

SECTION III  
TITLE PAGE OF PUBLISHED PAPERS  
(July 1976-June 1977)

## Monopole Excitation in the Giant-Resonance Region of $^{208}\text{Pb}^\dagger$

H. P. Morsch, P. Decowski,\* and W. Benenson

*Cyclotron Laboratory and Physics Department, Michigan State University, East Lansing, Michigan 48824*

(Received 29 December 1975; revised manuscript received 20 May 1976)

Inelastic scattering of 45-MeV protons and 70-MeV  $^3\text{He}$  particles has been used to study the giant-resonance region of  $^{208}\text{Pb}$ . The giant resonance is found to be highly structured with states of different multipolarities, such as dipole, quadrupole, and octupole. A monopole state is found at 9.11 MeV which exhausts about 2% of the monopole-sum-rule strength.

Among the important open questions in studies of giant resonances is the location of the monopole state. This breathing mode of the nucleus is particularly important because it gives information on the compressibility of nuclear matter, a property which has not experimentally been determined up to present. Theoretical estimates of the excitation energy of the monopole state vary considerably because they depend strongly on the choice of effective interaction.

Recent experimental attempts to observe a giant monopole resonance have centered on  $^{208}\text{Pb}$  but have not been conclusive. As a result of inelastic-electron-scattering experiments, Pitthan *et al.*<sup>1</sup> proposed a monopole state at 8.9 MeV which exhausts 50% of the sum-rule strength. However, it was shown by Schwierczinski *et al.*<sup>2</sup> that this state could equally well be quadrupole. Marty *et al.*<sup>3</sup> have compared inelastic deuteron and proton scattering and found that a possible explanation of the differences in the spectra obtained could be a giant monopole resonance at 13 MeV.

In an attempt to clarify the questions raised above we have studied the giant-resonance region in  $^{208}\text{Pb}$  using high-resolution, high-statistics, inelastic proton and  $^3\text{He}$  scattering. To summarize the results, we find that the giant-resonance region is highly structured and that the structure is angle dependent in a way that indicates that some of the peaks are pure dipole, quadrupole, and octupole excitations. One peak has an angular distribution which can be described only by an  $L=0$  calculation and hence may comprise part of the long-sought giant monopole resonance. Additional evidence for the monopole character of this state is found from the absence of the peak in the  $^3\text{He}$  inelastic scattering spectra in agreement with expectations for this type of excitation.

The experiments were performed with 45-MeV protons and 70-MeV  $^3\text{He}$  particles from the Michigan State University cyclotron. The scattered particles were detected in a delay-line counter<sup>4</sup> on the focal plane of an Enge split-pole spectro-

graph. The energy resolution (35 keV for protons and 45 keV for  $^3\text{He}$  particles) was limited by the thick targets (5.4 and 1.8 mg/cm<sup>2</sup>, respectively) required to keep impurities to a minimum relative to the  $^{208}\text{Pb}$ . A plastic scintillator provided time-of-flight information. This information permitted the elimination of most of the slit-scattered particles, which arrived at the detector 3–10 nsec later than the real inelastic events. Long runs were taken to eliminate statistical fluctuations in the spectra. Nonlinearities in the detector system create a gradual modulation of the spectra at a maximum excursion of about 5%. That the structure discussed in the present paper is not due to these nonlinearities was checked by comparing spectra taken at different field settings.

The raw proton spectra at 12° and 33° are shown in Fig. 1. Gross structures (width of 300 keV or more) similar to these observed in electron and proton scattering<sup>5–7</sup> are seen on top of a continuum which is slowly varying with angle. The scattering from light contaminants shows up mostly as narrow peaks which were identified by comparison to scattering from Mylar (C<sub>10</sub>H<sub>8</sub>O<sub>4</sub>). In addition to the gross structure, the good energy resolution of our experiment permits the observation of a strong fine structure in the giant-resonance region (width limited by the 35-keV resolution). It is interesting to note that the fine-structure peaks show distinct differences in the angular dependence, which implies the excitation of different multipolarities. There are peaks which show up mainly at forward angles indicated by cross hatching in the 12° spectrum. There are also other peaks which are dominant at larger angles, e.g., at 9.35 and 10.3 MeV. The angular distributions for some of the states with characteristic angle dependence are shown in Fig. 2 along with distorted-wave Born-approximation (DWBA) predictions. To determine the intensities a background was assumed of the type shown in Fig. 1. The assigned  $L=3$  excitation at 9.35 MeV

High-Spin Multiquasiparticle Yrast Traps in  $^{176}\text{Hf}\dagger$ 

T. L. Khoo, F. M. Bernthal, R. G. H. Robertson, and R. A. Warner  
*Cyclotron Laboratory and Departments of Physics and Chemistry, Michigan State University,  
 East Lansing, Michigan 48824*

(Received 14 June 1976)

We have identified several high- $K$  four- and six-quasiparticle states between 2.5 and 5 MeV excitation in  $^{176}\text{Hf}$ , which are well described by the collective model with axial symmetry. Isomers with  $K^\pi = 14^-, 19^+$ , and  $22^-$  form traps at or near the yrast line. The yrast structure changes from the ground band to a  $K^\pi = 16^+$  band at  $I = 16$  and again to a  $K^\pi = 22^-$  state at  $I = 22$ , providing the first demonstration that intrinsic excitations of a heavy deformed nucleus can become yrast.

The high-spin states of deformed nuclei that have been observed to date arise largely from collective rotation, involving the coherent motion of many nucleons. This is true whether the yrast structure remains the ground-state band, or develops into decoupled or unpaired bands, as occurs after back bending. The question arises as to whether few-nucleon degrees of freedom can also play an important role in the structure of nuclei at high spin. This matter is of relevance to nuclear behavior at spins exceeding  $30\hbar$ . Indeed, Bohr and Mottelson<sup>1,2</sup> have predicted that in this domain the large angular momentum of yrast states may in some cases be generated by aligning the spins of a few nucleons. Present experimental techniques do not allow us to observe individual levels at such ultrahigh spins. Nevertheless, it may be possible to investigate the interplay of collective and few-nucleon motion through the study of discrete levels by judiciously selecting a system in which the intrinsic excitations lie close to the yrast line at relatively low spins  $[(10-20)\hbar]$ .

Such an investigation entails the study of multi-quasiparticle (qp) configurations in a region of nuclear excitation (2.5-5 MeV) that has hitherto not been explored in detail. It is hence also of interest to determine whether the collective model, which has been remarkably successful at lower spins and energies, is still applicable in this new regime. Specifically, are there still simple intrinsic excitations with well-behaved rotational bands built on them, and are the radiative transitions adequately described? It is also important to ascertain whether  $K$  remains a good quantum number. Numerous (heavy-ion,  $\alpha n$ ) studies have identified no high-spin isomers which can be associated with band heads of high  $K$ ; this may imply a breakdown of a coupling scheme associated with axial symmetry.<sup>2</sup>

A promising system to investigate is  $^{176}\text{Hf}$  in

which we had previously identified a 401- $\mu\text{sec}$  four-qp isomer at 2866 keV, in addition to many high- $K$  two-qp states at lower excitation.<sup>3,4</sup> In the reaction  $^{176}\text{Yb}(\alpha, 4n)^{176}\text{Hf}$  with a 48-MeV  $\alpha$  beam, the 401- $\mu\text{sec}$  isomer receives  $\sim 30\%$  of the  $(\alpha, 4n)$  cross section. We have employed a delayed coincidence technique similar to that described in Ref. 3 to isolate the  $\gamma$  rays populating this isomer. Some of these  $\gamma$  rays were themselves found to be delayed in separate experiments in which  $\gamma$ -ray, conversion-electron,<sup>5</sup> and three-parameter  $\gamma$ - $\gamma$ - $t$  coincidence data were accumulated with the beam pulsed off. In addition, in-beam prompt  $\gamma$ - $\gamma$  coincidence,  $\gamma$ -ray angular distribution, and excitation function data were obtained. Thus, we used a large variety of spectroscopic information to develop the level scheme of Fig. 1. The transition multipolarities

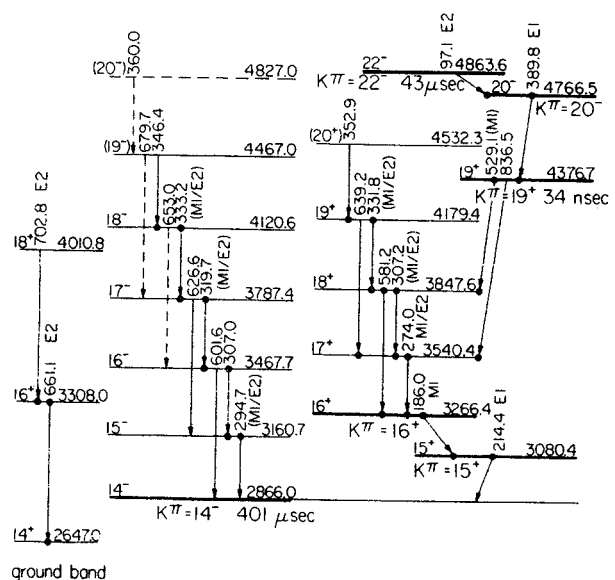


FIG. 1. Partial level scheme for  $^{176}\text{Hf}$  showing four- and six-qp excitations and upper portion of ground band. Assignments in parentheses are tentative. Filled circles indicate  $\gamma$  rays entering and leaving a level in prompt coincidence.

Anomalous Quenching of  $S = 1$  Two-Nucleon Transfer\*

H. Nann and B. H. Wildenthal

*Cyclotron Laboratory and Department of Physics, Michigan State University, East Lansing, Michigan 48824*  
(Received 14 June 1976)

Examination of the ground-state transitions of the  $(p, t)$  and  $(p, {}^3\text{He})$  reactions on all  $T_z = \frac{1}{2}$  nuclei from  ${}^{21}\text{Ne}$  through  ${}^{39}\text{K}$  reveals a systematic suppression of the  $S = 1, T = 0$  component of the  $(p, {}^3\text{He})$  transfer cross sections which is not explained in terms of current structure and reaction theories.

In this Letter we wish to call attention to a strikingly persistent feature of the ground-state transitions of  $(p, t)$  and  $(p, {}^3\text{He})$  reactions on the  $T = \frac{1}{2}$  nuclei of the  $sd$  shell. These transitions populate mirror states with  $T = \frac{1}{2}$  and  $T_z = \pm \frac{1}{2}$ ; hence both members of each isospin doublet should have essentially identical nuclear wave functions. The  $(p, t)$  reaction can populate these states only via pickup of a  $S = 0, T = 1$  nucleon pair, while the  $(p, {}^3\text{He})$  reaction can proceed via pickup of both  $S = 0, T = 1$  and  $S = 1, T = 0$ , pairs. We have observed<sup>1</sup> that for every  $T = \frac{1}{2}$  target in the  $sd$  shell from  ${}^{21}\text{Ne}$  through  ${}^{39}\text{K}$ , the ground-state  $(p, {}^3\text{He})$  transition appears to proceed by pure  $S = 0, T = 1$  transfer. The presence of any incoherent  $S = 1, T = 0$  contribution would result in cross sections for  $(p, {}^3\text{He})$  relative to  $(p, t)$  larger than those observed.

At present we are unable to explain this anomaly. Significant  $S = 1, T = 0$  strength is predicted by the best available shell-model wave functions for these ground-state transitions. Also, such strength is both predicted and observed for various excited states. Thus, some aspect of either nuclear structure or direct-reaction mechanism serves to quench systematically the ground-state  $S = 1, T = 0$  transfer strengths. The source of the quenching appears to lie outside the conventional realm of such theories. If this anomaly is confirmed by further experimental work, it will present a significant challenge to either current shell-model theory or distorted-wave Born-approximation (DWBA) theory, or both.

The experimental measurements employed 40-MeV protons from the Michigan State University cyclotron. The reaction products were momentum analyzed in a split-pole magnetic spectrograph and detected with position-sensitive proportional counters. This apparatus yielded excellent particle identification and energy resolutions in the range 15–30 keV. Angular distributions were usually measured in the region of  $6^\circ$  to  $50^\circ$ . In the context of the present note, the key experi-

mental measurements were of the  $(p, {}^3\text{He})$ -to- $(p, t)$  cross-section ratios. These measurements were typically made by measuring both  $(p, t)$  and  $(p, {}^3\text{He})$  differential cross sections during the same experimental run, with the same configuration of target, beam, and counter. Only the magnetic field of the spectrograph was changed in order to bring both  ${}^3\text{He}$ 's and tritons to the same position on the focal plane. The errors in these relative cross-section measurements are estimated to be less than 10%. Absolute cross-section scales are estimated to be accurate to 20%. These were assigned by measuring elastic proton-scattering counting rates relative to the  $(p, t)$  and  $(p, {}^3\text{He})$  rates and assuming standard<sup>2</sup> optical-model estimates for the elastic cross sections.

The ground-state angular distributions are shown in Fig. 1, with the  $(p, t)$  values elevated by one order of magnitude. The curves through the  $(p, t)$  distributions are DWBA calculations with a single set of optical-model parameters, the proton values being adapted from Greenlees and Pyle<sup>3</sup> and the mass-3 values from Urone *et al.*<sup>4</sup> (The parameters used for the outgoing tritons and  ${}^3\text{He}$ 's are identical and have the characteristic that they fit  ${}^3\text{He}$  and triton elastic scattering simultaneously.) The DWBA curves have been generated with current<sup>5-7</sup> mixed-configuration shell-model wave functions. However, the  $(p, t)$  shapes are independent of any variation of wave function within the  $sd$  shell and the absolute normalization of theory to experiment does not directly concern us in the present context. For the  $(p, {}^3\text{He})$  reaction, the contributions to the complete calculated differential cross sections (solid curves) from  $S = 0, T = 1$  transfer (dotted curves) and  $S = 1, T = 0$  transfer (dot-dashed curves) are added incoherently. A spin-isospin exchange term in the interaction potential<sup>8</sup> with values of  $[D(0, 1)]^2 = 0.71$  for the  $S = 0, T = 1$  transfer strength and of  $[D(1, 0)]^2 = 0.30$  for the  $S = 1, T = 0$  transfer strength<sup>9</sup> was employed in the DWBA calculations. The

---

## Pion-Absorption Contribution to the $\pi$ - $d$ Scattering Length in a Simple Dispersion-Theoretic Approach

R. Rockmore and P. Goode

*Physics Department, Rutgers, The State University, New Brunswick, New Jersey 08903*

and

H. McManus

*Cyclotron Laboratory, Michigan State University, East Lansing, Michigan 48824*

(Received 13 September 1976)

The pion-absorption contribution to the  $\pi$ - $d$  scattering length ( $a_{\pi d}'$ ) is calculated in the Hulthén model in a simple dispersion-theoretic approach with Koltun-Reitan input modified through the introduction of the off-shell  $S$ -wave range parameter  $\alpha_0$  with  $\alpha_0 = 500$  MeV/ $c$ . In this approach one finds the uncrossed result,  $a_{\pi d}' = -2.69 \times 10^{-3} m_{\pi}^{-1}$ , increased by  $1.30 \times 10^{-3} m_{\pi}^{-1}$  with the inclusion of crossing.

The role of pion-absorption in low-energy pion-nucleus scattering as well as the possible importance of crossing in this context has generated renewed interest in the study of such effects in threshold  $\pi$ - $d$  elastic scattering. The quantity of experimental and theoretical interest in this process is  $a_{\pi d}$ , the  $\pi$ -deuteron scattering length. For  $a_{\pi d}^S$ , the contribution to  $a_{\pi d}$  with *no* intermediate pion absorption, double scattering and ex-

plicit Fadeev calculations<sup>1</sup> yield the value  $a_{\pi d}^S \approx -0.035 m_{\pi}^{-1}$ . The remaining contribution to  $\text{Re} a_{\pi d}$  coming from intermediate pion absorption,  $a_{\pi d}'$  which is less well understood theoretically and for which, it has been noted, few calculations exist, is thought to be of the order of 10% (although this estimate is based on a recent measurement<sup>2</sup> of  $\text{Re} a_{\pi d}$  for which the uncertainty is about 50%).

1720

## A DETERMINATION OF THE MASS AND SOME ENERGY LEVELS OF THE NUCLIDE $^{44}\text{Ar}^{\star}$

G.M. CRAWLEY, W.F. STEELE, J.N. BISHOP, P.A. SMITH and S. MARIPUU\*

*Cyclotron Laboratory and Physics Department  
Michigan State University, East Lansing, Michigan 48824, USA*

Received 20 July 1976

The mass and some energy levels of the nuclide  $^{44}\text{Ar}$  have been determined from the  $^{48}\text{Ca}(^3\text{He}, ^7\text{Be})^{44}\text{Ar}$  reaction. A comparison with theoretical values of the mass is made.

The lifetime of the nucleus  $^{44}\text{Ar}$  has been reported [1, 2] but until now its mass and energy levels were unknown. This letter reports a measurement of the mass of  $^{44}\text{Ar}$  and the excitation energies of several of its excited states as determined from the  $^{48}\text{Ca}(^3\text{He}, ^7\text{Be})^{44}\text{Ar}$  reaction at 70 MeV  $^3\text{He}$  bombarding energy.

The  $^3\text{He}$  beam was produced by the Michigan State University isochronous cyclotron. The reaction products were analyzed by an Enge split-pole magnetic spectograph [3]. Detection of ions in the focal plane of the spectrometer was accomplished by a system composed of a plastic scintillator photomultiplier unit behind a 25 cm single wire charge division gas proportional counter [4]. The counter measures both position along the focal plane and differential energy loss of an ion, while the scintillator is used to measure time-of-flight of ions through the spectrograph.

As the  $Q$ -values for many ( $^3\text{He}, ^7\text{Be}$ ) reactions are nearly equal [5], contaminants in the target often produce peaks which interfere with those of primary interest. Contamination by carbon and oxygen is particularly severe because they are commonly present on calcium targets and the ( $^3\text{He}, ^7\text{Be}$ ) reaction on these nuclides has a relatively large cross section [6]. Consequently, an effort was made to minimize the amount of carbon and oxygen to come into contact with the  $^{48}\text{Ca}$  target. Targets were prepared by evaporating a layer, approximately  $200\ \mu\text{g}/\text{cm}^2$  thick, of 97.16% isotopically enriched  $^{48}\text{Ca}$  onto both gold and silver foils

of between 100 and  $200\ \mu\text{g}/\text{cm}^2$ . The metal evaporated after reduction of calcium carbonate mixed with molybdenum powder in a molybdenum tube. The silver backing foils gave a smoother target presumably because the coefficient of expansion of silver is closer to that of calcium than is the expansion coefficient of gold. The targets were prepared, stored and transferred to the target chamber under vacuum. Nevertheless, as can be seen from fig. 1, peaks arising from carbon and oxygen are still larger than the peaks corresponding to levels in  $^{44}\text{Ar}$ .

To help minimize the effect of the oxygen impurities in the  $^{44}\text{Ar}$  ground-state region, 1.5 mm diameter pins were placed at the positions where  $^7\text{Be}$  ions from the oxygen contaminant in the target would focus. This reduced the size of the peaks due to the 4.4 MeV state of  $^{12}\text{C}$  arising from the oxygen impurity by about a factor of ten. This technique is described in detail elsewhere [7]. In addition to contaminants, the  $^7\text{Be}$  spectra are complicated by those outgoing  $^7\text{Be}$  ions which are in the 0.43 MeV particle stable first excited state. Thus each level in the residual nucleus produces two peaks in the  $^7\text{Be}$  spectrum which are separated by about 0.4 MeV, the exact amount depending on the kinematical parameters. The experimental resolution (FWHM), due primarily to target thickness, of the spectrum measured at  $7^\circ$  laboratory angle (fig. 1) is about 66 keV, which allows discernment of these peak pairs, including those of impurities.

Ten independent spectra were measured at angles ranging from  $5^\circ$  to  $15^\circ$ . Small angles were chosen because the cross sections are larger at forward angles and to maximize the separation of the peaks corresponding to  $^{44}\text{Ar}$  from the contaminant peaks. Even

\* Work supported by the National Science Foundation.

\* Present address, Duke University, Durham, North Carolina, USA.

HIGH-SPIN LEVEL SYSTEMATICS IN  $^{177-182}\text{W}$ : YRAST BAND ANOMALY IN  $^{180}\text{W}$ \*

F.M. BERNTHAL, C.L. DORS, B.D. JELTEMA, T.L. KHOO and R.A. WARNER

*Departments of Chemistry and Physics and Cyclotron Laboratory,  
Michigan State University, East Lansing, Michigan 48824, USA*

Received 21 July 1976

High-spin levels in  $^{177-182}\text{W}$  have been populated in  $(\alpha, xn\gamma)$  reactions. Backbending-type behavior appears most prominently in  $^{180}\text{W}$ . The role of  $i_{13/2}$  neutrons and  $h_{9/2}$  protons in the  $^{180}\text{W}$  *yrast* behavior is examined. A strongly-coupled  $K^\pi = 10^+$  band structure is identified in  $^{182}\text{W}$ , the first seniority-two  $i_{13/2}$  configuration to be characterized in a deformed nucleus.

The more neutron rich even-even tungsten isotopes are the only nuclei accessible by  $(\text{particle}, xn)$  reactions in the rare-earth region of deformation for which high-spin data on the *yrast* bands have yet to be reported [1]. The tungsten isotopes are of some interest in this regard, because they bridge a region between no backbending in the more neutron-rich hafnium isotopes [2], and a region of sharp *yrast* anomalies in the osmium isotopes [3, 4]. The latter phenomena have recently been attributed by Neskakis et al. [4] to decoupling of  $h_{9/2}$  protons. In contrast, backbending in the neutron-deficient lower- $Z$  rare earth region is believed to result from decoupling of  $i_{13/2}$  neutrons [5]. Thus, *yrast* band anomalies in the heavier tungsten isotopes might be expected to arise from influences similar to those at work in the osmium isotopes, but the tungsten isotopes have the added attraction of being in a region where the axially symmetric nuclear shape is expected to be quite stable.

In this letter, we summarize results of  $(\alpha, xn\gamma)$  experiments carried out to populate levels in tungsten isotopes 177–182. Self-supporting foils of  $^{177}\text{Hf}$  and  $^{180}\text{Hf}$  were bombarded with beams of 26–50 MeV  $\alpha$ -particles from the Michigan State University Cyclotron. Prompt and delayed  $\gamma$ - $\gamma$  coincidence data,  $\gamma$ -ray excitation functions and angular distributions, and  $\gamma$ -time data relative to variable beam burst frequencies were obtained for each isotope studied. Details of the work on the odd- $A$  isotopes 179 and 181 have been published previously [6–8], and are discussed here only

as they pertain to the *yrast* behavior in the neighboring even-even isotopes.

The *yrast* band data for  $^{177-182}\text{W}$  are summarized in fig. 1. A conventional  $2\mathcal{G}/\hbar^2$  vs  $(\hbar\omega)^2$  plot of the even- $A$  data is shown in fig. 2. The salient aspect of the data is the  $^{180}\text{W}$  anomaly. The behavior of the *yrast* band very nearly qualifies  $^{180}\text{W}$  for the family of “backbending” nuclei, and is at least as striking as the  $^{170}\text{Yb}$  case which has recently received so much theoretical attention [9–13]. Furthermore, the effect is unique to  $^{180}\text{W}$  among all the W isotopes with  $N = 98-108$ , though some evidence for the behaviour persists in  $^{178}\text{W}$ . No such backbending behavior is seen in the corresponding Hf or Yb isotones, with the important exception of  $^{170}\text{Yb}$ . An additional feature of interest in this context is our characterization (from  $\gamma$ -ray crossover/cascade ratios) of the  $1.4\ \mu\text{s}$ ,  $K^\pi = 10^+$  isomer [14] in  $^{182}\text{W}$  as a triplet coupling of the  $9/2^+$  [624] and  $11/2^+$  [615] neutrons. This provides the first experimental data on the location and behavior of a seniority-two,  $i_{13/2}$  intrinsic configuration in the rare-earth deformed region.

Understanding the *yrast* behavior in  $^{180}\text{W}$  within the framework of conventional explanations of backbending thus becomes an intriguing problem. The recent experiments at Jülich would lead one to expect that the backbending-type behavior in  $^{180}\text{W}$  may simply be an extension into the W isotopes of the  $h_{9/2}$  proton-induced backbending proposed in the Os isotopes [4]. However, the data for the neighboring odd- $A$  W isotopes, 177, 179, and 181, show a remarkable correlation between the degree of decoupling in the  $i_{13/2}$  bands in those nuclei, and the behavior of the *yrast* band in their

\* Research supported by the U.S. National Science Foundation and the U.S. Energy Research and Development Agency.

## ON THE ROLE OF INDIRECT PROCESSES IN THE INELASTIC EXCITATION OF LOW LYING $0^+$ STATES<sup>\*</sup>

H.P. MORSCH

*Williams Laboratory of Nuclear Physics, University of Minnesota and Cyclotron Laboratory\*,  
Michigan State University, East Lansing, Michigan 48824, USA*

and

P.J. ELLIS

*School of Physics and Astronomy, University of Minnesota, Minneapolis, Minnesota 55455, USA*

Received 26 May 1976

Using simple microscopic form factors, we have studied the indirect excitation of low lying  $0^+$  states by inelastic scattering through the lowest  $2^+$  states in the case of  $\alpha$  scattering from  $^{24}\text{Mg}$  and  $^{28}\text{Si}$  and  $^3\text{He}$  scattering from  $^{46}\text{Ti}$ . Scaling amplitudes according to the inelastic scattering and  $B(E2)$  data we found that only for  $\alpha$  scattering from  $^{24}\text{Mg}$  was the indirect excitation small. For the other cases studied, our estimate yields indirect cross sections which were significant in comparison with the data, although this has been well described by the direct one-step process alone. The shape of the indirect cross section may be either strongly oscillatory or flat, depending on the radius of the real optical potential.

Several studies of the excitation of low lying  $0^+$  states in inelastic  $^3\text{He}$  and  $\alpha$  scattering have recently been made [1, 2] in which a one-step mechanism was assumed so that the conventional DWBA could be employed. The shape of the predicted angular distributions was found to be very sensitive to the form factor assumed, and this was used to obtain information on the particle-hole admixtures in the transition amplitude. It thus seems important to estimate the size of multi-step processes, particularly in view of early work by Love on  $^{90}\text{Zr}$  [3], where multi-step processes were suggested to be significant. The multi-step process we consider here, is as in ref. [3], first the inelastic excitation of the lowest  $2^+$  state, and then, subsequently, inelastic scattering to the  $0_2^+$  state in question. We refer to this as indirect excitation to distinguish it from the direct ( $0_1^+ - 0_2^+$ ) monopole mode.

We study inelastic excitations in  $\alpha$  scattering from  $^{24}\text{Mg}$  and  $^{28}\text{Si}$  and in  $^3\text{He}$  scattering from  $^{46}\text{Ti}$  using microscopic form factors. We take a Gaussian nucleon-nucleon interaction of range 1.85 fm and volume integral 446 MeV fm<sup>3</sup> and fold this with the  $^3\text{He}$  and  $\alpha$

internal wave functions of ref. [4]. Using this particle-nucleus interaction and assuming simple valence configurations it has been found [5] that the inelastic excitation of  $2_1^+$  levels can be described if the strength of the interaction is increased by an amount consistent with the effective charges necessary to reproduce the observed  $B(E2)$ . We use this procedure here for the ( $0_1^+ - 2_1^+$ ) step of the reaction, slightly adjusting the strength so as to account for the magnitude of the observed  $2_1^+$  cross sections [5, 6]. The configurations assumed for the  $0_1^+$  and  $2_1^+$  levels are  $(f_{7/2})^6$  for  $^{46}\text{Ti}$ ,  $(d_{5/2})^8$  for  $^{24}\text{Mg}$  and  $(d_{5/2})^{12}$  and  $(d_{5/2})^{11} s_{1/2}$ , resp. for  $^{28}\text{Si}$ . The single particle radial wave functions needed are generated in a Woods-Saxon well with a radius parameter of 1.25 fm, a diffuseness of 0.65 fm and a depth adjusted to reproduce the observed separation energy. For the second step, ( $2_1^+ - 0_2^+$ ), we simply use the same form factors as for the ( $0_1^+ - 2_1^+$ ) step and scale the strength according to the experimental  $B(E2)$  values [7, 8]. This procedure implies specific configurations for the  $0_2^+$  levels, however we do not believe that this assumption is severe. The shape of the  $0^+ - 2^+$  transition form factors is generally substantially the same if more complicated structure assumptions are made. Indeed we investigated the effect of  $2p_{3/2}$  admixtures in the  $0_2^+$  level of  $^{46}\text{Ti}$  and found very little change in the results.

<sup>\*</sup> Work supported in part by ERDA Contracts E(11-1) 1265 and At(11-1) 1764.

\* Present address.



## MONOPOLE EXCITATION OF ${}^4\text{He}$ IN $\alpha$ -PARTICLE SCATTERING FROM ${}^{12}\text{C}$ , ${}^{13}\text{C}$ , AND ${}^{16}\text{O}$ \*

R. JAHN<sup>1</sup>, D.P. STAHEL, G.J. WOZNIAK, Joseph CERNY

*Department of Chemistry and Lawrence Berkeley Laboratory,  
University of California, Berkeley, Calif. 94720, USA*

and

H.P. MORSCH<sup>2</sup>

*Cyclotron Laboratory, Michigan State University, East Lansing, Michigan 48824, USA*

Received 15 October 1976

The excitation of the  $0^+$  state in  ${}^4\text{He}$  at 20.1 MeV has been studied in  $\alpha$ -scattering from  ${}^{12}\text{C}$ ,  ${}^{13}\text{C}$ , and  ${}^{16}\text{O}$  at  $E_\alpha = 65$  MeV by measuring the decay  $\alpha^* \rightarrow p + t$  with a coincidence method. DWBA calculations of this monopole transition using both microscopic and collective model transition densities are presented.

Monopole excitations of nuclei are of considerable interest. One of the simplest examples of a monopole state is the first excited state of  ${}^4\text{He}$ , which in the shell model is largely described by a  $(1s_{1/2}^{-1} 2s_{1/2})$  particle-hole excitation [1]. This unbound state at 20.1 MeV excitation energy ( $\alpha^*$ ,  $\Gamma = 0.27$  MeV) lies 0.3 MeV above the  $t + p$  breakup threshold of the  $\alpha$ -particle and decays entirely via this channel [2, 3]. An experimental system has been developed [4] which is capable of selectively detecting an  $\alpha$ -particle excited to this  $\alpha^*$  state by measuring its correlated decay products in coincidence and identifying them as a proton and a triton.

In this letter we present a first observation of the monopole (projectile) excitation of  ${}^4\text{He}$  in 65 MeV  $\alpha$ -scattering from light nuclei ( ${}^{12}\text{C}$ ,  ${}^{13}\text{C}$ ,  ${}^{16}\text{O}$ ). For the (target) ground-state transitions, microscopic calculations have been performed using both microscopic and collective model transition densities. Although the absolute cross sections in the forward angular region are remarkably well predicted, this approach fails to reproduce the shape of the experimental an-

gular distributions, indicating that higher-order effects may be significant in this projectile excitation.

Our experimental setup [4] consisted of two counter telescopes capable of detecting the two breakup-particles in coincidence. In the laboratory system the protons and tritons arising from the decay of the  $\alpha^*$  state are emitted into a cone, which is defined by the lab. energy of the  $\alpha^*$  and by its decay energy. In order to achieve good detection efficiency, the acceptance angle of the two telescopes has to be similar to the size of the breakup cone, which is approximately  $12^\circ$  for 40 MeV  $\alpha^*$  events. Opposing this, energy resolution considerations require a small angular acceptance. A good compromise has been made by arranging the two telescopes vertically, thus achieving relatively good efficiency due to the large vertical acceptance angle and reasonable energy resolution by limiting the horizontal acceptance angle.

Fig. 1(a) shows the  $\alpha^*$  detection system. The  $\Delta E$  detectors were phosphorus-diffused silicon,  $380 \mu\text{m}$  thick and the  $E$  counters were Si(Li), 5 mm thick, all having the same area of  $1.0 \times 1.4 \text{ cm}^2$ . The divided collimator subtended a  $15^\circ$  vertical and a  $4^\circ$  horizontal opening angle. Standard particle identification techniques were used to identify the  $\alpha^*$  events. Both telescopes were capable of detecting protons as well as tritons, so that both possible combinations of  $\alpha^*$  decay products entering the two telescopes ( $p + t$  and  $t + p$ ) were detected, thus doubling the efficiency. In

\* Work performed under the auspices of the U.S. Energy Research and Development Administration.

<sup>1</sup> On leave from Institut für Strahlen- und Kernphysik der Universität Bonn, Germany. Supported by Deutscher Akademischer Austauschdienst.

<sup>2</sup> Present address: Kernfysisch Versnellend Instituut, Universiteit Groningen, The Netherlands.

STRUCTURAL CHANGES IN THE YRAST STATES OF  $^{178}\text{Hf}^*$ 

T.L. KHOO

*Cyclotron Laboratory and Department of Physics, Michigan State University, East Lansing, MI 48824, USA<sup>1</sup>,  
and McMaster University, Hamilton, Ontario L8S 4K1, Canada*

and

G. LØVHØIDEN

*McMaster University, Hamilton, Ontario L8S 4K1, Canada,  
and Institute of Physics, University of Bergen, Bergen, Norway<sup>1</sup>*

Received 14 February 1976

High-spin levels in  $^{178}\text{Hf}$ , including the ground-state band, several 2-quasiparticle (qp) bands, and two 4-qp isomers have been identified from  $(\alpha, 2n)$  studies. Changes in the structure of the yrast line are observed. The 4-qp isomers with  $K^\pi = 16^+$  and  $14^-$  are yrast traps.

The present interest in nuclei at high spin is partly motivated by a desire to understand how nuclei behave under the stress of large angular momentum. In this connection, it is pertinent to ask how angular momentum is generated in nuclei with the least expenditure of energy. In deformed nuclei, collective rotation has been commonly observed to be energetically the most favourable mode for generating spin. However, one might enquire whether few-particle degrees of freedom can be a competitive mode in this respect. That they indeed can has been demonstrated in a recent study of  $^{176}\text{Hf}$  [1], where it has been found that some 4- and 6-quasiparticle (qp) states can occur lower in energy than members of the ground-state band (gsb) with corresponding spin. It is important to determine if there are other systems where similar few-qp states become yrast.

A good candidate is  $^{178}\text{Hf}$ , where a 31 y  $K^\pi = 16^+$  isomer is known [2, 3] to exist at  $\approx 2.45$  MeV, an unusually low energy for a state of such high spin. In fact, if one extrapolated the gsb, previously known only to its  $8^+$  member, one would expect its  $16^+$  member to lie above the  $K^\pi = 16^+$  isomer. Therefore, we set out to find the higher-lying members of the gsb and also other high-K qp states.

\* Work supported in part by the U.S. National Science Foundation and National Research Council, Canada.

<sup>1</sup> Present address.

We employed the  $^{176}\text{Yb}(\alpha, 2n)^{178}\text{Hf}$  reaction, using 24–35 MeV  $\alpha$ -particle beams, and performed conventional in-beam  $\gamma$ -ray spectroscopic measurements with Ge(Li) detectors. Gamma-ray spectra were recorded in singles and coincidence modes with the McMaster FN tandem accelerator;  $\gamma$ -ray angular distribution, excitation function, and delayed- $\gamma$ -ray measurements were performed with the Michigan State University Cyclotron. In searching for isomers,  $\gamma$ -rays were observed (a) in a 580 ns beam-off interval corresponding to the period between every ninth pulse from the cyclotron, and (b) in a 500  $\mu\text{s}$  period between beam bursts of 100  $\mu\text{s}$  duration. The experimental techniques are described in more detail in refs. [4] and [5].

A partial level scheme for  $^{178}\text{Hf}$  which includes only states with  $K \geq 4$  is shown in fig. 1. The gsb to spin 8, the lower  $K^\pi = 8^-$  band to spin 13, and the  $K^\pi = 8^-, 4^+, 16^+$  states at 1479, 1514 and  $\approx 2450$  keV, respectively, were known from previous studies [2, 3, 6, 7]. The remaining levels of fig. 1 are reported here for the first time. These include the members of the gsb to spin 14, the  $K^\pi = 14^-$  isomer, and the rotational bands built on the  $K^\pi = 8_2^-, 5^-,$  and  $6^+$  states. The newly discovered isomers at 1554 and 2574 keV have half-lives of  $78 \pm 1$  ns and  $68 \pm 2$   $\mu\text{s}$ , respectively. The probable configurations of the band-heads are given in table 1. The spins and parities have been as-

## HIGH-SPIN NEUTRON HOLE EXCITATIONS IN LIGHT ODD-A Pb NUCLEI\*

H. HELPPI, S.K. SAHA and P.J. DALY

*Chemistry Department, Purdue University, West Lafayette, Indiana 47097, USA*

and

S.R. FABER, T.L. KHOO and F.M. BERNTHAL

*Cyclotron Laboratory and Departments of Physics and Chemistry  
Michigan State University, East Lansing, Michigan 48824, USA*

Received 15 February 1977

The high-spin level structures of  $^{195,197,199,201,203}\text{Pb}$  have been investigated by  $(\alpha, xn\gamma)$  and  $(^3\text{He}, xn\gamma)$  spectroscopy. The resulting level schemes are interpreted in terms of the weak coupling of an  $\nu i_{13/2}$  hole to known states of the even-A core nuclei.

In odd mass Pb nuclei with  $A < 205$ ,  $13/2^+$  isomers of  $\nu i_{13/2}^{-1}$  character are well established, and some low-spin levels are known from radioactivity studies [1]. However, nothing has been known up to now about the high-spin level structures of these semi-magic nuclei. In marked contrast, high-spin levels in the even-A Pb nuclei down to  $A = 194$  have been studied in detail by two groups [2, 3], and the results have been interpreted in terms of neutron hole excitations. We have investigated the five odd-A Pb nuclei in the mass range  $A = 195-203$  by in-beam  $\gamma$ -ray spectroscopy. The main results are reported briefly here, with most emphasis on systematic features of the high-spin level spectra.

The experiments were performed at the Michigan State University cyclotron by means of  $(\alpha, 3n\gamma)$  and  $(^3\text{He}, xn\gamma)$  reactions on isotopically enriched HgO targets. Strong yrast cascades terminating in the known  $\nu i_{13/2}^{-1}$  isomeric states were observed in all five nuclei. Isotopic identifications were based on excitation function measurements and on the requirement of approximate intensity balance, at all bombarding energies, between the transitions populating and depopulating the  $13/2^+$  isomers. The experiments included  $\gamma$ -ray singles, comprehensive  $(\gamma\text{-}\gamma\text{-}t)$  coincidence measurements, and  $\gamma$ -ray angular distribution determinations. In addition, lifetime measurements spanning a range from 2 ns to

many seconds were performed, and many new isomers in the odd-A Pb nuclei were identified.

The principal results of the investigations are summarized in the partial level schemes shown in fig. 1, which also includes the even-A Pb level spectra [2, 3].

*The nucleus  $^{203}\text{Pb}$ .* A pulsed beam  $^{202}\text{Hg}(\alpha, 3n\gamma)$  experiment revealed a  $^{203}\text{Pb}$  isomer with  $t_{1/2} = 0.48 \pm 0.04$  s, and subsequent  $\gamma\text{-}\gamma$  coincidence and prompt angular distribution measurements firmly established the complete isomeric decay scheme. The 0.5 s isomeric state is placed at 2949 keV and assigned  $J^\pi = 29/2^-$ . It decays by 153 keV E3 and 1027 keV M4 transitions to  $23/2^+$  and  $21/2^+$  levels, which de-excite in turn by several cascades leading to the known 6.2 s  $13/2^+$  isomer at 825 keV. The dominant neutron hole configuration  $f_{5/2}^{-1}, i_{13/2}^{-2}$  is clearly indicated for the  $29/2^-$  state in  $^{203}\text{Pb}$ , which can be ascribed to the coupling of the  $^{204}\text{Pb}$   $9^-$  state (fig. 1) with the additional  $\nu i_{13/2}$  hole.

The 0.5 s  $^{203m}\text{Pb}$  activity has also been observed recently by Linden et al. [4].

*The nuclei  $^{201}\text{Pb}$  and  $^{199}\text{Pb}$ .* These nuclei have been investigated by  $(\alpha, 3n\gamma)$  reactions on  $^{200}\text{Hg}$  and  $^{198}\text{Hg}$  targets. As illustrated in fig. 1, three new isomers have been identified in each nucleus. The data showed clearly that the 0.54  $\mu\text{s}$  and 10.6  $\mu\text{s}$  isomers in  $^{201}\text{Pb}$  and  $^{199}\text{Pb}$ , respectively, de-excite to the  $25/2^-$  levels in these nuclei, but the connecting transitions were not observed even in the delayed  $\gamma$ -ray spectra. If, as the level systematics suggest, these transitions are of

\* Supported in part by U.S. Energy Research and Development Administration and U.S. National Science Foundation.

**$\alpha + \alpha$  PHASE SHIFTS AND THE  $p + {}^7\text{Li}$  AND  $n + {}^7\text{Be}$  CHANNELS\***C.H. KING, Sam M. AUSTIN, W.S. CHIEN and H.H. ROSSNER<sup>1</sup>*Cyclotron Laboratory and Physics Department,  
Michigan State University, East Lansing, Michigan 48824, USA*

Received 15 December 1976

Calculations reported recently in this journal indicate a discrepancy between measurements of  $\alpha + \alpha \rightarrow n + {}^7\text{Be}$  cross sections and phase shifts deduced from  $\alpha + \alpha$  elastic scattering. It is demonstrated that these calculations are erroneous.

Spallation reactions between cosmic rays and interstellar matter have apparently been important in the nucleosynthesis of the light elements. For  ${}^6\text{Li}$  and the Be and B isotopes, in fact, spallation appears to have been the dominant production mechanism [1]. In the production of  ${}^7\text{Li}$ , two important spallation reactions are  $\alpha + \alpha \rightarrow p + {}^7\text{Li}$  and  $\alpha + \alpha \rightarrow n + {}^7\text{Be}$  (with the  ${}^7\text{Be}$  subsequently decaying to  ${}^7\text{Li}$  by electron capture). From our measurements of the cross sections for these reactions [2], we concluded that existing spallation models [1] were unlikely to yield sufficient  ${}^7\text{Li}$  production to explain the observed cosmic abundance of  ${}^7\text{Li}$ . Thus, other  ${}^7\text{Li}$  production mechanisms might be required.

Recently, Slobodrian [3] has made an interesting comparison between the cross sections we measured and the results of  $\alpha + \alpha$  elastic-scattering phase-shift analyses. Since the  $p + {}^7\text{Li}$  and  $n + {}^7\text{Be}$  channels are the only open reaction channels in  $\alpha + \alpha$  scattering below 39.6 MeV, the sum of the cross sections for these channels is the total reaction cross section in this energy region. Slobodrian calculated the total reaction cross section (incorrectly, as we shall show) using phase shifts determined in two analyses [4, 5] of  $\alpha + \alpha$  elastic-scattering data. In both cases, the calculated values of the total reaction cross section  $\sigma_R$  significantly exceeded that implied by our measurements. In his paper, Slobodrian presents previously unpublished data from Berkeley [6] which are generally in excellent agreement with our measurement of

$\alpha + \alpha \rightarrow p + {}^7\text{Li}$ . Hence, he suggests the apparent discrepancy must lie in the measurement of the  $\alpha + \alpha \rightarrow n + {}^7\text{Be}$  cross sections.

The purpose of this note is to indicate that Slobodrian's calculations are apparently erroneous. When the presence of the identical  $\alpha$ -particles is properly treated, the expression for the total reaction cross section is

$$\sigma_R = 2\pi\lambda^2 \sum_{\substack{l=0 \\ \text{even}}}^{\infty} (2l+1)(1 - |e^{2i\delta_l}|^2), \quad (1)$$

Here the  $\delta_l$  are the complex elastic-scattering phase shifts. We have calculated  $\sigma_R$  using expression (1) and the phase-shift-set of Darriulat [4] (published in a paper by Kumar and Barker [7]), which is one of the sets used by Slobodrian, and have obtained values smaller than those obtained by Slobodrian by a factor very close to 2. It therefore appears likely that Slobodrian has used an expression for  $\sigma_R$  which is twice that of eq. (1). Since such an incorrect expression for  $\sigma_R$  has appeared elsewhere [8] in the literature, it seems worthwhile to present here a short derivation of the correct result.

The properly symmetrized scattering amplitude for identical bosons is well-known [9] to be

$$f^{1B}(\theta) = f(\theta) + f(\pi - \theta), \quad (2a)$$

where  $f(\theta)$  is the usual scattering amplitude for distinguishable particles:

$$f(\theta) = \frac{\lambda}{2i} \sum_{l=0}^{\infty} (2l+1)P_l(\cos\theta)(e^{2i\delta_l} - 1). \quad (2b)$$

The total cross section  $\sigma_T$  can then be determined

\* Research supported by the U.S. National Science Foundation.

<sup>1</sup> Present address: Hahn-Meitner-Institut für Kernforschung, Berlin GmbH, 1 Berlin-West 39, Germany.

## LETTER TO THE EDITOR

### Measuring short-range correlations †

G Bertsch and J Borysowicz

Physics Department and Cyclotron Laboratory, Michigan State University, East Lansing, Michigan 48824, USA

Received 4 June 1976

**Abstract.** We re-examine the problem of determining short-range correlations by sum rules for cross sections at constant momentum transfer. Using the model-independent analysis technique, we find that knowledge of the summed cross sections for momentum transfers  $3 \text{ fm}^{-1}$  to  $4.5 \text{ fm}^{-1}$  is crucial for observation of short-range repulsion. Unfortunately, meson production will obscure the interpretation of the data in just this region.

The character of the short-range interaction between nucleons is basic to nuclear theory. The most frequently used model, the potential of Reid (1968), has strong repulsion at short distance, as do many other models. At one point measurement of the resulting correlation was contemplated (McVoy and Van Hove 1962), but rejected as experimentally not possible. We here re-examine this old question, using model-independent analysis of theoretically generated 'data'. The conclusion of McVoy and Van Hove is affirmed by our work, but we are able to provide a more quantitative specification of the requirements of the measurement. Specifically, the experimental requirements are

- (a) an electron beam of  $> 1.5 \text{ GeV}$  energy,
- (b) data out to momentum transfers of  $4.5 \text{ fm}^{-1}$  and
- (c) precision of 1%, relative to the cross sections on hydrogen and deuterium.

However, meson production will cause uncertainties of the order of 1%, thus ruling out unambiguous interpretation of an experiment which measures only the final electron.

The basic theoretical construct we consider is the structure function

$$S(q) = \langle 0 | \sum_{i < j} \exp [i \mathbf{q} \cdot (\mathbf{r}_i - \mathbf{r}_j)] | 0 \rangle.$$

Its Fourier transform is the desired two-body correlation function

$$\rho(r_{12}) = \frac{1}{(2\pi)^3} \int d^3 q \frac{S(q)}{\binom{N}{2}}.$$

On the experimental side, we will consider a simple system, the  $^4\text{He}$  nucleus, and measurement of the difference in cross sections between helium and deuterium:

$$I(q) = \int_{E-\Delta E}^E dE' (\sigma_{\text{He}}(q, E') - 2\sigma_{\text{d}}(q, E'))$$

† Work supported in part by NSF, USA.

## Comparison of measured neutron spectra with predictions of an intranuclear-cascade model\*

Aaron Galonsky

*Cyclotron Laboratory and Physics Department, Michigan State University, East Lansing, Michigan 48824  
and Institut für Kernphysik der Kernforschungsanlage Jülich, D-517 Jülich, West Germany*

R. R. Doering and D. M. Patterson†

*Cyclotron Laboratory and Physics Department, Michigan State University, East Lansing, Michigan 48824*

H. W. Bertini

*Neutron Physics Division, Oak Ridge National Laboratory, Oak Ridge, Tennessee 37830*

(Received 30 March 1976)

Neutron spectra resulting from bombardment of targets of  $^{48}\text{Ca}$ ,  $^{90}\text{Zr}$ ,  $^{120}\text{Sn}$ , and  $^{208}\text{Pb}$  with 45-MeV protons have been measured at many angles between  $0^\circ$  and  $160^\circ$ . Intranuclear-cascade, Monte Carlo calculations predict too many high-energy neutrons in the forward direction and too few neutrons, particularly high-energy neutrons, at angles greater than  $\sim 45^\circ$ . Beyond  $90^\circ$  the underprediction is by factors of 10 to 100. For angle-integrated spectra, however, there is reasonable agreement between theory and experiment.

[ NUCLEAR REACTIONS  $^{48}\text{Ca}$ ,  $^{90}\text{Zr}$ ,  $^{120}\text{Sn}$ ,  $^{208}\text{Pb}(p, nx)$ ;  $E = 45$  MeV; measured  $\sigma(E_n, \theta)$  and  $\int d\Omega \sigma(E_n, \theta)$ ; enriched targets. Intranuclear-cascade model. ]

For proton spectra initiated by 62- and 39-MeV protons, a detailed comparison has recently been made between experiment and intranuclear-cascade models.<sup>1</sup> In that comparison it was seen that the models predicted relatively too many high-energy protons at small angles and too few protons of all energies at large angles. In this Communication we compare the predictions of the ORNL model<sup>2</sup> with neutron spectra produced by 45-MeV protons incident on thin targets of  $^{48}\text{Ca}$  (1 mg/cm<sup>2</sup>),  $^{90}\text{Zr}$  (10 mg/cm<sup>2</sup>),  $^{120}\text{Sn}$  (10 mg/cm<sup>2</sup>), and  $^{208}\text{Pb}$  (10–30 mg/cm<sup>2</sup>).<sup>3,4</sup> Experimental details may be found in Refs. 3 and 4. The spectra were measured at Michigan State University, and the calculations were performed at Oak Ridge National Laboratory. Similar data exist for the same target nuclei but for lower proton bombarding energies, viz. 35 and 25 MeV. A comparison between theory and experiment was made for  $^{48}\text{Ca}$  and  $^{208}\text{Pb}$  at 35 MeV. As the results were qualitatively similar to those at 45 MeV, only the 45-MeV work is presented here. No cascade calculations were

made at 25 MeV, where the range of neutron energy is rather small.

In terms of angle-integrated spectra, Fig. 1 shows the comparison between theory and experiment for each of the four targets. The prediction of the cascade model is given in each case by a histogram having a 5-MeV bin width. The histories of 50 000 incident protons were followed for each target, resulting in statistical errors ranging from 2% for neutrons in the lowest-energy bin to 5% in the highest. As the cascade progresses in time, the kinetic energy brought in by the proton is accounted for, but there is no accounting of the mass difference between target and residual nuclei. One consequence of this neglect is, for example, the ejection of neutrons having the same kinetic energy as the incident protons, whereas the maximum neutron energy must trail the incident proton energy by the magnitude of the  $(p, n)$   $Q$  value. These magnitudes are (in MeV) 0.51, 6.89, 3.46, and 3.65 for  $^{48}\text{Ca}$ ,  $^{90}\text{Zr}$ ,  $^{120}\text{Sn}$ , and  $^{208}\text{Pb}$ , respectively. An approximate correction

## Nuclear rotational current and velocity fields, the cranking model, and transverse electroexcitation of the first excited state of $^{12}\text{C}^\dagger$

Mark Radomski

*Cyclotron Laboratory, Physics Department, Michigan State University, East Lansing, Michigan 48824*

(Received 19 July 1976)

We examine current and velocity fields of rotating deformed nuclei. Although the harmonic oscillator cranking model gives rigid moments of inertia, the velocity field is not a rigid rotation in the examples studied. Such fields are partially observable via electroexcitation, and we compare  $^{12}\text{C}$  to experiment. A slight improvement in experimental precision would allow different models to be distinguished.

[NUCLEAR REACTIONS Inelastic electron scattering, deformed nuclei; trans-verse electroexcitation probability, rotational model;  $^{12}\text{C}(e, e')^{12}\text{C}^*(4.4 \text{ MeV})$ .]

The nature of nuclear rotation has received much attention and interest in nuclear physics. Initial recognition of the phenomenon was hindered by a preconception in favor of rigid-body rotation. The fluid drop picture with irrotational flow<sup>1</sup> has also been used extensively. The actual nature of the flow need follow no assumption based on a classical ideal, but is dynamically determined by the interplay of collective and intrinsic degrees of freedom, in a manner as yet not understood.

I shall present some dynamically calculated velocity fields for rotation of idealized versions of  $^8\text{Be}$  and  $^{12}\text{C}$ , compare them with classical expectations, and show how they manifest their nature in the transverse electroexcitation of the rotational states. My model for carbon may already be marginally in conflict with experiments on excitation of the  $2^+$  (4.44 MeV) state. Thus a modest increase of experimental precision may enable this and other models to be distinguished.

The cranking model will be used to generate current density fields from which velocity fields will be deduced. An axially symmetric potential well is rotated with constant angular velocity  $\omega$  about the  $x$  axis, the symmetry axis starting in the  $z$  direction at time  $t=0$ . Time-dependent wave functions for the motion of a particle are found, through first order in  $\omega$ , in, e.g., Ref. 2. The extension to many particles is straightforward. Current density fields are arrived at by taking expectation values, using these wave functions, of a local current operator. The time dependence of the current field, and of other local fields such as the density, consists of rotation to follow the potential. It is thus sufficient to regard the fields obtained at  $t=0$  and to treat them as being related to body-fixed axes.

For independent particles one thus obtains the current<sup>3</sup>

$$\vec{j}(\vec{x}) = 2\text{Re} \sum_{\mu \text{ occupied}}^A \sum_{\nu \neq \mu} \langle \mu | \vec{j}_{op}(\vec{x}) | \nu \rangle \langle \nu | -\omega j_x | \mu \rangle \times (\epsilon_\mu - \epsilon_\nu)^{-1} + O(\omega^3), \quad (1)$$

where  $\vec{j}_{op}(\vec{x})$  is the local one-body current density operator. The current at  $\omega=0$  vanishes for a time-reversal invariant intrinsic structure such as is appropriate to the ground-state band of even-even nuclei. The density field  $\rho(\vec{x})$  is equal to that for  $\omega=0$ , except in order  $\omega^2$ , under the same conditions.

Equation (1) contains much more information than just the moment of inertia, for which the cranking model result has long been known.<sup>4</sup> But if the mass-convection current is used for  $\vec{j}_{op}$ , and  $\vec{x} \times \vec{j}(\vec{x})$  is integrated over space, one finds  $L_x = \omega \mathcal{G}_{\text{crank}}$ , where  $\mathcal{G}_{\text{crank}}$  is given by Inglis's result.

In a fluid drop picture, the current is a product of density and velocity. It is natural to define a velocity field by

$$\vec{v}(\vec{x}) = \vec{j}(\vec{x}) / \rho(\vec{x}). \quad (2)$$

Rigid-body flow has  $\vec{v} = \vec{\omega} \times \vec{x}$ . Irrotational flow has a  $\vec{v}$  field with zero curl. In general, different current and density operators (e.g., electromagnetic vs baryon number currents and densities) produce different velocities. For definiteness, let us take the electromagnetic convection current and charge; for proton states

$$\langle \mu | \vec{j}_{op}(\vec{x}) | \nu \rangle = \frac{1}{2im} \{ \psi_\mu(\vec{x})^\dagger \vec{\nabla} \psi_\nu(\vec{x}) - [\vec{\nabla} \psi_\mu(\vec{x})]^\dagger \psi_\nu(\vec{x}) \}.$$

Then  $\vec{v}(\vec{x})$  is the average velocity field of the protons. For the doubly even, self-conjugate nuclei explicitly to be considered, the neutron velocity field is the same. If the cranked Hamiltonian is furthermore spin independent, the magnetic mo-

## Observation of highly neutron-rich $^{43}\text{Cl}$ and $^{59}\text{Mn}^\dagger$

E. Kashy, W. Benenson, D. Mueller, H. Nann, and L. Robinson

Cyclotron Laboratory and Department of Physics, Michigan State University, East Lansing, Michigan 48824

(Received 19 May 1976)

We report the observation and mass measurement of  $^{43}\text{Cl}$  and  $^{59}\text{Mn}$  by the ( $^3\text{He}$ ,  $^8\text{B}$ ), five-nucleon pickup reaction. Mass excess values of  $-23.14 \pm 0.06$  for  $^{43}\text{Cl}$  and  $-55.49 \pm 0.03$  MeV for  $^{59}\text{Mn}$  have been measured.

[NUCLEAR REACTIONS  $^{48}\text{Ca}$ ,  $^{64}\text{Ni}$ ( $^3\text{He}$ ,  $^8\text{B}$ );  $E = 74$  MeV; measured mass excess]  
 $^{43}\text{Cl}$ ,  $^{59}\text{Mn}$ .

### INTRODUCTION

In this paper, we report the use of the ( $^3\text{He}$ ,  $^8\text{B}$ ) reaction to reach the highly neutron-rich nuclei  $^{43}\text{Cl}$  and  $^{59}\text{Mn}$  and to measure their masses.  $^{43}\text{Cl}$  has six neutrons more than the stable  $^{37}\text{Cl}$  and is predicted bound against neutron decay.<sup>1</sup> Its high value of isospin,  $T_z = \frac{9}{2}$ , makes its mass important as a test of the numerous mass relations in the region far from  $\beta$  stability. A recent paper of Jelley *et al.*<sup>2</sup> discusses one of these relations and also summarizes the current status of experimental data on very neutron-rich light nuclei.

Only a few light nuclei as far from  $\beta$  stability have experimentally measured masses, e.g.,  $^{22}\text{O}$  with  $T_z = 4^3$  and  $^{30,31,32}\text{Na}$  with  $T_z = 4, \frac{9}{2}$ , and  $5^4$ . For the  $T_z = \frac{9}{2}$  nucleus  $^{31}\text{Na}$  an experimental accuracy of about 800 keV was achieved.<sup>4</sup> Interestingly  $^{31}\text{Na}$  and  $^{32}\text{Na}$  differ from recent predictions<sup>1,2</sup> by 2 to 5 MeV, a discrepancy which has been interpreted in terms of a shape transition of the ground state.<sup>5</sup> These deviations are significant since these relations tend to yield agreement at the 200–300 keV level for nuclei closer to  $\beta$  stability. The present results for  $^{43}\text{Cl}$  represent a significantly higher precision in mass values of highly neutron-rich nuclei in addition to adding to the scarce data available.  $^{59}\text{Mn}$  also has  $T_z = \frac{9}{2}$  but lies much nearer the line of  $\beta$  stability. Its decay properties have recently been reported concurrently with our mass measurements.<sup>6</sup>

Multinucleon pickup reactions leading to nuclei far from stability have extremely small cross sections, ranging from  $1 \mu\text{b}/\text{sr}$  for the ( $^3\text{He}$ ,  $^6\text{He}$ ) three-neutron pickup reaction to a few nb/sr for ( $p$ ,  $^6\text{He}$ ) or ( $^3\text{He}$ ,  $^8\text{Li}$ ) five-nucleon pickup reaction. For the ( $^3\text{He}$ ,  $^8\text{B}$ ) reaction, the targets have to be even thinner than those in the aforementioned five-nucleon pickup to compensate for the larger specific ionization of the  $^8\text{B}$  ions, whereas the cross sections are comparable. The intense 74

MeV  $^3\text{He}$  beam available from the Michigan State University cyclotron (2–3  $\mu\text{A}$  on target) makes these studies feasible using a few days of beam time.

### EXPERIMENTAL PROCEDURE AND RESULTS

The experimental apparatus is essentially that which has been previously described.<sup>7</sup> The  $^8\text{B}$  ions were detected, identified, and momentum analyzed in the focal plane of an Enge split-pole spectrograph by combining in a Sigma-7 computer the information on energy loss and position in two resistive wire proportional detectors, and time-of-flight information from a thin plastic scintillator.

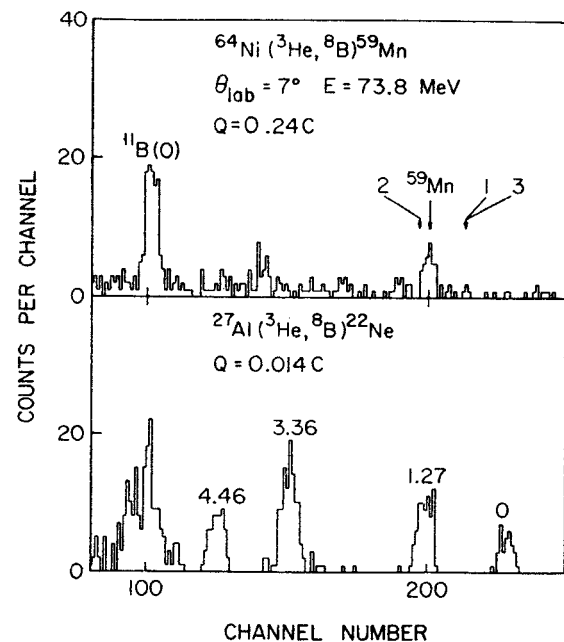


FIG. 1. Energy spectra of  $^8\text{B}$  ions from the ( $^3\text{He}$ ,  $^8\text{B}$ ) reaction on  $^{27}\text{Al}$  and  $^{64}\text{Ni}$ . The theoretical predictions labeled 1 and 2 are taken from Ref. 9, that labeled 3 is from Ref. 10.



## Finite-range distorted-wave Born-approximation study of the ( ${}^4\text{He}$ , ${}^6\text{Li}$ ) reaction on ${}^{12}\text{C}$ , ${}^{24}\text{Mg}$ , and ${}^{40}\text{Ca}$ †

R. G. Markham and M. A. M. Shahabuddin

Cyclotron Laboratory and Physics Department, Michigan State University, East Lansing, Michigan 48824

(Received 4 August 1976)

Angular distributions have been obtained for the ( $\alpha$ ,  ${}^6\text{Li}$ ) reaction at 46 MeV on targets of  ${}^{12}\text{C}$ ,  ${}^{24}\text{Mg}$ , and  ${}^{40}\text{Ca}$ . A finite-range distorted-wave Born-approximation analysis is performed using shell model wave functions to describe the target and various cluster wave functions to describe  ${}^6\text{Li}$ . Finite-range effects are evident in the predicted absolute magnitudes but not in the shapes of the angular distributions, which are poorly fitted. Reasonable agreement between measured and predicted absolute cross sections is obtained if the product of the  $\alpha$ - $d$  wave function and potential for the  ${}^6\text{Li}$  has no node away from the origin.

[ NUCLEAR REACTIONS  ${}^{12}\text{C}$ ,  ${}^{24}\text{Mg}$ ,  ${}^{40}\text{Ca}(\alpha, {}^6\text{Li})$ ,  $E=46$  MeV; measured  $\sigma(E_{\alpha\text{Li}}, \theta)$ ; Finite-range DWBA analysis with microscopic wave functions. ]

### I. INTRODUCTION

In recent years, there has been a great deal of interest in the ( ${}^6\text{Li}$ ,  $d$ ) " $\alpha$ " transfer reaction. Studies<sup>1</sup> have found that the angular distributions have shapes which are characteristic of the transferred  $L$  and reproducible with both finite-range and zero-range distorted-wave Born-approximation (DWBA) calculations. Thus, the reaction has been very useful for making spin assignments, but so far it has only been possible to discuss the relative cross sections. The significance of the absolute cross sections is completely unknown. The prediction of absolute cross sections based on shell model wave functions requires a microscopic four nucleon form factor and a reliable reaction theory. The difficulties inherent in the construction of such a form factor and the lack of knowledge of the structure of  ${}^6\text{Li}$  [which is required in a finite-range DWBA (FRDWBA) calculation] preclude a simultaneous solution to these problems. Thus, it is necessary to isolate the two problems and solve each independently. The ( $\alpha$ ,  ${}^6\text{Li}$ )—or ( ${}^6\text{Li}$ ,  $\alpha$ )—reaction allows one to make this separation since its analysis requires the same relative motion wave function and interaction potential of the  $\alpha$  and deuteron in  ${}^6\text{Li}$  but it only requires a two nucleon form factor which is relatively well understood.

Very little data exist for either the ( $\alpha$ ,  ${}^6\text{Li}$ ) or ( ${}^6\text{Li}$ ,  $\alpha$ ) reactions. The very negative  $Q$  values (–15 to –25 MeV) for the ( $\alpha$ ,  ${}^6\text{Li}$ ) reaction demand a high beam energy and so the few existing experiments<sup>2</sup> have been done on light nuclei with poor resolution. Tentatively it is concluded from these works that the reaction is direct. However, Rudy *et al.*<sup>3</sup> conclude that large compound nucleus con-

tributions are present for the ( $\alpha$ ,  ${}^6\text{Li}$ ) reaction on targets of  ${}^{12}\text{C}$  and  ${}^{16}\text{O}$  at 42 MeV. On the other hand, White, Charlton, and Kemper<sup>4</sup> conclude that the  ${}^{12}\text{C}(\alpha, \alpha){}^{14}\text{N}$  reaction is direct at  $E_{\alpha\text{Li}} = 33$  MeV but that multistep mechanisms may be very important. Both works included excitation functions, angular distributions and comparisons to Hauser-Feshbach calculations. The implications for  ${}^{12}\text{C}(\alpha, {}^6\text{Li})$  at 46 MeV are just not clear and, as will be demonstrated, the existing data on  ${}^{12}\text{C}$  are not able to distinguish between the different mechanisms.

Here we report a study of the ( $\alpha$ ,  ${}^6\text{Li}$ ) reaction on targets of  ${}^{12}\text{C}$ ,  ${}^{24}\text{Mg}$ , and  ${}^{40}\text{Ca}$ . Calculations are performed using FRDWBA with shell model form factors and two sets of  ${}^6\text{Li}$  cluster wave functions and potentials. The emphasis is on reproducing the absolute magnitudes of the cross sections to all states for which angular distributions have been obtained subject to the assumption of a one-step, direct transfer. Obviously, this may not be completely the case for  ${}^{12}\text{C}$  or  ${}^{24}\text{Mg}$  (due to multistep processes) but if the cross sections are even just indicative of the one-step direct contribution, we will be able to learn something about this mechanism which is vital to our understanding of the ( ${}^6\text{Li}$ ,  $d$ ) reaction.

### II. EXPERIMENT

The reactions were induced using 46 MeV  $\alpha$  particles from the Michigan State University cyclotron. Average beam intensities varied from 200 to 800 nA. The outgoing  ${}^6\text{Li}$  ions were analyzed in a split-pole spectrograph and detected in a dual proportional counter in the focal plane. The front counter was a single-wire, position-sensitive

$(f_{7/2})^{-3}$  configuration states in  $^{45}\text{Ca}^\dagger$ 

H. Nann, D. Mueller, and E. Kashy

Cyclotron Laboratory and Department of Physics, Michigan State University, East Lansing, Michigan 48824

(Received 18 August 1976)

The  $^{48}\text{Ca}(^3\text{He}, ^6\text{He})^{45}\text{Ca}$  reaction has been studied at 70 MeV bombarding energy and angular distributions to strongly populated states in  $^{45}\text{Ca}$  up to 5 MeV of excitation have been obtained. Evidence for  $(f_{7/2})^{-3}$  configuration states at 0.17, 1.43, 1.56, 1.89, and 2.88 MeV is discussed. The experimental  $(f_{7/2})^{-3}$  spectrum is compared with calculations based on the  $(f_{7/2})^{-2}$  spectrum of  $^{46}\text{Ca}$ .

[ NUCLEAR REACTIONS  $^{48}\text{Ca}(^3\text{He}, ^6\text{He})$ ,  $E_{^3\text{He}} = 70$  MeV, measured  $(E_{^6\text{He}}, \theta)$ ; enriched target, deduced excitation energies. ]

## I. INTRODUCTION

There has been a great interest in the description of nuclei with  $Z$  and  $N$  between 20 and 28 in terms of the spherical shell model with a suitable residual interaction between nucleons in a  $(f_{7/2})^n$  configuration outside the  $A = 40$  closed shell.<sup>1,2</sup> The simplest systems to check the basic assumptions of such a model are the  $(f_{7/2})^{2,3}$  configuration states.  $^{45}\text{Ca}$  is the least known of these nuclei. The present paper intends to fill this gap.

Since all  $(f_{7/2})^{-3}$  levels, except for the  $7/2^-$  state, have seniority  $\nu = 3$ , these states are expected to be very weakly excited in single-nucleon transfer reactions, but strongly in the  $^{48}\text{Ca}(^3\text{He}, ^6\text{He})^{45}\text{Ca}$  reaction. The single-particle or single-hole states in  $^{45}\text{Ca}$  have been studied by Rapaport, Dorenbusch, and Halbert<sup>3</sup> and Yntema<sup>4</sup> via  $^{44}\text{Ca}(d, p)^{45}\text{Ca}$  and  $^{46}\text{Ca}(d, t)^{45}\text{Ca}$ . The comparison of these results to those obtained in the present  $^{48}\text{Ca}(^3\text{He}, ^6\text{He})^{45}\text{Ca}$  reaction yields evidence for all of the high-spin members of the  $(f_{7/2})^{-3}$  configuration states in  $^{45}\text{Ca}$ .

## II. EXPERIMENTAL PROCEDURE AND RESULTS

The  $^{48}\text{Ca}(^3\text{He}, ^6\text{He})^{45}\text{Ca}$  reaction was performed with a 70 MeV  $^3\text{He}$  particle beam from the Michigan State University cyclotron. The reaction products were detected in a position sensitive detector system on the focal plane of an Enge split-pole magnetic spectrograph. The detector system consisted of two resistive-wire proportional counters backed by a plastic scintillator. The two proportional counters provided redundant information of the energy loss in the gas, while the signal from the plastic scintillator was employed to give both time of flight in the spectrograph and light-output information.

The target was made by evaporating metallic calcium, enriched to 97% in  $^{48}\text{Ca}$ , onto a thin carbon foil. The metallic calcium was reduced from

$\text{CaCO}_3$  by means of Zr powder as a part of the evaporation process. The target was kept under vacuum at all times. The thickness was about  $130 \mu\text{g}/\text{cm}^2$ .

Figure 1 shows two  $^6\text{He}$  spectra taken at  $10^\circ$  and  $24^\circ$ . The resolution was about 30 keV full width at half maximum. Although the level density in  $^{45}\text{Ca}$  is quite high in the 2 to 5 MeV excitation energy range,<sup>5</sup> only relatively few states are strongly excited. The excitation energies of the levels observed in the present experiment are given in Table I.

Angular distributions were obtained over the region from  $6^\circ$  to  $35^\circ$ . They are displayed in Figs. 2-4. Error bars reflect only statistical

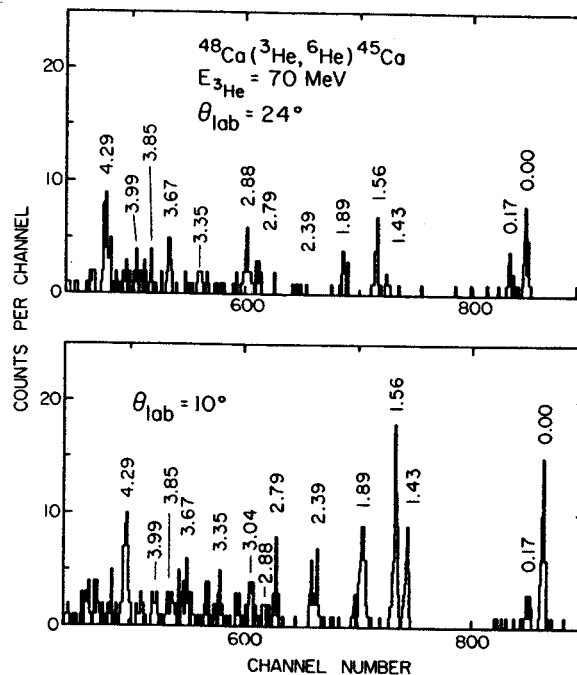


FIG. 1. Spectra of the  $^{48}\text{Ca}(^3\text{He}, ^6\text{He})^{45}\text{Ca}$  reaction at  $\theta_{\text{lab}} = 10^\circ$  and  $24^\circ$ .

Mass of  $^{57}\text{Ni}$ 

H. Nann, E. Kashy, D. Mueller, and A. Saha

Cyclotron Laboratory, Michigan State University, East Lansing, Michigan 48824

S. Raman

Physics Division, Oak Ridge National Laboratory, Oak Ridge, Tennessee 37830

(Received 16 August 1976)

A measurement of the  $Q$  values of the  $^{59}\text{Ni}(p,t)^{57}\text{Ni}$  and the  $^{58}\text{Ni}(^3\text{He},\alpha)^{57}\text{Ni}$  reactions shows a significant discrepancy with the current tabulated mass values. We find  $-12738.2 \pm 3.3$  keV and  $+8360.3 \pm 4.0$  keV, respectively, leading to a new improved mass excess for  $^{57}\text{Ni}$  of  $-56078.4 \pm 3.0$  keV.

[NUCLEAR REACTIONS  $^{59}\text{Ni}(p,t)$ ;  $^{58}\text{Ni}(^3\text{He},\alpha)$ ; measured  $Q$  values, deduced mass excess for  $^{57}\text{Ni}$ .]

Since the 1971 Wapstra-Gove mass tables<sup>1</sup> were published, several reaction  $Q$  values have been found<sup>2-4</sup> which disagree with the tables by several standard deviations. In this note, we report new results for the mass for  $^{57}\text{Ni}$  found during the course of studying the  $^{59}\text{Ni}(p,t)^{57}\text{Ni}$  and  $^{58}\text{Ni}(^3\text{He},\alpha)^{57}\text{Ni}$  reactions. The  $^{57}\text{Ni}$  mass excess of  $-56104 \pm 7$  keV reported in the 1971 mass table is based on the end point energy for the  $^{57}\text{Ni}-^{57}\text{Co}$  decay.<sup>5</sup> A previously measured  $Q$  value of  $+8400 \pm 50$  keV for the  $^{58}\text{Ni}(^3\text{He},\alpha)^{57}\text{Ni}$  reaction<sup>6</sup> was not used to determine the mass excess of  $^{57}\text{Ni}$ .

In the  $^{59}\text{Ni}(p,t)^{57}\text{Ni}$  experiment, we used a 40 MeV proton beam from the Michigan State University cyclotron. The reactor produced  $^{59}\text{Ni}$  target (37.4%  $^{58}\text{Ni}$ , 43.0%  $^{59}\text{Ni}$ , 15.2%  $^{60}\text{Ni}$ , 1.0%  $^{61}\text{Ni}$ , 2.1%  $^{62}\text{Ni}$ , and 1.2%  $^{64}\text{Ni}$ ) was a rolled foil of about  $230 \mu\text{g}/\text{cm}^2$  thickness. The reaction products were detected in the focal plane of an Enge split-pole spectrograph by a position sensitive proportional counter. The resolution obtained was about 15 keV full width at half maximum (FWHM). Figure 1 shows an example of the spectra obtained. As one can see, the ground and 0.769 MeV state transitions of the  $^{59}\text{Ni}(p,t)^{57}\text{Ni}$  reaction fall in the same region as the ground and 1.454 MeV state transitions of the  $^{60}\text{Ni}(p,t)^{58}\text{Ni}$  reaction and the ground state transition of the  $^{58}\text{Ni}(p,t)^{56}\text{Ni}$  reaction. These three transitions thus serve as calibration lines for the  $^{59}\text{Ni}(p,t)$   $Q$ -value determination. The spectrograph calibration method and fitting procedure is described extensively elsewhere.<sup>7</sup> Since the present measurement involves only the position of the tritons from the different Ni isotopes in the target, the uncertainties attributed to the beam energy and the scattering angle and due to target thickness effects are negligible. The main sources of errors are the  $Q$  values of the calibration re-

actions and local nonlinearities in the position-sensitive detector. The uncertainties of both sources are estimated to be  $\leq 3$  keV. Using the most recent mass excess values of Jolivet *et al.*<sup>4</sup> for the calibration  $Q$  values we obtain  $-12738.2 \pm 3.3$  keV for the  $Q$  value of the  $^{59}\text{Ni}(p,t)^{57}\text{Ni}$  ground state transition. This value is 18.4 keV more negative than the  $-12719.8 \pm 7.6$  keV result calculated from the 1971 mass table.

The  $^{58}\text{Ni}(^3\text{He},\alpha)^{57}\text{Ni}$  experiment was performed with a 70 MeV  $^3\text{He}$  beam using a similar setup as described before. The target was prepared by vacuum evaporation of  $^{58}\text{Ni}$  (isotopically enriched

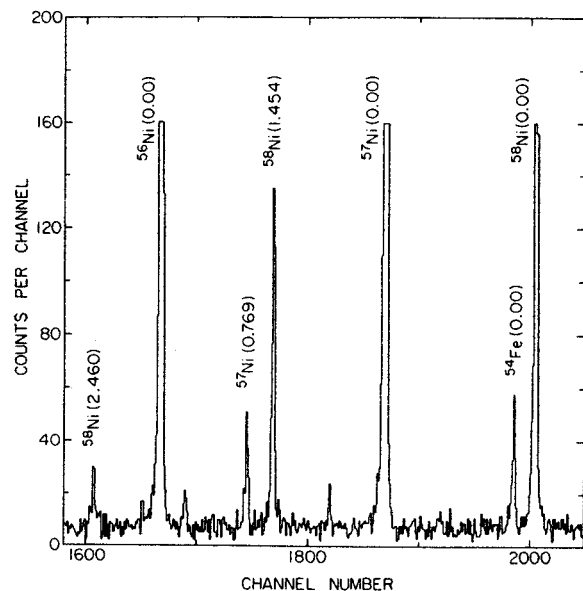


FIG. 1. Triton spectrum of the  $^{58,59,60}\text{Ni}(p,t)^{56,57,58}\text{Ni}$  reactions. The peaks are labeled by the final nucleus and its excitation energy.

## High-spin levels in $^{191}\text{Pt}$ and $^{193}\text{Pt}$ and the triaxial rotor model\*

S. K. Saha, M. Piiparinen,<sup>†</sup> J. C. Cunnane,<sup>†</sup> and P. J. Daly  
 Chemistry Department, Purdue University, West Lafayette, Indiana 47907

C. L. Dors, T. L. Khoo, and F. M. Bernthal

Departments of Chemistry and Physics and Cyclotron Laboratory, Michigan State University, East Lansing, Michigan 48824  
 (Received 27 August 1976)

The high-spin level structures of the transitional nuclei  $^{191}\text{Pt}$  and  $^{193}\text{Pt}$  have been studied by  $(\alpha, 3n\gamma)$  reactions on enriched Os targets. The measurements included  $\gamma$ -ray singles, comprehensive  $\gamma$ - $\gamma$  coincidences, half-life determinations, and  $\gamma$ -ray angular distributions. The extensive  $^{191}\text{Pt}$  and  $^{193}\text{Pt}$  level schemes established are reported here. In both nuclei, decoupled  $\nu i_{13/2}^{-1}$  bands, strongly resembling the ground bands of the adjacent core nuclei, and many other high-spin positive parity states have been located. Low-lying  $21/2^-$  bands have also been observed in both nuclei and they are described as semidecoupled bands with microscopic structures dominated by three-quasiparticle components of the type  $(\nu i_{13/2}^{-2}, \nu j^{-1})$ . The abundant information about  $\nu i_{13/2}$  level families obtained in these experiments and in a complementary  $^{191}\text{Au}$  decay study is discussed, and it is shown that these complex level spectra can be accounted for rather well in terms of the coupling of an  $i_{13/2}$  neutron hole to a triaxially deformed core.

[NUCLEAR REACTIONS  $^{190}\text{Os}$ ,  $^{192}\text{Os}(\alpha, 3n\gamma)$ ,  $E = 31\text{--}46$  MeV; measured  $E_\gamma$ ,  $I_\gamma(\theta)$ ,  $\gamma$ - $\gamma$  coin,  $T_{1/2}$ ;  $^{191,193}\text{Pt}$  deduced level schemes,  $J$ ,  $\pi$ .]

### I. INTRODUCTION

Recently there has been a sharp revival of interest in the asymmetric rotor description of shape transitional nuclei. Of particular significance has been the work of Meyer ter Vehn,<sup>1</sup> who showed that the complex unique parity level spectra of odd- $A$  nuclei observed in the  $A = 135$  and  $A = 190$  mass regions can be closely reproduced using a model of a high- $j$  particle (or hole) coupled to a rotating triaxial core. Toki and Faessler<sup>2</sup> have extended the model to include the known softness of the core by a generalized variable moment of inertia (VMI) treatment.

We have investigated<sup>3</sup> the high-spin level structures of the transitional nuclei  $^{186\text{--}194}\text{Pt}$  by  $(\alpha, xn\gamma)$  in-beam spectroscopy. In the odd- $A$  nuclei, strongly populated  $\nu i_{13/2}$  decoupled bands, resembling the ground bands of the adjacent core nuclei, were observed. Several additional strong deexcitation cascades connecting other high-spin ( $\geq 11/2$ ) positive parity members of the  $\nu i_{13/2}$  family were also identified. In a complementary study<sup>4</sup> of the electron capture decay of 3.1-h  $^{191}\text{Au}$ , low-spin  $\nu i_{13/2}$  levels in  $^{191}\text{Pt}$  were located and characterized. We have already reported briefly<sup>5</sup> on the rather complete  $\nu i_{13/2}$  level family established by the combined studies, and have shown that the model of an  $i_{13/2}$  hole coupled to a triaxial core ( $\gamma \sim 30^\circ$ ) is impressively successful in accounting for the experimental findings.

Here we present and discuss the detailed results

of the in-beam  $\gamma$ -ray investigations of the  $^{191}\text{Pt}$  and  $^{193}\text{Pt}$  level structures.

### II. EXPERIMENTAL PROCEDURE

The  $^{191}\text{Pt}$  and  $^{193}\text{Pt}$  level schemes were investigated by  $(\alpha, 3n\gamma)$  reactions on isotopically enriched targets of  $^{190}\text{Os}$  (95%) and  $^{192}\text{Os}$  (98%), using  $\alpha$ -particle beams from the Michigan State University cyclotron. Since the instruments and experimental techniques employed were similar to those described in our earlier article<sup>6</sup> on the  $^{190}\text{Pt}$  and  $^{192}\text{Pt}$  level structures, only a summary of the procedures and some samples of the data obtained are given here.

Singles  $\gamma$ -ray spectra were measured with Ge(Li) spectrometers at seven different  $\alpha$ -particle bombarding energies spanning the range 31–46 MeV, and the  $\gamma$  rays of  $^{191}\text{Pt}$  and  $^{193}\text{Pt}$  were identified from their excitation functions. A typical  $\gamma$ -ray spectrum recorded is shown in Fig. 1. For both reactions,  $\gamma$ -ray angular distributions with respect to the beam direction were measured at five angles in the range  $90^\circ\text{--}140^\circ$ , and values of the  $A_2/A_0$  and  $A_4/A_0$  coefficients were extracted for all well-resolved  $\gamma$  rays of moderate to strong intensity. Comprehensive three-parameter  $(\gamma, \gamma, t)$  coincidence measurements were performed using two Ge(Li) detectors, and prompt coincidence spectra gated on approximately 80 different  $\gamma$  rays in each nucleus studied were obtained. Some important  $^{193}\text{Pt}$  coincidence spectra are shown in Fig. 2.

## Threshold pion production in heavy-ion collisions\*

G. F. Bertsch†

Lawrence Berkeley Laboratory, Berkeley, California 94720

(Received 20 September 1976)

Pion production from heavy-ion collisions is calculated in the independent-particle model, using nucleon-nucleon cross section data as input information. The assumption is made that only the first collision of a nucleon pair can create a pion, and also all collective effects are neglected. For the representative case of  $^{16}\text{O}$  bombardment of  $^{238}\text{U}$  at 250 MeV/nucleon, one out of seven inelastic collisions should produce a pion. One-third of these pions should be able to escape to the outside. The pion spectrum peaks at 20 MeV with an average energy of 50 MeV, viewed in the nucleon-nucleon center-of-mass frame.

[NUCLEAR REACTIONS Pion production in heavy-ion collisions, calculate  $\sigma$ ,  $\sigma(E_p)$ .]

### I. INTRODUCTION

The energy range 100–300 MeV/nucleon in heavy-ion collisions is interesting because while the energy is high enough to allow strong interpenetration of the nuclei, with a density increase of a factor of 2, it is still low enough that collective effects associated with the higher density might have a chance to manifest themselves. As it happens, this energy region encompasses the threshold for significant pion production. Of the observable effects that can be easily measured, the pion production cross section at threshold is particularly sensitive to collective phenomena. The purpose of this paper, however, is to calculate the pion production with the most economical theoretical assumptions and, in particular, with no collective effects at all. This model could provide a baseline for theoretical discussions of experiments: Discrepancies by orders of magnitude one way or the other would provide an indication of various possible collective effects.

Our picture of the threshold production is that the Fermi momentum of the two nuclei combine to permit pion-producing nucleon-nucleon collisions. However, the initial distribution of nucleons in momentum space rapidly degrades to a thermal distribution, which is much less favorable for producing pions. The created pions have a relatively long mean free path ( $\sim 5$  fm) and thus provide a probe of the nuclear interior at the initial stages of collision.

Following this picture, we need the following ingredients for the calculation: first, the initial distribution of nucleons in phase space; second, the total nucleon-nucleon cross sections in order to calculate the rate of depletion of nucleons from the initial distribution; and, finally, the pion production cross sections for nucleon-nucleon collisions.

We shall neglect the possibility of pion production after the initial collision of a nucleon. Consequently, the calculation will be unreliable at higher energies.

To gain some perspective, we can view this model as a simple approximation to the solution of the classical Boltzmann equation for the particles. Our model contains all the assumptions of incoherence built into the Monte Carlo statistical cascade calculations of pion production by protons<sup>1,2</sup> as well as the further assumption that only the first collision is important. We now examine the various ingredients of the model in detail.

### NUCLEON DISTRIBUTION FUNCTION

For individual nuclei, we assume the distribution function of the Fermi gas model, specifically

$$f(p, r) = \rho(r)\theta(|p| - p_F)/(4\pi p_F^3/3). \quad (1)$$

This model differs in the surface region from the more customary Thomas-Fermi approximation, which utilizes a local Fermi momentum depending on position. The ansatz Eq. (1) is easier to apply than the Thomas-Fermi approximation, because the spatial dependence is separable from the momentum dependence.

Before proceeding, it would be useful to have a gauge of reliability of the Fermi gas approximation. A good test is provided by the response function, which is simply the probability of exciting the nucleus as a function of energy and momentum transfer. Threshold pion production by two nuclei requires a large momentum transfer to each nucleus with only small excitation energy. In the Fermi gas model, this restricts momentum transfers to around  $2k_F \sim 2.5 \text{ fm}^{-1}$ . Experimentally, the response to electrons has been measured near this

### Odd-parity rotational band structure in $^{48}\text{V}^\dagger$

L. E. Samuelson,\* W. H. Bentley, W. H. Kelly, and R. A. Warner

Cyclotron Laboratory and Department of Physics, Michigan State University, East Lansing, Michigan 48824

F. M. Bernthal and Wm. C. McHarris<sup>†</sup>

Cyclotron Laboratory, Department of Chemistry, and Department of Physics, Michigan State University, East Lansing, Michigan 48824

(Received 2 December 1974; revised manuscript received 7 September 1976)

A second odd-parity rotational band in the  $f_{7/2}$ -shell nucleus  $^{48}_{23}\text{V}_{25}$ , based on a 1099.1 keV state with  $K^\pi = 4^-$ , has been identified up to the  $8^-$  member. Also, corrections are given for the previously reported  $1^-$  band. These bands can be interpreted as the singlet and triplet couplings of the  $\Omega^\pi[Nn_2\Lambda\Sigma] = 3/2^+ [202_i]$  proton and  $5/2^- [312_+]$  neutron Nilsson orbitals, indicating prolate deformation.

NUCLEAR REACTIONS  $^{46}\text{Ti}(\alpha, pn)$ ,  $^{48}\text{Ti}(p, n)$ ; measured  $\gamma$ - $\gamma$  coin, ce,  $^{48}\text{V}$  deduced levels,  $J$ ,  $\pi$ ,  $\Lambda$ , ICC. Splitting of Nilsson levels.

An odd-parity rotational-like band built on a proposed  $J^\pi = 1^-$ , 518.7-keV state in  $^{48}_{23}\text{V}_{25}$  has been reported by Haas and Taras.<sup>1</sup> We have outlined arguments in favor of associating the 1099.1-keV state in  $^{48}\text{V}$  with a related  $K^\pi = 4^-$  rotational band.<sup>2</sup> In view of the apparently contradictory data regarding the proposed  $4^-$  assignment, however, we undertook to measure  $\alpha_K$ , the  $K$ -shell internal conversion coefficient, for the 1099.1-keV transition that depopulates this state to the  $4^+$  ground state. In this case, such a measurement is definitive with respect to the parity.

Here we report the unambiguous characterization of the 1099.1-keV transition as  $E1$  and the confirmation of the  $4^-$  assignment for the 1099.1-keV state. To our knowledge this is the first reported in-beam application of the conversion-coefficient technique to such a low- $Z$  nucleus. Moreover, the  $^{48}\text{V}$  data provide a very clear example of one of the few singlet-triplet coupling doublets to be identified in such a light nucleus, and they give a clear indication of permanent prolate deformation at low energies in a nucleus close to the  $Z = 20$ ,  $N = 28$  closed shells. We also show that the  $1^-$  band built on the 518.7-keV state is strongly perturbed with a large odd-even shift.

We have performed  $\gamma$ - $\gamma$  coincidence experiments and measured  $\gamma$ -ray excitation functions using the  $^{46}\text{Ti}(\alpha, pn\gamma)$  and  $^{45}\text{Sc}(\alpha, n\gamma)$  reactions to populate high-spin  $^{48}\text{V}$  states. New  $^{48}\text{V}$   $\gamma$  rays were identified by their appearance in gates on peaks well known from the  $(p, n\gamma)$  work.<sup>3</sup> The  $^{48}\text{Ti}(p, ne^-)$  studies reported here were specifically aimed at determining the parity of the 1099.1-keV state. Details of all of these experiments will be published later with the results for both positive and negative parity levels.

A portion of the level scheme of  $^{48}\text{V}$  showing the revised and extended odd-parity band structure is shown in Fig. 1. Important coincidence spectra

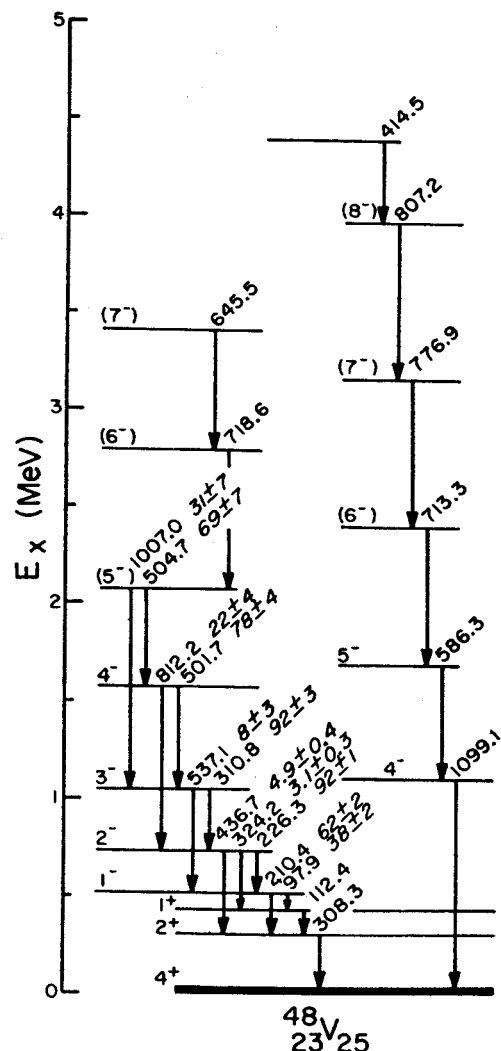


FIG. 1. A partial level scheme of  $^{48}\text{V}$  showing odd-parity band structures and their decay modes.

## Measurement of the internal pair emission branch of the 7.654-MeV state of $^{12}\text{C}$ , and the rate of the stellar triple- $\alpha$ reaction\*

R. G. H. Robertson,<sup>†</sup> R. A. Warner, and Sam M. Austin

Cyclotron Laboratory and Physics Department, Michigan State University, East Lansing, Michigan 48824

(Received 2 December 1976)

The internal pair decay of the  $0^+$  7.65-MeV state of  $^{12}\text{C}$  has been observed in coincidence with inelastic protons from  $^{12}\text{C}(p,p')^{12}\text{C}(7.65)$ , using a plastic scintillator of essentially  $4\pi$  sr solid angle. The branching ratio measured,  $\Gamma_r/\Gamma = (6.0 \pm 1.1) \times 10^{-6}$ , is in excellent agreement with the previous measurement by Alburger, and reduces the uncertainty in the stellar triple- $\alpha$  reaction rate by almost a factor of 2. Implications for the astrophysical production of  $^{12}\text{C}$  and  $^{16}\text{O}$  are discussed.

[NUCLEAR STRUCTURE  $^{12}\text{C}$ , 7.654-MeV state; measured  $\Gamma_r/\Gamma$ . Stellar helium burning.]

### I. INTRODUCTION

The steps by which a star burns helium to produce  $^{12}\text{C}$  and  $^{16}\text{O}$  seem now to be well understood. Öpik and Salpeter<sup>1</sup> showed that the gaps in the chain of stable nuclides which occur at  $A = 5$  and  $A = 8$  could be bridged by the triple- $\alpha$  process, the fusion of three  $\alpha$  particles to form  $^{12}\text{C}$ . In the next stage of helium burning,  $^{16}\text{O}$  is formed by the  $^{12}\text{C}(\alpha, \gamma)^{16}\text{O}$  reaction, which eventually competes with the triple- $\alpha$  reaction for use of the available  $^4\text{He}$ . Consequently, at the completion of helium burning, the relative abundance of  $^{12}\text{C}$  and  $^{16}\text{O}$  depends on the specific nuclear parameters governing the rates of the two reactions. To the extent that the end product is returned to the interstellar medium without further modification, the  $^{12}\text{C} : ^{16}\text{O}$  ratio calculated should correspond to the observed cosmic ratio.

Hoyle<sup>2</sup> realized this helium burning process could account for the observed abundances of  $^{12}\text{C}$  and  $^{16}\text{O}$  if the triple- $\alpha$  reaction were resonant in both the 2- $\alpha$  and 3- $\alpha$  systems. It was already known that the  $0^+$  ground state of  $^9\text{Be}$  lay at about 100 keV in the 2- $\alpha$  system, and Hoyle was able to infer the existence of a low-lying  $0^+$  state in the 3- $\alpha$  system. The excitation energy and radiative width of this state, now known to be the second excited state of  $^{12}\text{C}$ , play a crucial role in the triple- $\alpha$  process and have thus become the subject of intensive experimental work.

The rate  $P_{3\alpha}$  for the triple- $\alpha$  reaction can be written<sup>3</sup>

$$P_{3\alpha} = n_\alpha^3 \hbar^5 \left( \frac{2\pi\sqrt{3}}{kTM_\alpha} \right)^3 \Gamma_{\text{rad}} \exp(-Q_{3\alpha}/kT) \text{ cm}^{-3} \text{ sec}^{-1}, \quad (1)$$

where  $n_\alpha$  is the number density of  $\alpha$  particles,

$M_\alpha$  the atomic mass of  $^4\text{He}$ ,  $T$  the temperature,  $Q_{3\alpha}$  the energy released in the decay  $^{12}\text{C}(7.6541) \rightarrow 3^4\text{He}$ , and  $\Gamma_{\text{rad}}$  the radiative width of the 7.65-MeV state of  $^{12}\text{C}$ . The value of  $Q_{3\alpha}$  has recently been measured to be  $(379.38 \pm 0.20)$  keV,<sup>4</sup> a value sufficiently precise that its uncertainty no longer influences that in  $P_{3\alpha}$ . On the other hand  $\Gamma_{\text{rad}}$  is known only to  $\pm 31\%$ , and has become the chief limitation in the accuracy with which  $P_{3\alpha}$  can be calculated.

Experimentally  $\Gamma_{\text{rad}}$  is determined indirectly as the product of three quantities:

$$\Gamma_{\text{rad}} = \left( \frac{\Gamma_{\text{rad}}}{\Gamma} \right) \left( \frac{\Gamma}{\Gamma_r} \right) (\Gamma_r), \quad (2)$$

where  $\Gamma$  is the total width of the 7.65-MeV state and  $\Gamma_r$  its partial width for the  $E0$  internal pair transition to the ground state. The total radiative width  $\Gamma_{\text{rad}}$  is the sum of  $\Gamma_r$  and  $\Gamma_\gamma$ , the partial width for photon decay, essentially all of which proceeds through the  $2^+$  state at 4.44 MeV. The value of  $\Gamma_{\text{rad}}$  has been the subject of several recent experimental studies (summarized by Markham, Austin, and Shahabuddin<sup>5</sup>), resulting in a recommended weighted average of  $(4.13 \pm 0.11) \times 10^{-4}$  for that quantity. Electron scattering measurements<sup>6,7</sup> of the  $E0$  matrix element connecting the ground and 7.65-MeV states yielded a value for  $\Gamma_r$  of  $(60.5 \pm 3.9)$   $\mu\text{eV}$ . Thus, by far the largest contribution to the uncertainty in  $\Gamma_{\text{rad}}$  came from the remaining quantity,  $\Gamma/\Gamma_r$ , the reciprocal of the pair branching ratio. The single measurement of this ratio prior to the present work was that of Alburger.<sup>8</sup> Alburger excited the 4.44- and 7.65-MeV states of  $^{12}\text{C}$  by the  $^9\text{Be}(\alpha, n)$  reaction and compared the intensity of internal pairs from the two states. Since the 4.44-MeV state must decay radiatively its pair branch could be calculated

## Coulomb displacement energies of the $A = 4n + 3$ , $T = 1/2$ mirror nuclei in the $1f_{7/2}$ shell\*

D. Mueller,<sup>†</sup> E. Kashy, and W. Benenson

*Cyclotron Laboratory and Physics Department, Michigan State University, East Lansing, Michigan 48824*

(Received 6 January 1977)

The  $Q$  values of the ( $^3\text{He}, ^6\text{He}$ ) reaction on  $^{46}\text{Ti}$ ,  $^{50}\text{Cr}$ ,  $^{54}\text{Fe}$ , and  $^{58}\text{Ni}$  have been measured, and the excitation energy of levels up to 7 MeV has been determined. Angular distributions from the more strongly populated states have been taken from 4.5 to 27.0° in the laboratory. These angular distributions together with comparison to their  $T_z = +1/2$  mirrors have been used as empirical guides to determine the spin and parity of several of the states. The Coulomb displacement energies of particle-hole states in the  $T = 1/2$  mirrors have been compared to a simple model.

[ NUCLEAR REACTIONS  $^{25}\text{Mg}$ ,  $^{27}\text{Al}$ ,  $^{46}\text{Ti}$ ,  $^{50}\text{Cr}$ ,  $^{54}\text{Fe}$ ,  $^{58}\text{Ni}$ ( $^3\text{He}$ ,  $^6\text{He}$ ),  $E_{3\text{He}} = 70$  MeV, measured  $Q$ ,  $\sigma(\theta)$ , excitation energies, obtained mass excess of  $^{43}\text{Ti}$ ,  $^{47}\text{Cr}$ ,  $^{51}\text{Fe}$ ,  $^{55}\text{Ni}$ , deduced Coulomb displacement energies. ]

### I. INTRODUCTION

Coulomb displacement energies have been employed in the past to deduce charge radii of nuclei. However, more direct measurements of nuclear charge radii have been provided in recent years by electron scattering and muonic x-ray data. In their review article,<sup>1</sup> Nolen and Schiffer pointed out that the nuclear charge radii extracted from Coulomb displacement energies were too small when compared with other more accurate data. Equivalently, if nuclear charge radii which were determined by electron scattering or muonic x-rays are employed to calculate Coulomb displacement energies, the calculated values are too small by 5–10% throughout the Periodic Table. Nolen and Schiffer pointed out that this discrepancy persists even when both the exchange and electromagnetic spin-orbit terms are included. Several theoretical papers have investigated other correction terms including vacuum polarization, higher order magnetic terms, the finite size of the proton, the proton-neutron mass difference, isospin mixing in the core, and charge symmetry breaking of the nuclear force.<sup>2–11</sup> Despite the refinements of the theoretical model, a solution to the problem has not been found.

The experimental results presented in this paper are of interest because they allow accurate determination of Coulomb displacement energies for the ground and a few excited states of the  $T = 1/2$  mirror nuclei throughout the  $1f_{7/2}$  nuclear subshell. Although the displacement energies between isobaric analog states in heavier nuclei are known, the present results include the heaviest known mirror nuclei. The displacement energy of a mirror pair is expected to depend only on the

Coulomb interaction and possibly a charge-symmetry-breaking nuclear force, i.e., a difference in the nuclear part of the  $p$ - $p$  and  $n$ - $n$  interactions. The displacement energy of a nonmirror isobaric analog pair may depend, in addition, upon a charge dependent nuclear force, i.e., a difference in the  $T = 1$ ,  $p$ - $n$  and  $n$ - $n$  interactions. As Sherr and Talmi have shown,<sup>11</sup> it may be possible to extract the  $p$ - $n$  and  $n$ - $n$  difference by comparing the displacement energies of  $T > 1/2$  analog pairs with those of the  $T = 1/2$  mirror pairs.

The results of the present experiment provide more accurate measurements of the ground state masses of  $^{43}\text{Ti}$ ,  $^{47}\text{Cr}$ ,  $^{51}\text{Fe}$ , and  $^{55}\text{Ni}$  than were obtained previously.<sup>12,13</sup> The accurate determination of the excitation energy of several levels in these nuclei provides the necessary data to extract Coulomb displacement energies of the  $J^\pi = 7/2^-, 3/2^+$ , and  $1/2^+$  levels for the  $T = 1/2$  mirror pairs. The angular distributions of these low cross-section reactions and comparison with the  $T_z = +1/2$  mirror nuclei provided evidence for the spin and parity assignments. The displacement energies of the  $1/2^+$  and  $3/2^+$  particle-hole states are compared with a model of Sherr and Bertsch,<sup>14</sup> and excellent agreement is found. However, the data show the same phenomenon which Nolen and Schiffer found in a wide range of nuclei.

### II. EXPERIMENTAL METHOD

The measurement of the reaction  $Q$  values was made by comparing the magnetic rigidity of the  $^6\text{He}$  particles from the reactions of interest with those from the  $^{27}\text{Al}(^3\text{He}, ^6\text{He})^{24}\text{Al}(\text{g.s.})$  and  $^{25}\text{Mg}(^3\text{He}, ^6\text{He})^{22}\text{Mg}(3.3082)$  reactions in a magnetic spectrograph. The  $Q$  values of the calibration re-



# High-spin states of $(fp)^2$ character in $^{34,35,36}\text{Cl}$ and $^{37,39}\text{Ar}^\dagger$

H. Nann, W. S. Chien, A. Saha, and B. H. Wildenthal

Cyclotron Laboratory and Department of Physics, Michigan State University, East Lansing, Michigan 48824

(Received 10 February 1977)

Angular distributions of the  $(\alpha, d)$  reaction on  $^{32,33,34}\text{S}$  and  $^{35,37}\text{Cl}$  have been measured at 40 MeV bombarding energy. High-spin states of  $(fp)^2$  character in the final nuclei were identified on the basis of their strength and characteristic  $L = 4$  and  $L = 6$  angular distributions. For some states, spin assignments are suggested. The properties of the high-spin states are discussed.

[NUCLEAR REACTIONS  $^{32,33,34}\text{S}, ^{35,37}\text{Cl}(\alpha, d); E = 40$  MeV; measured  $(E_d, \theta)$ ; enriched targets; deduced  $L$  transfer.]

## I. INTRODUCTION

Within the last several years increasing information about high-spin states at the onset of the  $fp$  shell has become available. These high-spin states were studied via  $\gamma$ -ray spectroscopy utilizing either heavy-ion induced fusion evaporation<sup>1,2</sup> or  $(\alpha, n)^{3,4}$  and  $(\alpha, p)^{5,6}$  reactions, experiments which typically yield information only about states along the yrast line.

In an effort to determine the possible configurations of these high-spin states, and beyond that to get information about high-spin states away from the yrast line, we have performed the  $(\alpha, d)$  reaction on  $^{32}\text{S}$ ,  $^{33}\text{S}$ ,  $^{34}\text{S}$ ,  $^{35}\text{Cl}$ , and  $^{37}\text{Cl}$ . Using the known selectivity of direct  $(\alpha, d)$  transfer reactions,<sup>7-9</sup> particularly the preferential transfer of the proton-neutron pair in a completely aligned configuration with maximum possible spin, high-spin states in  $^{34}\text{Cl}$ ,  $^{35}\text{Cl}$ ,  $^{36}\text{Cl}$ ,  $^{37}\text{Ar}$ , and  $^{39}\text{Ar}$  of

$$[(\text{target})_J \otimes (f_{7/2})^2_{J=7, T=0}]$$

and

$$[(\text{target})_J \otimes (f_{7/2} p_{3/2})_{J=5, T=0}]$$

configurations are located. The transitions to these states are characterized by  $L = 6$  and  $L = 4$  angular distributions, respectively. A preliminary account<sup>10</sup> of the present data concentrated upon identification of the highest spin states ( $\frac{17}{2}^+$ ) which can be reached via  $(f_{7/2})^2_{7,0}$  transfer on  $J^\pi = \frac{3}{2}^+$  targets.

## II. EXPERIMENTAL PROCEDURE AND RESULTS

A 40 MeV  $\alpha$ -particle beam from the Michigan State University cyclotron was used for carrying out the present experiments. The sulfur targets consisted of a layer of the enriched S isotopes sandwiched between layers of Formvar and carbon foils in order to inhibit evaporation during the bombardment. The chlorine targets were made by

evaporation of NaCl or LiCl onto a thin carbon backing. One difficulty with the Cl targets, however, was that some deuteron groups from the  $\text{Cl}(\alpha, d)\text{Ar}$  reaction coincided with groups from the contaminant  $\text{Na}(\alpha, d)\text{Mg}$  or  $\text{Li}(\alpha, d)\text{Be}$  reactions. In such cases, the results from the runs with the different targets were combined. Details of the targets are given in Table I. The target thicknesses were determined by measuring the elastic differential cross sections with the same experimental configurations as used for the transfer measurements and normalizing these data to calculations with standard optical-model parameters. A silicon detector placed in the scattering chamber allowed continuous monitoring of the target conditions. The reaction products were detected in the focal plane of an Enge split-pole magnetic spectrograph with a proportional-counter plastic-scintillator combination.

Deuteron spectra from the various targets are shown in Fig. 1. The resolution obtained was between 40 and 60 keV, full width at half maximum. Although the known level densities in the excitation energy regions of interest are quite high,<sup>11</sup> only a few states are observed to be strongly excited. In some cases the observed levels are considerably above the threshold for particle emission. For example, in  $^{35}\text{Cl}$  the strongest excited

TABLE I. Target details.

Target	Thickness ( $\mu\text{g}/\text{cm}^2$ )	Isotopic abundance
$^{32}\text{S}$	110	99.9% $^{32}\text{S}$
$^{33}\text{S}$	15	22.3% $^{32}\text{S}$ , 76.8% $^{33}\text{S}$ , 0.9% $^{34}\text{S}$
$^{34}\text{S}$	140	9.6% $^{32}\text{S}$ , 0.4% $^{33}\text{S}$ , 90.0% $^{34}\text{S}$
$\text{Li}^{35}\text{Cl}$	56	99.4% $^{35}\text{Cl}$ , 0.6% $^{37}\text{Cl}$
$\text{Na}^{35}\text{Cl}$	95	99.4% $^{35}\text{Cl}$ , 0.6% $^{37}\text{Cl}$
$\text{Li}^{37}\text{Cl}$	45	3.9% $^{35}\text{Cl}$ , 96.1% $^{37}\text{Cl}$
$\text{Na}^{37}\text{Cl}$	74	4.0% $^{35}\text{Cl}$ , 96.0% $^{37}\text{Cl}$

## Calculation of recoil-order matrix elements for the beta decays of $^{20}\text{F}$ and $^{20}\text{Na}^\dagger$

Frank P. Calaprice\*

*Department of Physics, Princeton University, Princeton, New Jersey 08540*

W. Chung and B. H. Wildenthal

*Cyclotron Laboratory, Michigan State University, East Lansing, Michigan 48824*

(Received 1 November 1976)

The matrix elements which affect the shapes of the  $\beta$  spectra and the  $\beta$ - $\gamma$  angular correlations are calculated for the  $^{20}\text{F}$ - $^{20}\text{Na}$  mirror Gamow-Teller decays to the 1634 keV level of  $^{20}\text{Ne}$ . The dominant effects are due to the weak-magnetism and the axial-vector tensor form factors. Matrix elements relevant to the  $\beta$ - $\alpha$  correlations for other  $^{20}\text{Na}$  decays are also evaluated, with similar conclusions.

[ RADIOACTIVITY  $^{20}\text{F}$ ,  $^{20}\text{Ne}$ ,  $^{20}\text{Na}$ , calculated  $\beta$  decay form factors,  $M1$ ,  $E2$  matrix elements; predict  $\beta$  spectrum shape,  $\beta$ - $\gamma$  and  $\beta$ - $\alpha$  angular correlations. ]

### I. INTRODUCTION

Some of the best tests for the presence of the second-class<sup>1</sup> weak interaction involve measurements of certain angular correlations<sup>2</sup> in nuclear  $\beta$  decay. The  $\beta$ - $\gamma$  correlations for the mirror Gamow-Teller decays of the mass-20 system are particularly interesting in this respect, because of the relative simplicity of the decay schemes and the large energies released.

To first order in recoil, the  $\beta$ - $\gamma$  correlation depends on a linear combination of the weak magnetism and the axial-vector tensor form factors. For  $\Delta T = 1$  decays the form factors are each, in principle, combinations of first and second class components. Thus to determine the second class tensor term it is usually necessary to invoke the conserved vector current (CVC) theory to determine the weak magnetism form factor and to combine the  $\beta$ - $\gamma$  correlations of mirror  $e^+$  and  $e^-$  decays to eliminate the first-class tensor form factor. To higher order in recoil, other form factors also contribute and the procedure of isolating second-class contributions becomes a little more complicated. In order to assess the importance of these higher order form factors in the case of the  $A = 20$  decays, we have evaluated them with nuclear shell model wave functions.

Our procedure is to utilize the relationships between the nuclear form factors and matrix elements of one-body operators, which are given by the impulse approximation.<sup>2</sup> While the validity of the impulse approximation can be questioned for these higher order terms, there is evidence that the extended shell model is adequate for calculating the matrix elements. Within the limitations of

this procedure we evaluate the form factors and their effect on the  $\beta$ - $\gamma$  correlations. In addition, we calculate the shapes of the  $\beta$  spectra with the goal of assessing the possibility of determining the weak magnetism form factor from the spectrum shape. Finally, we have attempted to present these results for  $A = 20$  in a thoroughly detailed context so that comparable analyses in other  $sd$  shell nuclei can be carried out in a straightforward fashion from other nuclear wave functions.

### II. DISCUSSION OF DECAY PROCESS

A simplified version of the mass-20 decay scheme is illustrated in Fig. 1. The decay rate for unpolarized nuclei for a process in which the  $\beta$  particle is detected in coincidence with the delayed  $E2$   $\gamma$  ray (spins and neutrino unobserved) is given by the following<sup>2</sup>:

$$d\lambda = \frac{G_V^2 \cos^2 \theta_C}{2(2\pi)^5} F_0(Z, E) p E (E_0 - E)^2 dE d\Omega_\beta d\Omega_\gamma \\ \times [G_0(E) + \Delta_1(E)(p/E) \cos \theta \\ + \frac{1}{2} G_2(E)(p/E)^2 (\cos^2 \theta - \frac{1}{3})]. \quad (1)$$

In the above,  $p$  and  $E$  are the  $\beta$  momentum and total energy, respectively,  $G_V$  and  $\theta_C$  are the vector coupling constant and Cabibbo angle,  $F_0$  is the point charge Fermi function, and  $\theta$  is the angle between the  $\beta$  and  $\gamma$  particle directions. The spectral functions  $G_0(E)$ ,  $\Delta_1(E)$ , and  $G_2(E)$  for Gamow-Teller decays are given by the following:

## AN ENERGY-DEPENDENT LANE-MODEL NUCLEON-NUCLEUS OPTICAL POTENTIAL<sup>†</sup>

D. M. PATTERSON<sup>††</sup>, R. R. DOERING and AARON GALONSKY

*Cyclotron Laboratory, Physics Department, Michigan State University, East Lansing, Michigan 48824  
USA*

Received 13 January 1976

**Abstract:** An energy-dependent Lane-model nucleon-nucleus optical potential is presented. The isovector strength parameters of the potential have been determined by fitting (p, n) IAS angular-distribution data between 25 and 45 MeV for targets from <sup>48</sup>Ca to <sup>208</sup>Pb. The isoscalar strength parameters have been obtained by requiring that the Lane-model potential reproduce the Becchetti-Greenlees Coulomb-corrected proton potential. The energy associated with the proton in all energy-dependent parts of the potential is reduced by the average Coulomb potential inside the nucleus. The main result of the parameter search, other than determining the strength of the isovector energy dependence, is to redistribute the isovector strength found by Becchetti and Greenlees between the real-volume and imaginary-surface terms. The Lane-model optical potential so obtained is reasonably successful in reproducing (p, p), (p, n) IAS, and (n, n) scattering over a wide mass and energy range.

E NUCLEAR REACTIONS <sup>48</sup>Ca, <sup>90</sup>Zr, <sup>120</sup>Sn, <sup>208</sup>Pb(p, n),  $E = 25, 35, 45$  MeV; analyzed previously measured IAS  $\sigma(\theta)$ ; deduced energy-dependent isovector parameters. <sup>27</sup>Al, Fe, Sn, <sup>209</sup>Bi(n, n),  $E = 7.0, 14, 24$  MeV; calculated  $\sigma(\theta)$ .

### 1. Introduction

It has been pointed out by Lane<sup>1)</sup> that the nuclear optical potential may be written in a charge-independent form. Such a potential may be used not only to describe both proton and neutron elastic scattering from nuclei, but also the (p, n) reaction to the isobaric analog of the target ground state (IAS). The Lane-model optical potential may be written as

$$U = -U_0 + 4U_1 (\mathbf{t} \cdot \mathbf{T})/A, \quad (1)$$

where  $\mathbf{t}$  and  $\mathbf{T}$  are the nucleon and nucleus isospins, respectively,  $A$  is the mass number of the nucleus, and  $U_0$  and  $U_1$  are functions that do not depend upon isospin in the isospin-independent and isospin-dependent parts of the potential, respectively. The functions  $U_0$  and  $U_1$  should, in general, depend upon relative position and momentum<sup>2-9)</sup>, and both may be complex<sup>7-12)</sup>. If a sufficiently general parameterization of the Lane-model optical potential were available, one would be able to calculate

<sup>†</sup> Supported by the National Science Foundation and the Office of Naval Research.

<sup>††</sup> Present address: Fusion Research Center, University of Texas, Austin, Texas 78712.

## A HIGH RESOLUTION STUDY OF $^{26}\text{Al}$ VIA THE (p, d) REACTION†

D. L. SHOW, B. H. WILDENTHAL, J. A. NOLEN, Jr. and E. KASHY

*Cyclotron Laboratory and Department of Physics, Michigan State University, East Lansing, Michigan  
48824*

Received 13 February 1976

**Abstract:** Excitation energies and angular distributions of  $^{26}\text{Al}$  levels in the first 6 MeV of excitation have been measured with the  $^{27}\text{Al}(p, d)^{26}\text{Al}$  reaction at  $E_p = 35$  MeV. Deuteron spectra were analyzed with an Enge split-pole magnetic spectrograph and recorded on nuclear emulsions (experimental resolution  $\approx 6$  keV, FWHM); supplementary data were recorded with position-sensitive wire proportional counters. The angular distributions were analyzed with the DWBA to extract the  $l$ -values and associated spectroscopic factors of the neutron transfers. The results for excitation energies,  $l$ -values, spectroscopic factors, and values of  $J^\pi$ ,  $T$  are discussed in terms of previous experimental and theoretical work and in the light of new shell-model calculations for this system.

E NUCLEAR REACTION  $^{27}\text{Al}(p, d)$ ,  $E = 35$  MeV; measured  $\sigma(E_d, \theta)$ ,  $^{26}\text{Al}$  deduced levels,  $L$ ,  $J$ ,  $\pi$ ,  $S$ . Magnetic spectrograph.

### 1. Introduction

The structure of the energy levels of  $^{26}\text{Al}$  is enigmatic. In terms of the simplest shell model, based on an  $^{16}\text{O}$  core, the active system consists of five protons and five neutrons, each in the  $d_{5/2}$  orbit. In such a model,  $^{26}\text{Al}$  could be treated as coupling of single neutron and proton holes in the  $d_{5/2}$  orbit. However, there is no simple relationship between the lowest observed states of  $^{26}\text{Al}$  and those of its particle conjugate in the  $d_{5/2}^n$  model,  $^{18}\text{F}$  [ref. 1)]. Simple rotational-model schemes 2) fare no better than the simplest shell-model analysis and the addition of considerable complexity to the rotational model, by considering several bands and extensive band-mixing via Coriolis coupling, still fails to yield a viable explanation of this system 3). Shell-model calculations which involve both the  $d_{5/2}$  and  $s_{1/2}$  orbits 4) and which quantitatively explain many features of the  $A = 20$ –28 region still fail to give even a qualitative representation of the  $T = 0$  part of the level structure of  $^{26}\text{Al}$ . In doubly odd, self-conjugate nuclei such as  $^{26}\text{Al}$ ,  $T = 1$  levels both occur in the first few MeV of excitation. The isobaric analogues of the  $T = 0$  and  $T = 1$  levels of  $^{26}\text{Al}$  which occur in  $^{26}\text{Mg}$  have been studied in some detail 5), and while the  $A = 20$ –28 shell-model analysis of ref. 4) can explain some features of this subset of levels, particularly the

† Research supported by the US National Science Foundation.

## WEAK INTERACTIONS IN DEUTERONS: EXCHANGE CURRENTS AND NUCLEON-NUCLEON INTERACTION

F. DAUTRY, M. RHO and D. O. RISKA<sup>†</sup>

*Service de Physique Théorique, Centre d'Etudes Nucléaires de Saclay, BP no. 2, 91190 Gif-sur-Yvette, France*

Received 19 January 1976

**Abstract:** While the meson-exchange electromagnetic current has been tested with an impressive success in the two-nucleon system, nothing much is known about the reliability of the exchange currents in weak interactions. We study this question using muon absorption in the deuteron,  $\mu^- + d \rightarrow n + n + \nu$ . The meson-exchange current, previously derived in parallel to those of the electromagnetic interaction, is checked for consistency against the p-wave piece of the  $p + p \rightarrow d + \pi^+$  process near threshold and then tested with the total capture rate for which some (though not so accurate) data are available. We then use the same Hamiltonian to calculate the matrix elements for the solar neutrino processes  $p + p \rightarrow d + e^+ + \nu$  and  $p + p + e^- \rightarrow d + \nu$  in the hope that they would be measured and help resolve the solar neutrino puzzle. Finally we make a detailed analysis of the differential capture rate  $d\Gamma/dE_n$ ,  $E_n$  being the kinetic energy in the c.m. of the two neutrons, in the expectation that it will be used to pin down the ever elusive n-n scattering length.

### 1. Introduction

It is now established beyond doubt that the meson-exchange currents account for most, if not all, of the 10% discrepancy in the np capture  $n + p \rightarrow d + \gamma$  at thermal neutron energy<sup>1)</sup> and in addition correctly explain the data for electrodisintegration of the deuteron at larger momentum transfer<sup>2)</sup>. The main reason for this success is that the principal part of the exchange currents is essentially given by low-energy theorems, the small remainder arising predominantly from the  $\Delta(1232)$  contribution<sup>3)</sup>. Although a similar low-energy theorem based on the PCAC plays an important role in extracting the meson-exchange weak currents<sup>3)</sup>, no one has yet done a truly convincing calculation to assess how good these currents are. Many calculations<sup>3,4)</sup> have been made on the triton beta decay; however because of the complications that are inherently three-body, we cannot be sure whether a success or failure is to be attributed to the exchange currents. It seems thus best to resort to a two-body system as in the electromagnetic case. The only two-body process that is feasible in the laboratory is

$$\mu^- + d \rightarrow n + n + \nu, \quad (1.1)$$

where the absorption occurs with the muon at rest. Some data are already available<sup>5)</sup> for the total capture rate  $\Gamma_{\text{tot}}$  and more precision measurements are in progress.

<sup>†</sup> Department of Physics, Michigan State University, East Lansing, Michigan 48824.

## THE LEVEL STRUCTURE OF $^{191}\text{Pt}$ FROM THE DECAY OF 3.2 h $^{191}\text{Au}$

M. PIIPARINEN†, S. K. SAHA and P. J. DALY

Chemistry Department, Purdue University, W. Lafayette, Indiana 47907, USA††

and

T. L. KHOO, C. L. DORS and F. M. BERNTHAL

Departments of Chemistry and Physics and Cyclotron Laboratory,  
Michigan State University, East Lansing, Michigan 48824, USA†††

Received 1 March 1976

**Abstract:** Levels of  $^{191}\text{Pt}$  populated in the decay of 3.2 h  $^{191}\text{Au}$  have been investigated by  $\gamma$ -ray singles and comprehensive  $\gamma$ - $\gamma$  coincidence measurements. A detailed  $^{191}\text{Au}$  decay scheme, which differs radically from earlier versions, has been established. The  $^{191}\text{Au}$  decay results are discussed with reference to those obtained in complementary ( $\alpha$ ,  $3n\gamma$ ) studies of odd- $A$  Pt nuclei and with particular emphasis on the locations and properties of low-spin members of the  $\nu_{1/2}^+$  level family in  $^{191}\text{Pt}$ .

E RADIOACTIVITY  $^{191}\text{Au}$  [from  $^{191}\text{Ir}(\alpha, 4n)$ ]; measured  $E_\gamma$ ,  $I_\gamma$ ,  $\gamma\gamma$ -coin.  $^{191}\text{Pt}$  deduced levels,  $J$ ,  $\pi$ , ICC. Enriched target, Ge(Li) detectors.

### 1. Introduction

During the course of extensive investigations of the  $^{186-194}\text{Pt}$  level structures by means of ( $\alpha$ ,  $xn$ ) in-beam  $\gamma$ -ray spectroscopy<sup>1,2</sup>, several fruitless attempts were made to discover some connections between the  $^{191}\text{Pt}$  levels strongly populated in the  $^{190}\text{Os}(\alpha, 3n)$  reaction and the low-lying  $^{191}\text{Pt}$  levels reported in earlier radioactivity studies<sup>3</sup>). In an effort to remedy this unsatisfactory and puzzling situation, we undertook a reinvestigation of the EC decay of 3.2 h  $^{191}\text{Au}$  ( $J^\pi = \frac{3}{2}^+$ ). We were hopeful that the decay study would also extend our knowledge of the  $\nu_{1/2}^+$  level family in  $^{191}\text{Pt}$  by locating low-spin family members not detectably populated in the ( $\alpha$ ,  $3n$ ) reaction.

The most notable previous study of the  $^{191}\text{Au}$  decay was that of Johansson *et al.*<sup>4</sup>), who performed comprehensive conversion electron measurements and some coincidence determinations; the  $^{191}\text{Au}$  decay scheme presented in ref. 3) is based on their results. Surprisingly, there has been no earlier high resolution  $\gamma$ -ray study of the  $^{191}\text{Au}$  decay.

† Present address: Department of Physics, University of Jyväskylä, Finland.

†† Work supported by the US ERDA.

††† Work supported by the US ERDA and the NSF.

A SURVEY OF THE ( $^3\text{He}$ ,  $^7\text{Be}$ ) REACTION AT 70 MeV†

W. F. STEELE, P. A. SMITH and J. E. FINCK

Cyclotron Laboratory, Michigan State University, East Lansing, Michigan 48824

and

G. M. CRAWLEY

Physics Department and Cyclotron Laboratory, Michigan State University, East Lansing, Michigan 48824

and

Nuclear Physics Department, Australian National University, Canberra, Australia

Received 2 October 1975

**Abstract:** A study of the ( $^3\text{He}$ ,  $^7\text{Be}$ ) reaction has been undertaken using a 70 MeV  $^3\text{He}$  beam. By surveying a wide range of target nuclides, namely  $^{12,13}\text{C}$ ,  $^{16}\text{O}$ ,  $^{24,26}\text{Mg}$ ,  $^{40,42,44}\text{Ca}$ ,  $^{58,60,62,64}\text{Ni}$ ,  $^{90}\text{Zr}$ ,  $^{120,124}\text{Sn}$ ,  $^{144}\text{Sm}$  and  $^{206}\text{Pb}$ , systematics of the  $\alpha$ -clustering phenomenon were investigated. In addition, masses and energy levels of  $^{60}\text{Fe}$  and  $^{120}\text{Cd}$  were measured. The  $^7\text{Be}$  particles were detected in a single wire proportional counter backed by a plastic scintillator in the focal plane of an Enge spectrometer to ensure adequate particle identification. Total energy resolution as small as 140 keV full width at half maximum was obtained, although in most cases the target thickness limited the energy resolution to larger values. Differential cross sections as low as 20 nb/sr were measured. The finite range programs LOLA and LOLITA were used to calculate differential cross sections for comparison to data, assuming the reaction to proceed by a direct  $\alpha$ -transfer. The spectroscopic factors which were extracted show a marked decrease with increasing atomic mass number, implying a decrease in surface  $\alpha$ -clustering for heavier nuclei.

NUCLEAR REACTIONS  $^{12,13}\text{C}$ ,  $^{16}\text{O}$ ,  $^{24,26}\text{Mg}$ ,  $^{40,42,44}\text{Ca}$ ,  $^{58,60,62,64}\text{Ni}$ ,  $^{90}\text{Zr}$ ,  $^{120,124}\text{Sn}$ ,  $^{144}\text{Sm}$ ,  $^{206}\text{Pb}$  ( $^3\text{He}$ ,  $^7\text{Be}$ ),  $E = 70.0$  MeV; measured  $\sigma(\theta)$ ; deduced  $S_\alpha$ .  $^{60}\text{Fe}$ ,  $^{120}\text{Cd}$  deduced mass excess.  $^8,^9\text{Be}$ ,  $^{12}\text{C}$ ,  $^{20,22}\text{Ne}$ ,  $^{36,38,40}\text{Ar}$ ,  $^{54,56,58,60}\text{Fe}$ ,  $^{86}\text{Sr}$ ,  $^{116,120}\text{Cd}$  deduced levels.

## 1. Introduction

Various attempts have been made to measure the amount of  $\alpha$ -clustering on the nuclear surface both by  $\text{K}^-$  meson capture experiments <sup>1, 2</sup>) and by ( $\alpha$ ,  $2\alpha$ ) reactions <sup>3</sup>). The results of these experiments are still inconclusive.

Another approach has been to look for  $\alpha$ -cluster transfer reactions. If reactions which transfer two protons and two neutrons like ( $^6\text{Li}$ , d) ( $^7\text{Li}$ , t) (d,  $^6\text{Li}$ ) or ( $^3\text{He}$ ,  $^7\text{Be}$ ) can be shown to proceed predominantly as the direct transfer of an  $\alpha$ -cluster, then reaction calculations might allow the extraction of  $\alpha$ -particle spectroscopic factors which may be taken as an indication of  $\alpha$ -clustering. For example, Gutbrat, Yoshida and Bok <sup>4</sup>), and Martin *et al.* <sup>5</sup>) have extracted  $\alpha$ -spectroscopic factors using the (d,  $^6\text{Li}$ ) reaction. However, the direct character of the (d,  $^6\text{Li}$ ) reaction is

† Work supported by the National Science Foundation.

**A COUPLED-CHANNEL BORN APPROXIMATION ANALYSIS  
OF  $^{22}\text{Ne}(p, t)^{20}\text{Ne}$  AND  $^{24}\text{Mg}(p, t)^{22}\text{Mg}$   
USING SHELL-MODEL WAVE FUNCTIONS†**

C. H. KING, M. A. M. SHAHABUDDIN and B. H. WILDENTHAL  
*Cyclotron Laboratory, Michigan State University, East Lansing, Michigan 48824*

Received 3 February 1976

**Abstract:** Coupled-channel Born approximation calculations for the reactions  $^{22}\text{Ne}(p, t)^{20}\text{Ne}$  and  $^{24}\text{Mg}(p, t)^{22}\text{Mg}$  to the  $0^+$ ,  $2^+$  and  $4^+$  members of the ground-state rotational bands have been carried out. The two-nucleon transfer spectroscopic amplitudes were determined from shell-model wave functions, the calculation of inelastic excitations was based on the collective model, and the reaction space was limited to the first  $0^+$ ,  $2^+$  and  $4^+$  states in each nucleus. The measured cross sections in the case of  $^{22}\text{Ne}(p, t)$  are reasonably well described by this model. However, significant deviations were observed between the calculated cross sections and the experimental data for the  $^{24}\text{Mg}(p, t)$  transitions to the  $2^+$  and  $4^+$  states. These discrepancies are possibly attributable to multistep processes involving higher-lying states in  $^{24}\text{Mg}$  not included in the reaction space. The effects on the calculations of other possible inadequacies of the reaction model and uncertainties in the parameters of this model are discussed.

### 1. Introduction

Considerable effort has been devoted in recent years toward achieving improved wave functions in a shell-model basis for the states of nuclei in the  $A = 16$ –40 region. Transfer-reaction experiments are a potentially useful tool for testing the quality of such wave functions, since the measured cross sections should be directly related to the overlaps between the wave functions of the initial and final states as long as only direct, one-step reaction processes are significant. Unfortunately, it is questionable whether a one-step reaction model is applicable to transfer reactions on the highly collective nuclei in the middle of this region. In fact, increasing evidence seems to indicate that multistep processes involving inelastic excitations of the collective states are an essential component of such reactions.

When multistep effects are important, it is necessary to replace the usual analysis based on the distorted-wave Born approximation (DWBA) with one using the coupled-channel Born approximation (CCBA). This necessarily complicates the relation between the theoretical wave function and the experimental cross sections, since any one cross section will depend coherently on matrix elements connecting several states in the initial and final nuclei while the DWBA requires only one. In particular, matrix elements between the wave functions of all states coupled strongly

† Work supported by the US National Science Foundation.



**A MEASUREMENT OF  $\Gamma_{\text{rad}}/\Gamma$   
FOR THE 7.654 MeV STATE OF  $^{12}\text{C}$   
AND THE RATE OF THE STELLAR  $3\alpha$  REACTION†**

R. G. MARKHAM, SAM M. AUSTIN and M. A. M. SHAHABUDDIN

*Cyclotron Laboratory and Physics Department, Michigan State University, East Lansing, Michigan  
48824*

Received 20 April 1976

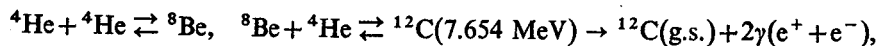
**Abstract:** The branching ratio  $\Gamma_{\text{rad}}/\Gamma$  for the radiative de-excitation of the 7.654 MeV,  $0^+$  state in  $^{12}\text{C}$  has been measured. Coincidences between  $\alpha$ -particles from  $^{12}\text{C}(\alpha, \alpha')^{12}\text{C}(7.654 \text{ MeV})$  and recoil  $^{12}\text{C}$  ions at the proper energy and angle were the signature of radiative decay. Conservative techniques were used throughout to avoid the need for large corrections. A value of  $\Gamma_{\text{rad}}/\Gamma = (3.87 \pm 0.25) \times 10^{-4}$  was obtained in good agreement with other recent results but substantially higher than the previously accepted value of  $(2.9 \pm 0.3) \times 10^{-4}$ . Available results are reviewed and a recommended value of  $\Gamma_{\text{rad}}/\Gamma$  is presented. The implication of this result for the rate of the  $3\alpha$  process in stellar helium burning is discussed and a recommended reaction rate is presented.

**E** NUCLEAR REACTIONS  $^{12}\text{C}(\alpha, \alpha')$ ,  $E = 40.2 \text{ MeV}$ ; measured  $\alpha'$   $^{12}\text{C}$ -coin, recoil  $^{12}\text{C}(\theta)$ .  $^{12}\text{C}$  7.654 MeV level deduced  $\Gamma_{\text{rad}}/\Gamma$ . Stellar helium burning. Enriched target.

### 1. Introduction

After hydrogen has been converted to  $^4\text{He}$  in the core of a star, the core contracts until temperatures sufficient to fuse  $^4\text{He}$  into  $^{12}\text{C}$  via the  $3\alpha$  reaction are reached. The  $^{12}\text{C}(\alpha, \gamma)^{16}\text{O}$  reaction then converts part of the  $^{12}\text{C}$  to  $^{16}\text{O}$ , the extent of the conversion depending on the relative rates of the two reactions. When the  $3\alpha$  reaction is relatively fast,  $^{12}\text{C}$  is the main product of helium burning; and when it is relatively slow,  $^{16}\text{O}$  is dominant<sup>1</sup>). Since the subsequent evolution of a star greatly depends on the ratio of  $^{12}\text{C}$  to  $^{16}\text{O}$  in the ashes of helium burning, it also depends in effect on a knowledge of the rates of the  $3\alpha$  and  $^{12}\text{C}(\alpha, \gamma)^{16}\text{O}$  reactions. The rate of the latter reaction is still rather uncertain<sup>2</sup>) and as we shall see recent measurements have cast doubt on the  $3\alpha$  rate as well.

In the  $3\alpha$  reaction  $^4\text{He}$  is converted into  $^{12}\text{C}$  via a two stage process



where the arrows denote an equilibrium situation. The rate  $P_{3\alpha}$  for this process depends on the  $Q$ -value of the reaction and the width  $\Gamma_{\text{rad}}$  for  $\gamma$ -ray plus pair decay

† Research supported by the US National Science Foundation.

## THE $\pi\omega$ MESON EXCHANGE CONTRIBUTION TO THE NUCLEON-NUCLEON INTERACTION

D. O. RISKA †

*Department of Physics and Cyclotron Laboratory, Michigan State University, East Lansing,  
Michigan 48824*

Received 8 June 1976

**Abstract:** The  $\pi\omega$  exchange contribution to the NN interaction is calculated. The spin-independent central and the spin-orbit components of the resulting interaction are found to be negligible compared to the corresponding components of the single  $\omega$ -meson exchange interaction. The tensor and spin-spin components due to  $\pi\omega$  exchange are of the same order of magnitude as the corresponding components due to single  $\omega$ -exchange.

### 1. Introduction

Recently models for the nucleon-nucleon (NN) interaction based on combinations of single-meson exchange and two-pion exchange mechanisms which give “almost” satisfactory results for the two-nucleon scattering phase parameters in the low energy region have been presented<sup>1,2</sup>). In those models the most important contributions apart from the one-pion exchange (OPE) and two-pion exchange (TPE) contributions are those due to exchange of the  $\rho$ - and  $\omega$ -vector mesons. Of course such meson exchange models also have to be amended to include a suitable phenomenological high momentum damping factor or alternatively a repulsive short range contribution.

While the  $\rho$ -meson exchange contribution is included with the two-pion exchange contribution, the  $\rho$ -meson being a two-pion resonance, the  $\omega$ -meson exchange contribution is added as a separate pole term to the NN amplitude. A certain cause for uncertainty resides in the interpretation of the  $\omega$ -nucleon coupling constant  $g_\omega$  that describes the strength of the  $\omega$ -pole term. In the first place it is not easy to separate the effect of the  $\omega$ -exchange contribution from that of the phenomenological high momentum damping factor (presumably describing more complicated exchange mechanisms), unless the mass scale of the cut-off factor is considerably larger than that of the vector meson mass. The common situation is thus that one has a trade-off between the repulsion due to the  $\omega$ -exchange contribution and that due to high momentum damping factors. If thus the  $\omega$ N coupling constant  $g_\omega$  is used as a free parameter one should not expect that the best fit to NN scattering data is obtained for that value of  $g_\omega$  which corresponds to the true  $\omega$ N coupling strength as some of

† Supported in part by the National Science Foundation.

## PION EXCHANGE CURRENTS AND NUCLEAR CHARGE FORM FACTORS<sup>†</sup>

MARK RADOMSKI and D. O. RISKA

*Department of Physics and Cyclotron Laboratory, Michigan State University, East Lansing,  
Michigan 48824*

Received 9 April 1976

**Abstract:** The effect of the pion exchange current due to the Born term in the photoproduction amplitude on the charge form factors and distributions of  ${}^4\text{He}$ ,  ${}^{16}\text{O}$  and  ${}^{40}\text{Ca}$  is calculated in the simple harmonic oscillator shell model. The exchange current contribution is most notable in the case of the  $\alpha$ -particle while it is rather unimportant in  ${}^{16}\text{O}$  and  ${}^{40}\text{Ca}$ . The contribution to the nuclear mean square radius is small ( $\approx 0.03 \text{ fm}^2$ ) and roughly independent of the mass number.

### 1. Introduction

It has recently been noted that pion exchange currents have a large effect on the charge form factors of the lightest nuclei ( $A \leq 4$ )<sup>1-3</sup> at relatively small values of momentum transfer ( $\geq 3 \text{ fm}^{-1}$ ). This observation raises several questions, as for example how well one can quantitatively calculate these exchange current contributions and how important such effects are in the case of heavier nuclei. The first of these two questions will eventually be decided by comparing experimental data for the charge form factors with the predictions obtained with the present models for the exchange current operators in conjunction with realistic wave functions for the few-nucleon bound states. We note in passing that a definite theoretical analysis is presently hindered by the absence of data on the deuteron charge form factor. The second question above is relatively simpler to answer, at least preliminarily, by explicit calculation of the exchange current contributions to the charge form factors of heavier nuclei. In this paper we present the results of such calculations.

The pion exchange current contributions to the charge form factors of the doubly closed shell nuclei  ${}^4\text{He}$ ,  ${}^{16}\text{O}$  and  ${}^{40}\text{Ca}$  are calculated using simple harmonic oscillator wave functions. The results indicate that, while the exchange currents are relatively unimportant at low momentum transfer, their effects rapidly increase with momentum transfer so as to give rise to corrections of the order 25% at  $10 \text{ fm}^{-2}$ . In the case of the  $\alpha$ -particle, the effect of the pion exchange current considered here is even more important, in agreement with the findings of Borysowicz and Riska<sup>3</sup>).

<sup>†</sup> Research supported by the National Science Foundation.

## THE TIME-DEPENDENT SINGLE-PARTICLE METHOD FOR QUASIELASTIC HEAVY ION COLLISIONS†

G. BERTSCH

*Physics Department, Michigan State University, East Lansing, Michigan 48824*

and

R. SCHAEFFER

*Centre d'Etude Nucléaire de Saclay, 91190 Gif-sur-Yvette, France*

Received 26 May 1976

(Revised 7 September 1976)

**Abstract:** The dynamics of heavy ion collisions are modeled by solving the time-dependent Schrödinger equation for potential wells moving on classical trajectories. We find that particle transfer is much more likely than particle excitation in the same nucleus. This is at variance with most experiments, and the likely reason is that the model neglects collective enhancements of low excitations. It is found that the DWBA underestimates the weak transitions by large factors. For the moderately strong transitions where the magnitude is correct, the phases can be significantly different. The observed anomalous of  $^{18}\text{O}(0^+ \rightarrow 2^+)$  correlates with the  $d \rightarrow 1s$  phase obtained in this calculation. We achieve quantitative agreement with experiment for one- and two-particle transfer. For grazing collisions of  $^{18}\text{O}$  and Sn at 100 MeV, the average energy loss is quite small, supporting the adiabatic picture of the single-particle degrees of freedom. For the earliest stages of the collision the single-particle dynamics can be easily characterized classically. However, at late stages of the collision a classical treatment does not give accurate velocities or transfer probabilities for the particles.

### 1. Introduction

There is a great interest in heavy ion collisions, with a wealth of experimental data now available. But there is as yet no theoretical framework to build an understanding of the data, especially at the higher energies where measurements are not of specific final states, but are averages over many final states. A promising method to appear is the time-dependent Hartree-Fock calculation<sup>1)</sup>. This describes not only single-particle behavior but also collective oscillations at low energies. However, the method is technically difficult to apply to three-dimensional geometry and much of the physics may well be contained in the time-dependent Schrödinger equation, without demanding Hartree-Fock self-consistency. With this in mind we shall investigate the consequences of the time-dependent single-particle model where the single-particle Hamiltonian is solved for colliding potential wells. Calculations of heavy ion reactions in this spirit were first attempted by Breit *et al.*<sup>2)</sup>. The approach of treating one aspect of the collision classically and another quantum mechanically has been exploited for inelastic as well as for transfer reactions by Broglia and Winther<sup>3)</sup>. The difference is

† Research supported by the National Science Foundation.

## ROTATIONAL AND INTRINSIC STRUCTURE OF $^{182}\text{W}$ FROM THE $(\alpha, 2n\gamma)$ REACTION AND DECAY OF $^{182\text{m}}\text{Re}$ †

B. D. JELTEMA, F. M. BERNTHAL<sup>††</sup>, T. L. KHOO  
and C. L. DORS

Departments of Chemistry and Physics and Cyclotron Laboratory, Michigan State University,  
East Lansing, Michigan 48824

Received 8 November 1976

**Abstract:** The  $^{180}\text{Hf}(\alpha, 2n\gamma)$  reaction was used to populate states in  $^{182}\text{W}$ . In-beam  $\gamma$ -ray spectroscopy experiments result in assignment of 59 levels to the  $^{182}\text{W}$  level scheme. Eleven rotational bands are identified, and most of these are characterized. A previously reported 1.4  $\mu\text{s}$  isomer is characterized as the  $K^\pi = 10^+$  triplet coupling of  $\frac{3}{2}^+$  [624] and  $\frac{5}{2}^+$  [615] neutrons, the first seniority two  $i_{1/2}$  configuration to be identified in the rare-earth deformed region. The strongly coupled band built on this isomer apparently becomes *yrast* above spin 16. Data from EC  $\beta^+$  decay of 64 h  $^{182\text{m}}\text{Re}$  were used to supplement the in-beam data.

E

NUCLEAR REACTION  $^{180}\text{Hf}(\alpha, 2n\gamma)$ ,  $E = 26$  MeV; measured  $E_\gamma$ ,  $I_\gamma(\theta)$ ,  $I_\gamma$  vs.  $E_\alpha$ ,  $\alpha\gamma$ -delay,  $\gamma\gamma$ -coin.  $^{182}\text{W}$  deduced levels  $J$ ,  $\pi$ ,  $\gamma$ -branching,  $K$ ,  $g_K$ . Ge(Li) detectors. Enriched target. RADIOACTIVITY  $^{182\text{m}}\text{Re}$  [from  $^{181}\text{Ta}(\alpha, 3n)$ ;  $E = 41$  MeV]; measured  $E_\gamma$ ,  $I_\gamma$ ,  $\gamma\gamma$ -coin; deduced  $\log ft$ .  $^{182}\text{W}$  deduced levels,  $J$ ,  $\pi$ . Natural target, Ge(Li) detectors.

### 1. Introduction

The level structure of  $^{182}\text{W}$  has been investigated extensively in  $\beta$ -decay and transfer reaction studies, but except for a half-life measurement of an  $I^\pi = 10^+$  isomeric state<sup>1)</sup>, the high-spin structure is essentially unknown. The  $(\alpha, 2n)$  reaction can transfer twelve or more units of angular momentum, so that in-beam  $\gamma$ -ray spectroscopy is expected to yield significant new information on the band structure of intrinsic and collective states in  $^{182}\text{W}$ .

We report in this paper the results of  $(\alpha, 2n\gamma)$  experiments on  $^{182}\text{W}$ . This nucleus is of interest for several reasons. A number of high- $\Omega$  orbitals are expected to lie near the Fermi surface in  $^{182}\text{W}$ . These should give rise to several low-lying, high- $K$  two-quasiparticle states, some of which are expected to be isomeric, since decay to the ground-state band would be  $K$ -forbidden. The earlier identified  $I^\pi = 10^+$  isomer was characterized in this work. The high-spin results of this work further extend the

† Research supported by the US National Science Foundation and the US Energy Research and Development Administration.

†† Address 1976–77: Niels Bohr Institute, Tandem Accelerator Laboratory, Risø, 4000 Roskilde, Denmark.

## INTERACTIONS FOR INELASTIC SCATTERING DERIVED FROM REALISTIC POTENTIALS †

G. BERTSCH, J. BORYSOWICZ and H. McMANUS

*Cyclotron Laboratory and Department of Physics, Michigan State University, East Lansing,  
 Michigan 48824*

and

W. G. LOVE

*Cyclotron Laboratory and Department of Physics, Michigan State University, East Lansing,  
 Michigan 48824*

and

*Department of Physics and Astronomy ††, The University of Georgia, Athens, Georgia 30602*

Received 30 June 1976

(Received 21 February 1977)

**Abstract:** An effective local interaction for inelastic scattering is derived by fitting the matrix elements of a sum of Yukawas and, for the tensor force, other closely related forms, to three selected sets of  $G$ -matrix elements. The ranges were selected to ensure OPEP tails in the relevant channels as well as a short-range part which simulates the “ $\sigma$ -exchange” process. Some of the implications of the various parts of the interaction are discussed in a distorted-wave context.

### 1. Introduction

This report describes a set of interactions for inelastic scattering which are derived from the nucleon-nucleon potentials of Hamada and Johnston <sup>1)</sup> and Reid <sup>2)</sup> and from the oscillator matrix elements of Elliott <sup>3)</sup>. The interactions are devised to be used with nuclear scattering codes. Exchange terms must be included. We are not discussing in this paper pseudopotentials which include approximately the effects of exchange. The route from the nucleon-nucleon potential to an inelastic scattering interaction is long and tedious, hence the necessity of a thorough description. The resulting potentials do not necessarily provide a good fit to experimental inelastic scattering data, but we hope that they will provide a fairly unambiguous prediction of inelastic scattering from the fundamental nucleon-nucleon interaction. In current distorted-wave programs <sup>4, 5)</sup>, the effective nucleon-nucleon interactions in inelastic scattering are frequently taken to be of the convenient forms †††

$$\begin{aligned}
 V &= \sum_i V_i Y(r_{12}/R_i), \quad \text{central,} \\
 V &= \sum_i V_i Y(r_{12}/R_i) \mathbf{L} \cdot \mathbf{S}, \quad \text{spin-orbit,}
 \end{aligned}
 \tag{1}$$

† Research sponsored in part by the National Science Foundation.

†† Permanent address.

††† Eq. (2) is from ref. <sup>4)</sup>, and eq. (3) from ref. <sup>5)</sup>.

## Proton Decay of the Isobaric Analogs of the Ground States of $^{207}\text{Pb}$ and $^{208}\text{Pb}$ \*

Ranjan Bhowmik\*\*, R. R. Doering\*\*\*, Aaron Galonsky, and P. S. Miller  
 Cyclotron Laboratory and Department of Physics, Michigan State University,  
 East Lansing, Michigan, USA

Received November 6, 1976

The proton decays  $\tilde{p}$  of isobaric analog states of  $^{207,208}\text{Pb}$  in the reactions  $^{207,208}\text{Pb}(p, n)$  have been studied using a neutron-proton coincidence technique. The width anomaly observed in  $(p, n)$  [4] and  $(p, n\tilde{p})$  singles spectra [11] is resolved in the coincident spectra.

Formation of isobaric analog states (IAS) in heavy nuclei has been extensively studied by proton elastic and inelastic resonance scattering [1–3] and by the  $(p, n)$  charge-exchange reaction [4–6]. Due to its unique nature, an IAS decays preferentially by proton emission to low-lying states of the final nucleus. Indirect observation of an IAS is therefore possible, and has been made, by detecting proton decay ( $\tilde{p}$ ) of the isobaric analog state [7–12].

The cross section for partial decay by  $\tilde{p}$  emission from the IAS of  $^{208}\text{Pb}$  [8, 13] has been reported to be greater than the  $(p, n)$  cross section [6, 14] for formation of the same IAS. A similar anomaly exists for the IAS of  $^{209}\text{Bi}$  [5, 6, 9]. It would appear that processes other than population of the IAS are contributing to the  $\tilde{p}$  yield. In addition to this discrepancy, the widths of the IAS of  $^{207,208}\text{Pb}$  and  $^{209}\text{Bi}$  as measured in  $(p, n\tilde{p})$  experiments [8, 9, 11], are considerably greater than the widths obtained in  $(p, n)$  experiments [4, 6] or in  $^{206}\text{Pb}+p$  [1] and  $^{207}\text{Pb}+p$  [2, 3] resonance experiments.

To explain these discrepancies, it has been suggested [5] that proton decay of analogs of excited states may contribute to the  $\tilde{p}$  yield. However, no direct evidence for the production of these excited analogs has been observed in  $(p, n)$  reactions on Pb and Bi, although they were looked for in many neutron spectra [6, 14]. Instead, it has been surmised that a proton evaporation and preequilibrium-emission peak underlying the  $\tilde{p}$  groups is responsible for excess

$\tilde{p}$  cross sections and widths [15]. We present data which tend to support this proposition.

We have investigated the reaction mechanism of the  $(p, n\tilde{p})$  process in  $^{208}\text{Pb}$  and in  $^{207}\text{Pb}$  by detecting the neutron and proton in coincidence. The proton bombarding energy was 25 MeV. Protons were detected at  $90^\circ$  with an  $E$ -veto telescope. A neutron time-of-flight (TOF) scintillation spectrometer [14] was used to detect the neutrons at  $30^\circ$  with respect to the beam. Pulse-shape discrimination was used to reject gamma rays. To achieve a reasonable coincidence counting rate, the neutron flight path was only 25 cm and the energy resolution 30%. The  $n$ - $p$  coincidences were recorded on a magnetic tape and later replayed with appropriate gates to sort out the kinematic region of interest.

Figure 1 shows the neutron TOF spectrum for the  $^{208}\text{Pb}$  target gated by protons between 10 and 12 MeV. The strong peak at 6 MeV corresponds to excitation of the target ground-state analog in  $^{208}\text{Bi}$ . The gating protons include the  $\tilde{p}$  decays of the IAS to the first three states of  $^{207}\text{Pb}$ , the only states with non-negligible population [8, 11]. The continuum background extending down to our threshold at 1.5 MeV indicates that an appreciable number of protons in the energy range 10–12 MeV are of non-IAS origin. The absence of a noticeable peak at 3.5 MeV speaks against the thesis that  $(p, n)$  excitation of the analog of the 2.61 MeV first-excited state of  $^{208}\text{Pb}$  leads to appreciable numbers of 10–12 MeV protons.

Proton energy spectra, gated by various regions of neutron energy, are shown in Figure 2. As the neutron energy is lowered, conservation of energy allows the proton spectrum to extend to higher energy. For

\* Supported by the National Science Foundation and the Office of Naval Research

\*\* Present address: Univ. Birmingham, England

\*\*\* Present address: Univ. Virginia, Charlottesville, VA, USA

## MIGMA DISTRIBUTION FUNCTIONS AND FUSION RATES\*

M. M. GORDON and FELIX MARTI

*Cyclotron Laboratory and Physics Department, Michigan State University, East Lansing, Michigan 48824, U.S.A.*

Received 7 October 1975 and in revised form 17 February 1976

Using a circular orbit model appropriate to a Migma fusion device, analytical expressions are obtained for the particle density and the colliding pair distribution functions in terms of a parameter which specifies the central ("core") density. Contrary to expectations, our distribution functions tend to favor colliding pairs with low relative velocities, and this tendency grows stronger as the central density increases. The reaction rate parameters for the  $d+d$  and  $d+^3\text{He}$  fusion reactions have been calculated for a wide range of deuteron energies, and our resultant values are not only significantly smaller than those found by Maglich, but are also generally smaller than those obtained from a comparable Maxwell distribution. We also find that the total pair density and the resultant fusion rate increase remarkably little with large increases in the central density, so that this basic Migma characteristic does not appear particularly advantageous for fusion production.

### 1. Introduction

In his discussion of fusion rates in the "Migma Cell", Maglich<sup>1)</sup> has emphasized the importance of two basic Migma properties, namely, the very high density of the central core, and the prevalence of nearly head-on collisions within this core. We report here on a systematic analysis of these properties with results which are more detailed and less favorable than those presented by Maglich.

Our analysis is based on a circular orbit model which is a sophisticated version of the model used by Harrison<sup>2)</sup>, and much earlier by Haegi<sup>3)</sup>. This model replaces the actual precessing orbits by circles, all of which pass within a small distance  $r_0$  of the magnetic field axis ( $r=0$ ). Maglich, Harrison, and Haegi consider  $r_0$  to be determined by the size of the focused beam spot or by the energy spread of the injected ions. However, these considerations determine only the minimum value of  $r_0$ , while its steady state value (after elastic collisions are considered) may be much larger. We shall therefore treat  $r_0$  as a "compactness parameter", with values ranging up to  $r_0 = 0.1a$ , where  $a$  is the average radius of the circular orbits. As shown by Haegi<sup>3)</sup>, the central core density is inversely proportional to  $r_0$ .

As usual, our analysis assumes the ion distribution to be axially symmetric and time independent. We further assume that  $p_z/p$  for the ions can be neglected, and that the density does not depend on  $z$  within an unspecified range  $\Delta z$ . These assumptions simplify the problem sufficiently so that analytical results can be derived for the important Migma distribution functions. These functions then provide a clear and direct

means for evaluating those quantities which determine the fusion rates.

For a system of self-colliding particles having a spatial density  $\rho(r)$ , the reaction rate per unit volume at a specified position  $r$  is given by:

$$dI/dV = \frac{1}{2} \rho^2(r) \langle v_{12} \sigma(v_{12}) \rangle_r, \quad (1)$$

where  $v_{12}$  is the relative velocity of an ion pair, and  $\sigma(v_{12})$  is the cross section. Here, the subscript  $r$  on the angular brackets indicates that the averaging is carried out at the specified position. That is, unlike the simple case of a plasma, the relative velocity distribution in a Migma depends on position.

Integration of the above formula yields the following result for the total reaction rate:

$$I = P \langle v_{12} \sigma(v_{12}) \rangle, \quad (2)$$

where  $\langle v_{12} \sigma(v_{12}) \rangle$  is the "reaction rate parameter", and where:

$$P = \frac{1}{2} \int \rho^2(r) dV, \quad (3)$$

is the "total pair density". Our analysis is aimed at evaluating these quantities and showing how they depend on various parameters characterizing the Migma.

### 2. Migma orbit distribution

Since we apply the methods of dynamics to solve a problem which is inherently geometric, it proves convenient to set the frequency  $\omega = qB_0/mc = 1$ , and the mass  $m = 1$ . In these units, the orbit period  $\tau = 2\pi$ , and the momentum  $p$  becomes identical to the orbit radius. In addition, the (generalized) angular

\* Work supported by the National Science Foundation.



## RESPONSE FUNCTIONS OF ORGANIC SCINTILLATORS TO HIGH ENERGY NEUTRONS

J. A. LOCKWOOD, C. CHEN, L. A. FRILING, D. SWARTZ, R. N. ST. ONGE\*

*Physics Department, University of New Hampshire, Durham, New Hampshire 03824, U.S.A.*

AARON GALONSKY and R. R. DOERING

*Cyclotron Laboratory, Physics Department, Michigan State University, East Lansing, Michigan 48824, U.S.A.*

Received 28 July 1976

Two cylindrical liquid scintillators of dimensions  $5\text{ cm} \times 5\text{ cm}$  and  $12.5\text{ cm} \times 12.5\text{ cm}$ , filled with NE213, were calibrated with high energy neutrons from  $E_n = 3\text{ MeV}$  to  $E_n = 75\text{ MeV}$  at the time-of-flight facility associated with the Michigan State University Cyclotron. Pulse shape discrimination was used on each detector to separate the protons and alphas produced by neutron interactions from the electrons produced by gamma rays. Response functions for monoenergetic neutrons from about 2 MeV to 75 MeV have been determined. These response functions are very different from the calculated response using the Monte Carlo method. The implications of these calibrations for measurements of high energy neutrons using liquid scintillators are discussed.

### 1. Introduction

Numerous measurements have been made of fast neutrons ( $1 < E_n < 15\text{ MeV}$ ) in the atmosphere using recoil proton detectors, primarily organic scintillators<sup>1</sup>). Most detectors used some type of pulse-shape-discrimination (PSD) technique to separate interactions due to neutrons and to gamma rays<sup>2</sup>). With the exception of the extensive results by Verbinski et al.<sup>3</sup>), few fast-neutron detectors have been calibrated with a neutron time of flight (TOF) system. As atmospheric neutron measurements have been extended to higher energies ( $15 < E_n < 75\text{ MeV}$ ), accurate knowledge of the neutron response function has become increasingly important because the contributions from neutron-induced reactions on carbon are competitive with elastic neutron-proton scattering. Recently, liquid scintillators filled with NE213 have been flown by the University of New Hampshire (UNH) group to measure the energy spectrum and fluxes of neutrons from  $E_n \approx 2\text{ MeV}$  to  $E_n \approx 75\text{ MeV}$  near the top of the atmosphere<sup>4</sup>). The same neutron detectors were then calibrated at the Michigan State University Isochronous Cyclotron Facility. In this calibration the TOF technique was used to select the monoenergetic neutron beams. The number of protons per MeV as a function of proton energy for each monoenergetic neutron beam was taken to be the neutron response function. It is the purpose of this paper to report the measured neutron response functions of these detectors to neutrons with  $2 < E_n < 75\text{ MeV}$ .

### 2. Neutron detectors

The two neutron detectors were cylindrical organic liquid scintillators of dimensions  $5\text{ cm} \times 5\text{ cm}$  and  $12.5\text{ cm} \times 12.5\text{ cm}$  filled with NE213 and encapsulated in glass. A description of the scintillators is presented in Klumpar et al.<sup>5</sup>). Pulse shape discrimination was used on the output of each NE213 detector and the detector with its associated RCA 8575 phototube was completely enclosed in a plastic anticoincidence (AC) scintillator shield to reject events due to incident charged particles<sup>6</sup>). Since both good particle resolution between neutron and gamma-ray events and a wide dynamic pulse-height range were required, the zero-crossover method of PSD was used<sup>7,8</sup>). The experimental set-up including PSD and TOF systems are indicated schematically in fig. 1. The PSD system utilizes a constant-fraction pickoff unit for the signal from the anode of an RCA 8575 phototube. In order to determine the particle type, the signal from the constant-fraction pickoff unit is delayed and used as the stop signal for the time-to-amplitude converter (TAC). Another signal derived from the dynode of the phototube is fed through the double-delay-line amplifier. A bipolar signal from the amplifier is fed through a timing single channel analyzer in which the zero-crossover technique is used to produce a start signal for the pulse shape (PS) TAC. From this start signal and the stop signal derived from the anode, the (PS) TAC yields a signal with pulse height characteristic of the type of charged particle interacting in NE213 scintillator. Also, the double-delay-line amplifier provides an unipolar signal for the pulse height (PH)

\* Deceased.

## A He-JET CHOPPER FOR MEASURING HALF-LIVES OF SHORT-LIVED NUCLEI\*

M. D. EDMISTON, R. A. WARNER, WM. C. McHARRIS†

*Cyclotron Laboratory, Department of Chemistry and Department of Physics  
and*

W. H. KELLY

*Cyclotron Laboratory and Department of Physics, Michigan State University, East Lansing, Michigan 48824, U.S.A.*

Received 14 October 1976

A He-jet chopper has been built to enable one to measure the half-lives of nuclear species from several seconds to as short as several tens of milliseconds. The chopper has been used to measure some of the mirror beta decays in the  $f_{7/2}$  shell.

### 1. Introduction

The He-jet recoil transport system (HeJRTS) has become a routinely used tool for the study of nuclei far from stability<sup>1,2</sup>). One type of experiment is the simple measurement of a half-life, usually performed by collecting a spot of radioactivity from the HeJRTS,

mechanically moving this spot in front of a detector, and watching it decay away. This method works quite well but does not permit one to measure half-lives as short as the HeJRTS is capable of handling, for it can transport activities in several tens of msec, while it takes about 1 s to move the spot to a well-shielded detector.

\* Work supported in part by the U.S. National Science Foundation.

† Alfred P. Sloan Fellow, 1972-1976.

Clearly it would be preferable not to move the spot, but rather turn the HeJRTS on and off. Unfortunately, this is difficult to do. If one attempts to pulse the

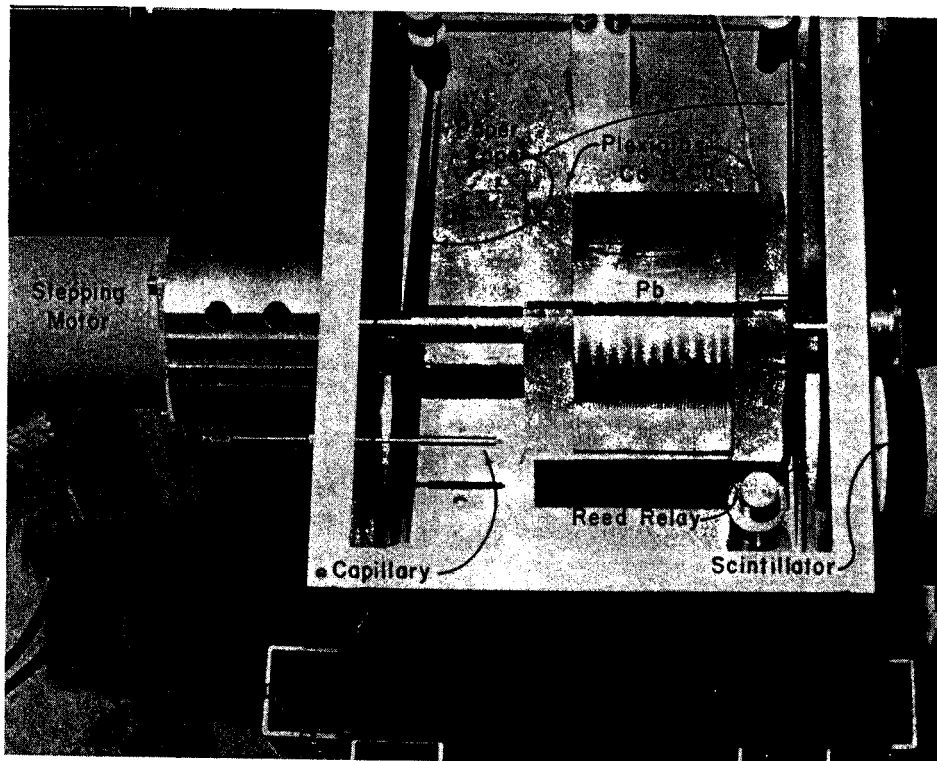


Fig. 1. Photograph of the Pb chopper in place ready for data to be taken.

## PREPARATION OF ISOTOPIC SULFUR TARGETS

MARK A. HEDEMANN\*

*Cyclotron Laboratory, Michigan State University, East Lansing, Michigan 48824, U.S.A.*

Received 17 November 1976

An evaporation technique for making sulfur isotope targets of approximately  $200 \mu\text{g}/\text{cm}^2$  in thickness or greater is discussed.

The preparation of a sulfur target presents several problems. Sulfur adheres poorly to carbon foils. Since we desired a target of approximately  $150\text{--}200 \mu\text{g}/\text{cm}^2$  in thickness, a different backing material was needed. Sulfur also sublimates at low temperatures in a vacuum, its vapor pressure being  $10^{-6}$  at  $19^\circ\text{C}$  and  $10^{-4}$  torr at  $57^\circ\text{C}$ . Sulfur compounds which have the desired property of not vaporizing upon exposure to the beam are often not useful because of the reaction products from the chemical partner. A target structure containing pure sulfur was therefore needed which would prevent the loss of the sulfur. The following method overcame these problems, and had the added advantage of requiring only a small quantity of the enriched isotopes.

A target frame was prepared by laying down a layer of Formvar<sup>1)</sup> film, picking up a floating carbon foil onto this layer, and laying down another layer of Formvar on top of the carbon layer. These layers were allowed to dry for one day. A layer of sulfur was then evaporated onto the Formvar layer. The sulfur was found to adhere more readily to Formvar than to carbon.

The container for the sulfur during the evaporation was a 2" long piece of  $\frac{1}{4}$ " diameter tantalum tubing. Three-quarters of an inch of one end was pinched shut. Approximately 1 mg of sulfur was put into the tube, and  $\frac{3}{4}$ " of the other end was pinched shut parallel to the first end. A hole was drilled in the center of one face of the remaining  $\frac{1}{2}$ " long cavity using a #80 drill bit. The ends were bent in order to have the tube fit into the electrodes with the top of the cavity above the electrodes (fig. 1). The Formvar surface was placed 1.0 cm above the top of the cavity.

The evaporation was done under vacuum. Before heating, the system was pumped down to approximately  $3 \times 10^{-6}$  torr. The valve to the pumping system

was then closed to prevent poisoning of the pumping system. This brought the pressure up to approximately  $2 \times 10^{-4}$  torr due to some leakage while closing the valve.

After closing the valve, the current between the electrodes was gradually raised over a period of about two minutes until the evaporation occurred. The actual evaporation itself was quite rapid, as is shown later. The evaporation typically occurred at 80 A current. Two glass slides were placed alongside the target frame in order to see the sulfur film as it formed. The film appeared white and was visible to a radius of about 2 cm. About three seconds after the film appeared on the glass, the current was turned off immediately and air was let in as rapidly as possible without breaking the film. These actions were designed to prevent immediate sublimation of vaporization of the newly deposited film. A layer of dry Formvar was put over the layer of sulfur. Moisture on the Formvar film would destroy the sulfur film. Another evaporation could be made on this layer of Formvar.

Although the evaporation lasted only three seconds, no sulfur residue was ever found in the cavity after any evaporation. The sulfur layers produced by this

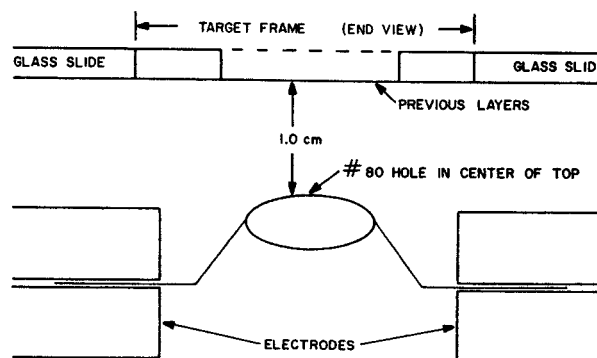


Fig. 1. Setup for the sulfur evaporation. The tantalum filament is shown clamped between the electrodes. The layer closest to the filament is a Formvar layer. The glass slides are essential in order to see the sulfur film form.

\* Present address: California Institute of Technology, Pasadena, California, 91109, U.S.A.

## CYCLOTRON HEAVY ION BEAM INTENSITY ENHANCEMENT BY USING AN EASILY IONIZED SUPPORT GAS IN THE ION SOURCE

E. D. HUDSON, G. A. PALMER, C. L. HALEY

*Oak Ridge National Laboratory\*, Oak Rige, Tennessee, 37830, U.S.A.*

and

M. L. MALLORY†

*Cyclotron Laboratory, Michigan State University, East Lansing, Mich. 48824, U.S.A.*

Received 8 November 1976

A large increase in the beam intensity of the Oak Ridge Isochronous Cyclotron (ORIC) has resulted from mixing easily ionized support gas with the primary gas in the cold cathode ion source.

The discovery of self bombardment<sup>1)</sup> of the arc chamber in a cyclotron by large mass-to-charge ions ( $^{132}\text{Xe}^{1+, 2+, \dots}$ ) led to experiments on a  $^{20}\text{Ne}^{7+}$  beam using xenon support gas. The primary arc gas (neon) was supplied to one end of the arc chamber through one gas line while xenon was supplied to the other end of the arc chamber through a separate gas line. The neon beam was found to increase by about a factor of 10 over previously observed intensities but was too low for planned experiments. In May 1976, a request for a  $^{20}\text{Ne}^{7+}$  beam for approximately the beam current obtained by xenon gas mixing led to a re-examination of the gas mixing data. Prior to the experiment with  $^{20}\text{Ne}^{7+}$ , an opportunity to try gas mixing with a  $^{20}\text{Ne}^{6+}$  beam occurred and a large beam enhancement was immediately detected. Since it was easy to mix the gases in the ion source, gas mixing was tried routinely with most of the following scheduled cyclotron runs and consistent beam enhancements found for lighter heavy ions (masses  $\leq 20$ ). For example,  $^{16}\text{O}^{5+}$  maximum beam intensity was increased to 35  $\mu\text{A}$  and also a  $^{12}\text{C}^{5+}$  beam of 150 nA has been extracted.

The result of mixing xenon with neon for a  $^{20}\text{Ne}^{6+}$  extracted beam from the cyclotron is shown in fig. 1. In the measurements of fig. 1, the xenon arc support gas was increased by small increments and the neon gas support was decreased until the arc was about to "drop out". The arc "drop-out point" is defined as the point where the arc voltage starts to increase sharply as the gas flow is decreased. The neon extracted beam intensity increases by approximately a factor of

five for a gas flow of 0.15  $\text{cm}^3/\text{min}$  of xenon, the corresponding neon gas flow was reduced from 4.4  $\text{cm}^3/\text{min}$  to 3.2  $\text{cm}^3/\text{min}$ . Experiments with gas

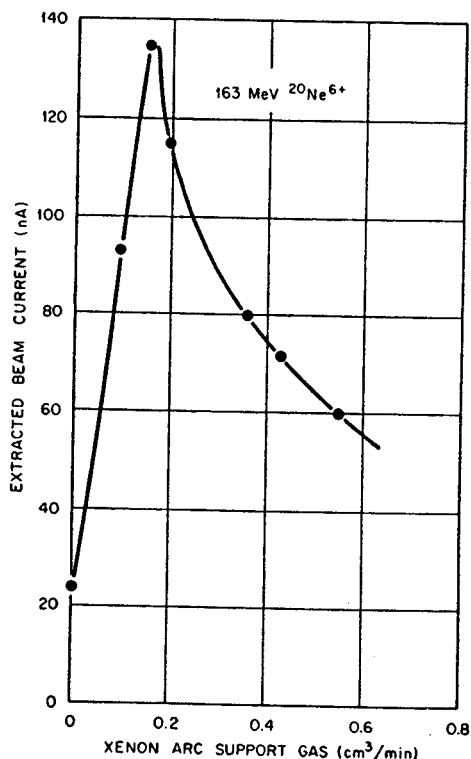


Fig. 1. The extracted beam current for a 163 MeV  $^{20}\text{Ne}^{6+}$  as a function of xenon support gas. The beam intensity increases by approximately as factor of 5 for mixing of xenon with neon for this charge state. The neon was reduced by  $\approx 1 \text{ cm}^3/\text{min}$  at the maximum enhancement. A similar enhancement factor is seen for argon and krypton gas mixing.

\* Operated by Union Carbide for the U.S. ERDA.

† Supported by the National Science Foundation.

## THE NEUTRON TIME-OF-FLIGHT FACILITY AT MICHIGAN STATE UNIVERSITY\*

RANJAN K. BHOWMIK, ROBERT R. DOERING, LAWRENCE E. YOUNG,  
SAM M. AUSTIN, AARON GALONSKY and STEVE D. SCHERY†

*Cyclotron Laboratory and Physics Department, Michigan State University, East Lansing, Michigan 48824, U.S.A.*

Received 29 December 1976

A new neutron time-of-flight facility at the Michigan State University Cyclotron Laboratory incorporates a magnetic beam swinger permitting measurement of angular distributions with a stationary detector. A large volume (2.7 l) liquid scintillation detector with a time resolution of less than 200 ps was developed to exploit the long flight paths (4–32 m) made possible by the swinger. For 33 MeV neutrons an overall time (energy) resolution of 550 ps ( $\approx 150$  keV) has been achieved.

### 1. Introduction

A neutron time-of-flight (TOF) facility incorporating a beam swinger<sup>1)</sup> has been constructed at the Michigan State University Cyclotron Laboratory. In this arrangement the neutron counter is held fixed; to change the reaction angle, the direction of the beam on target is changed by moveable magnets. Flight paths of 4–32 m are possible in a compact experimental area. The beam dump and the detector are housed in separate rooms facilitat-

ing good shielding. To have reasonable counting rates for the longer flight paths, a neutron detector with a volume of 2.7 l of NE224 scintillator has been developed. The analog signals from the detector are digitized and processed in a PDP11/45 computer connected to a CAMAC crate. An overall time resolution of 550 ps has been obtained with roughly equal contributions from beam resolution, target thickness and counter resolution.

\* Supported by the National Science Foundation.

† Presently at Moody College, Galveston, Texas, U.S.A.

### 2. Beam swinger

The physical layout of the beam swinger is

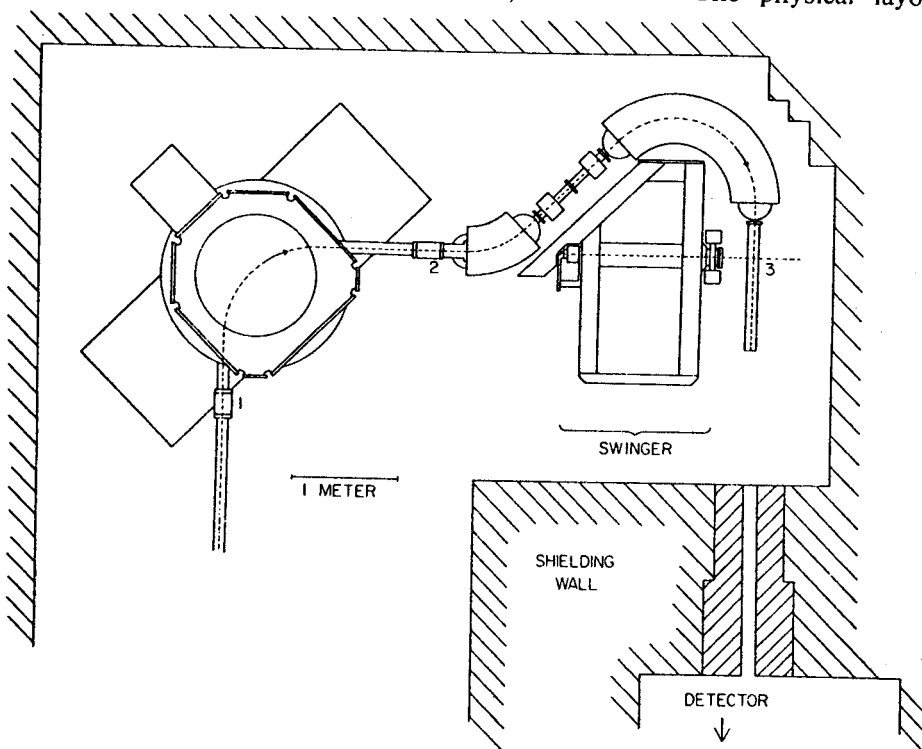


Fig. 1. Top view of the beam swinger set at a  $0^\circ$  reaction angle. Focuses occur at points 1, 2, and 3, and the target is placed at position 3. The (charged particle, n) chamber is shown in place.

# Pathway of Nitrogen Metabolism after Fixation of $^{15}\text{N}$ -labeled Nitrogen Gas by the Cyanobacterium, *Anabaena cylindrica*\*

(Received for publication, January 15, 1976)

C. PETER WOLK, JOSEPH THOMAS,† AND PAUL W. SHAFFER

From the MSU/ERDA Plant Research Laboratory, Michigan State University, East Lansing, Michigan 48824

SAM M. AUSTIN AND AARON GALONSKY

From the Cyclotron Laboratory and Department of Physics, Michigan State University, East Lansing, Michigan 48824

Methods have been developed for identifying the pathway of assimilation of  $\text{N}_2$ -derived nitrogen. The products of fixation of  $^{15}\text{N}$ -labeled nitrogen gas ( $[^{15}\text{N}]\text{N}_2$ ), and the distribution of  $^{15}\text{N}$  within glutamine, were determined after short periods of labeling (approximately 1 to 120 s) and also in pulse-chase experiments. Ammonia, the amide nitrogen of glutamine, and the  $\alpha$ -amino nitrogen of glutamate, in that order, were the first observed products of fixation of  $\text{N}_2$  by the cyanobacterium (blue-green alga), *Anabaena cylindrica*. This sequence of the formation of nitrogenous products was confirmed by the use of inhibitors. The presence of 1 mM methionine sulfoximine permitted continued formation of  $^{15}\text{NH}_3$ , while virtually preventing  $^{15}\text{N}$ -labeling of amino acids. In the presence of 1 mM azaserine, glutamine was labeled, but not other amino acids. Our observations demonstrate unequivocally that  $\text{N}_2$ -derived nitrogen fixed by this organism is metabolized initially by the glutamine synthetase/glutamate synthase pathway.

Most studies of the pathways considered potentially capable of initial metabolism of nitrogen in cyanobacteria (blue-green algae) have been enzymological. Activities of glutamic acid dehydrogenase and alanine dehydrogenase have been measured in *Anabaena cylindrica* (1, 2) and other cyanobacteria (3-5). Glutamine synthetase activity was observed in *A. cylindrica* at levels higher than required to account for *in vivo* rates of nitrogen assimilation (6; cf. also Ref. 1), and glutamate synthase (glutamine amide:2-oxoglutarate amidotransferase) activity was detected in the same cyanobacterium only when ferredoxin was used as reductant (7). Glutamine synthetase (8), like nitrogenase (9), is present at relatively high specific activity in heterocysts, differentiated cells which are major loci of nitrogen fixation in aerobically grown filaments (10-15). Little else is known about how the cellular localization of the enzymes assayed compares with the localization of the initial metabolism of fixed nitrogen. It is therefore not possible at this time to reach firm conclusions, on the basis of enzymological studies, about pathways operative in the metabolism of  $\text{N}_2$ -derived fixed nitrogen.

Addition of L-methionine-DL-sulfoximine, in other organisms an inhibitor of glutamine synthetase, to cultures of *A. cylin-*

*drica* (16) led to a great decrease in the size of the total intracellular pool of glutamine, and to about a halving of the glutamate pool, over a 12-h period. The concentrations of aspartate and of glycine plus alanine changed very little. Secretion of  $\text{NH}_3$  was increased greatly. These changes, being slow, could have been indirect, but they did support the idea that  $\text{N}_2$ -derived  $\text{NH}_3$  is metabolized initially by the glutamine synthetase/glutamate synthase pathway.

Early studies of products of fixation of  $^{15}\text{N}$ -labeled nitrogen gas, by Magee and Burris (17), showed that in hydrolysates of protein from the cyanobacterium *Nostoc muscorum*, the highest specific activity (atom per cent excess) of  $^{15}\text{N}$  was in glutamic acid. Because the products were analyzed only after 1.5 h of fixation, these studies could only suggest possible candidates for the earliest products of fixation. More recently, Stewart *et al.* (18) have referred to investigations involving 10 min exposures to  $^{15}\text{N}$ -labeled  $\text{N}_2$ . Although the period of labeling was such that several organic products had become labeled, the results were consistent with operation of the glutamine synthetase/glutamate synthase pathway. In such studies, as increasingly shorter intervals of labeling are employed, increasingly smaller amounts of fixed  $^{15}\text{N}$  must be detected and quantified. Efforts to compensate for decreased fixation by increasing the quantity of  $\text{N}_2$ -fixing cells are hampered by self-shading of the suspension of pigmented, photoautotrophic cells. In common practice, the content of  $^{15}\text{N}$  in fixed nitrogen is measured, after reoxidation of the nitroge-

\* This investigation was supported by the United States Energy Research and Development Administration under contract E(11-1)-1338, and by the United States National Science Foundation.

† Permanent address, Biology and Agriculture Division, Bhabha Atomic Research Centre, Trombay, Bombay 400 085, India.

## Formation of Glutamine from [ $^{13}\text{N}$ ]ammonia, [ $^{13}\text{N}$ ]dinitrogen, and [ $^{14}\text{C}$ ]glutamate by Heterocysts Isolated from *Anabaena cylindrica*

JOSEPH THOMAS,<sup>1</sup> J. C. MEEKS, C. PETER WOLK,\* PAUL W. SHAFFER, SAM M. AUSTIN, AND W.-S. CHIEN

MSU/ERDA Plant Research Laboratory,\* Cyclotron Laboratory, and Department of Physics, Michigan State University, East Lansing, Michigan 48824

Received for publication 5 August 1976

A method is described for the isolation of metabolically active heterocysts from *Anabaena cylindrica*. These isolated heterocysts accounted for up to 34% of the acetylene-reducing activity of whole filaments and had a specific activity of up to 1,560 nmol of  $\text{C}_2\text{H}_4$  formed per mg of heterocyst chlorophyll per min. Activity of glutamine synthetase was coupled to activity of nitrogenase in isolated heterocysts as shown by acetylene-inhibitable formation of [ $^{13}\text{N}$ ]NH<sub>3</sub> and of amide-labeled [ $^{13}\text{N}$ ]glutamine from [ $^{13}\text{N}$ ]N<sub>2</sub>. A method is also described for the production of 6-mCi amounts of [ $^{13}\text{N}$ ]NH<sub>3</sub>. Isolated heterocysts formed [ $^{13}\text{N}$ ]glutamine from [ $^{13}\text{N}$ ]NH<sub>3</sub> and glutamate, and [ $^{14}\text{C}$ ]glutamine from NH<sub>3</sub> and [ $^{14}\text{C}$ ]glutamate, in the presence of magnesium adenosine 5'-triphosphate. Methionine sulfoximine strongly inhibited these syntheses. Glutamate synthase is, after nitrogenase and glutamine synthetase, the third sequential enzyme involved in the assimilation of N<sub>2</sub> by intact filaments. However, the kinetics of solubilization of the activity of glutamate synthase during cavitation of suspensions of *A. cylindrica* indicated that very little, if any, of the activity of that enzyme was located in heterocysts. Concordantly, isolated heterocysts failed to form substantial amounts of radioactive glutamate from either [ $^{13}\text{N}$ ]glutamine or  $\alpha$ -[ $^{14}\text{C}$ ]ketoglutarate in the presence of other substrates and cofactors of the glutamate synthase reaction. However, they formed [ $^{14}\text{C}$ ]glutamate rapidly from  $\alpha$ -[ $^{14}\text{C}$ ]ketoglutarate by aminotransferase reactions, with various amino acids as the nitrogen donor. The implications of these findings with regard to the identities of the substances moving between heterocysts and vegetative cells are discussed.

Filamentous cyanobacteria that have been shown to be capable of fixing nitrogen gas (N<sub>2</sub>) aerobically are characterized by the presence of differentiated cells called heterocysts. A large amount of indirect evidence (6, 8, 22, 25, 27, 36) favors the hypothesis that heterocysts are major loci of nitrogen fixation in the filaments. This hypothesis was substantiated by autoradiographic experiments with [ $^{13}\text{N}$ ]N<sub>2</sub> (32). Early attempts (7, 10, 20, 21) to demonstrate substantial nitrogenase activity in isolated heterocysts free of vegetative cells were unsuccessful. Recently, however, Peterson and Burris (16), working with a strain of *Anabaena*, described a procedure for isolating heterocysts that can reduce  $\text{C}_2\text{H}_2$ , an alternate substrate for nitrogenase, at up to 1,840 nmol per mg of chlorophyll

(Chl) per min. When calculated on the basis of the heterocyst frequency in filaments, this rate accounted for 13% of the rate of  $\text{C}_2\text{H}_2$  reduction by intact filaments (1,060 nmol per mg of Chl per min). Tel-Or and Stewart (23) found up to 45% of the activity of whole filaments in heterocysts isolated from *Anabaena cylindrica*, but the specific activity of nitrogenase in whole filaments reported by the latter workers was only 0.194 nmol of  $\text{C}_2\text{H}_4$  per mg of protein per min. This rate is approximately 6 nmol of  $\text{C}_2\text{H}_4$  per mg of Chl per min if one assumes a ratio of protein to chlorophyll of approximately 30 (4).

The enzymatic pathway consisting of glutamine synthetase and glutamate synthase (glutamine amide: $\alpha$ -ketoglutarate amidotransferase) (24) was shown to be the major route of metabolism of ammonia in heterotrophic nitrogen-fixing bacteria (15). Using [ $^{13}\text{N}$ ]N<sub>2</sub>, we recently established that this pathway also me-

<sup>1</sup> Permanent address: Biology and Agriculture Division, Bhabha Atomic Research Centre, Trombay, Bombay 400 085, India.

A FACILITY FOR THE STUDY OF NEUTRON SCATTERING IN  
THE 20-40 MEV RANGE

R. R. Doering, L. E. Young, R. Bhowmik, S. M. Austin,  
A. Galonsky and S. Schery\*

Cyclotron Laboratory and Physics Department, Michigan State  
University, East Lansing, Michigan 48824

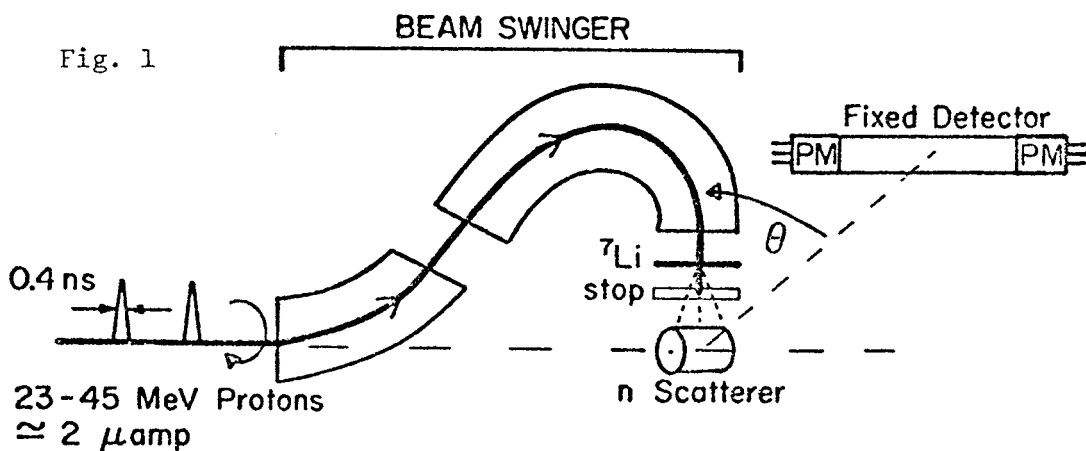
RÉSUMÉ

A facility including a sector focussed cyclotron, a beam swinging magnet and a fixed position large volume (1700 cm<sup>3</sup>) neutron detector has been developed for studies of neutron scattering cross sections. The overall time resolutions obtained so far are 490 psec for  $\gamma$  rays and 730 psec for neutrons.

ABSTRACT

A system including a beam-swinging magnet similar to that at Colorado and a large fixed neutron detector has been built for the study of neutron scattering (and other n-producing reactions). A pulsed proton beam from the MSU cyclotron ( $\sim 2\mu\text{s}$  time averaged,  $\Delta t \lesssim 400\text{ps}$ ) passes through a rotatable magnet ( $-45^\circ$  bend followed by  $+135^\circ$  bend), then through a  ${}^7\text{Li}$  neutron producing target and into a beam stop (see Fig. 1). Neutrons produced by the  ${}^7\text{Li}(p,n){}^7\text{Be}$  reaction strike a scattering sample placed on the rotation axis and may be scattered into a fixed detector placed at  $\theta$ . One can vary  $\theta$  between  $20^\circ$  and  $160^\circ$  by rotating the swinger magnet. The detector consists of a volume of liquid scintillator (NE 224) with dimensions of 100 cm long x 13 cm high x 1.3 cm deep and viewed at the ends by two 8850 photomultipliers. Overall resolutions of 490 psec for  $\gamma$  rays and 730 psec for neutrons have been achieved. The contribution of the counter and electronics to the n time spread is less than 200 psec. Preliminary results of n-scattering experiments will be described.

\* Research supported by the National Science Foundation.





GLUTAMINE FORMATION BY HETEROCYSTS OF ANABAENA CYLINDRICA

J. C. Meeks, Joseph Thomas, C. P. Wolk, MSU/ERDA Plant Research Laboratory, and Sam M. Austin, Cyclotron Laboratory and Department of Physics, Michigan State University, East Lansing, MI. 48824, U.S.A.

The initial organic products of fixation of  $^{13}\text{N}$ -labeled nitrogen gas ( $[^{13}\text{N}]\text{N}_2$ ) by whole filaments of Anabaena cylindrica are, sequentially, glutamine and glutamic acid. The capability of heterocysts isolated from A. cylindrica to form these amino acids from  $[^{13}\text{N}]\text{N}_2$  and  $[^{13}\text{N}]\text{NH}_3$  was investigated.

Heterocysts were isolated by a procedure which involves osmotic and brief sonic lysis of vegetative cells followed by low speed centrifugation. The suspensions of isolated heterocysts contained at most 2 per cent vegetative cells. These suspensions reduced acetylene in the presence of light, dithionite, ATP, and an ATP generating system at up to 34 per cent of the whole-filament rate on a per heterocyst basis. The isolated heterocysts had a specific activity of up to 1560 nmoles  $\text{C}_2\text{H}_4$  formed  $\cdot(\text{mg heterocyst chlorophyll})^{-1} \cdot \text{min}^{-1}$ , representing a five-fold increase over the whole-filament rate.

When incubated in the presence of light, dithionite, ATP and an ATP generating system, and glutamate, the isolated heterocysts fixed  $[^{13}\text{N}]\text{N}_2$  into ammonia and amide nitrogen at up to 23 per cent of the rate of whole filaments. Ammonia and amide nitrogen in the 80 per cent methanolic extract were fractionated by vacuum distillation at pH 10.0 and subsequent steam distillation in the presence of alkali, respectively. Amide nitrogen accounted for up to 67 per cent of the total  $^{13}\text{N}$  recovered, and ammonia for the balance of the  $^{13}\text{N}$ . The amide nitrogen was identified as glutamine-amide by coelectrophoresis of the  $^{13}\text{N}$ -labeled organic product with  $^{14}\text{C}$ -labeled glutamine. Fixation of  $[^{13}\text{N}]\text{N}_2$  into distill-

ROTATION- AND DEFORMATION-ALIGNED *YRAST* STRUCTURES IN W, Os AND Pt ISOTOPES\*

F. M. Bernthal

Michigan State University, East Lansing, Michigan 48824, U.S.A.

Recent  $(\alpha, xn\gamma)$  studies near the large- $A$  limit of the rare-earth region of deformation provide new insight into phenomena associated with the interplay between collective and single particle motion in nuclei. On the one hand, in a number of well-deformed Hf and W isotopes, a profusion of strong-coupled high- $\Omega$  orbitals near the Fermi surface gives rise to clear examples of deformation-aligned *yrast* structures.<sup>1</sup> On the other hand, systematics in lighter rare-earth nuclei generally seem consistent with the dominant role of decoupled  $i_{13/2}$  neutrons in backbending behavior of *yrast* bands. Attempts to extend this description to the W and Os isotopic series are complicated by the question of the role of  $h_{9/2}$  protons,<sup>2</sup> but there is a striking consistency between *yrast* band behavior in even- $A$  nuclei and the degree of decoupling displayed by  $i_{13/2}$  band structures in odd- $N$  neighbors throughout the rare earth region.<sup>3</sup> In the shape-transitional Pt isotopes 190 and 192, one finds direct evidence for the intersection of  $\pi h_{11/2}^{-2}$  and  $\nu i_{13/2}^{-2}$  structures with the ground rotational band.<sup>4</sup> The data thus suggest that both proton and neutron decoupling effects may influence *yrast* band behavior throughout the W-Os-Pt region.

We have most recently completed a study of the *yrast* structures in the more neutron-rich tungsten isotopes, of special interest because they bridge a region between no backbending in the hafnium isotopes and sharp *yrast* anomalies in the osmium isotopes. *Yrast* band anomalies in the W isotopes might therefore be expected to arise from influences similar to those at work in their osmium isotones, and the W isotopes have the added attraction of an axially symmetric nuclear shape that is expected to be quite stable. The high-spin tungsten *yrast* data generally seem consistent with the dominant role of  $i_{13/2}$  neutron structures.

In summary, the experimental *yrast* data throughout this region now suggest a rather smooth transition from conventional backbending in  $^{180}\text{W}$ ,  $^{182}\text{Os}$ , and  $^{186}\text{Pt}$  for example, to a more distinctive and transparent phenomenon where two or more bands are seen to intersect in the heavier Os and Pt isotopes. One also encounters the added dimension of deformation-aligned *yrast* structures in certain favorable cases.

\* Research supported by the U. S. National Science Foundation.

<sup>1</sup>T. L. Khoo, *et al.*, MSUCL Report No. 212 (1976), to be published.

<sup>2</sup>A. Neskakis, *et al.*, Nucl. Phys. A261 (1976) 189.

<sup>3</sup>F. M. Bernthal, *et al.*, Phys. Rev. Letters 33 (1974) 1313.

<sup>4</sup>M. Piiparinen, *et al.*, Phys. Rev. Letters 34 (1975) 1110.

COLLECTIVE AND INTRINSIC ASPECTS OF YRAST STRUCTURE

F. M. Bernthal

The Niels Bohr Institute

Risø, 4000 Roskilde, Denmark

and

Departments of Chemistry and Physics and Cyclotron Laboratory

Michigan State University

East Lansing, Michigan 48824 U.S.A.

1. Introduction

The broad subject of the yrast family of states and their structure is one which has become increasingly complex in recent years, particularly as the imagination of our theorists has opened the prospect for spectroscopic investigation of nuclei at very high spins. While the title of these lectures may have arisen from an early desire to conceive a label sufficiently global to allow absolutely anything remotely related to high spins to be discussed, it is in fact concise and accurate in its description of the current status of what I will call yrast line spectroscopy.

Spectroscopy of the yrast region has recently encountered distinctive phenomena which are associated on the one hand with the familiar collective degrees of freedom, and on the other hand with independent particle motion. As we shall see, a rich and varied array of phenomena lies between these two extremes; as usual, it is the interaction of the two that provides the experimentalist with some of the most fascinating systems for study.

These discussions will focus on recent experimental progress in yrast line spectroscopy and the insights for nuclear structure such studies afford. Most of the data are taken from the region of the nuclear chart between the elements hafnium and lead. Nuclei in this region are particularly instructive for yrast line spectroscopic study, influenced as they are by changing nuclear shapes, shell effects, and strong Coriolis forces. These are the general features expected to dominate nuclear structure at still higher spins, and they find their counterparts in the transition from prolate to oblate deformation in the Os and Pt isotopes, in the appearance of high-spin, multiquasiparticle yrast traps in certain Hf and W isotopes, and in the reappearance of strong rotation-alignment effects in Os, Pt and Hg isotopes.

To be sure, many of the phenomena which I will describe also appear in lighter nuclei, and several groups have made elegant interpretations of data that a few years ago would have seemed inscrutable. I will not attempt to summarize these data, but will confine my remarks to the Hf-Pb nuclei with which I am most familiar.

2. Backbending, Rotation-Aligned Yrast Structures, and All That Stuff: What are experiments telling us?

The yrast sequence of states generally holds little interest at lower spins, since strictly collective phenomena are presumed to predominate. It was the experimental observation of "backbending" that focused attention on irregularities in the ground band structure of rotational nuclei,

T. Faestermann, O. Häusser, D. Ward, H.R. Andrews,  
T.K. Alexander and D. Horn

Atomic Energy of Canada Limited, Chalk River Nuclear Laboratories,  
Chalk River, Ontario, Canada

and T.L. Khoo, Michigan State University, East Lansing

High-K isomers are prevalent towards the end of the rare-earth deformed region where the valence particles fill high  $\Omega$  orbitals. Very little is known about the g-factors for these isomers, mainly because in the half-life range encountered, 50 ns-50  $\mu$ s, quadrupole and paramagnetic relaxation effects can destroy the nuclear alignment very rapidly. The  $K=6, J^\pi=6^+$  state in  $^{176}\text{Hf}$  at 1554 keV decays predominantly to the ground band ( $K=0$ )  $6^+$  and  $4^+$  levels with  $\gamma$ -rays of 921.8 keV and 1247.3 keV respectively and its half-life has previously been measured<sup>1)</sup> as  $78 \pm 1$  ns. According to Khoo and Løvghøiden<sup>2)</sup> its structure is a mixture of two quasi-particle proton  $[404]7/2 \otimes [402]5/2$  and neutron  $[514]7/2 \otimes [512]5/2$  states.

We have measured the g-factor by the method of spin rotation i.e. observing the time dependence of the  $\gamma$ -ray intensity in a fixed detector resulting from the precession of the nuclear moment in an external magnetic field. The state was populated in the reaction  $^{176}\text{Yb}({}^4\text{He}, 2n){}^{176}\text{Hf}$  at 27 MeV using the pulsed beam facility at the Chalk River MP Tandem. Beam bursts were of 2 ns duration spaced by 0.8  $\mu$ s. Hafnium lies outside the rare-earth region proper in that the 4f atomic shell is closed, consequently there should be no paramagnetic relaxation or paramagnetic enhancement of the applied field. Ytterbium metal has an fcc crystal structure and at elevated temperatures, quadrupole relaxation should not be too severe despite the large moment expected for the isomer. The target was heated to a temperature of 505°C during the experiment. The external magnetic field was measured by an NMR probe to be 0.97856 T. Analysis of the time differential data gave  $g = 0.96 \pm .01$ .

Analysis of the branching ratios within the  $K=6$  band<sup>1)</sup> according to the usual rotational model expressions gives  $(g_K - g_R)/Q_0 = 0.067 \pm 0.0025$ . Assuming  $Q_0$  is the same for this band as for the ground band, namely  $Q_0 = 6.69$  b, then  $g_K - g_R = 0.448 \pm 0.017$ . For antiparallel spin coupling in a two quasi-particle state we have<sup>2)</sup>  $\mu = [I/(I+1)]\{Kg_K + g_R\}$ , where  $g_K$  is expected to be 1 for protons and 0 for neutrons. Combining the two results for  $g_K$  and  $g_R$  we find  $g_K = 1.02 \pm 0.01$  and  $g_R = 0.57 \pm 0.02$ .

Clearly the isomer is a rather pure two-proton configuration. A surprising feature of the result is the large value for  $g_R$  compared to that for the ground band ( $g_R = 0.24 \pm 0.014$ ). It is well known that the addition of an odd proton to a paired system typically raises  $g_R$  by 0.05 - 0.10 and we might expect a somewhat larger effect for two unpaired protons.

The observed relaxation time,  $\tau(K=2) \sim 200$  ns, is too short to enable measurement of longer lived high K isomers in Hf isotopes, however this might be improved by further increasing the target temperature.

1) T.L. Khoo and G. Løvghøiden, Preprint 1977.

2) T.L. Khoo, J.C. Waddington and M.W. Johns, Can. J. Phys. 51 (1973) 2307.

## HEAVY ION SOURCE SUPPORT GAS MIXING EXPERIMENTS

E. D. Hudson  
Oak Ridge National Laboratory,\* Oak Ridge, Tennessee 37830

and

M. L. Mallory  
Michigan State University,† East Lansing, Michigan 48824

### Summary

Experiments on mixing an easily ionized support gas with the primary ion source gas have produced large beam enhancements for high charge state light ions (masses  $\leq 20$ ). In the Oak Ridge Isochronous Cyclotron (ORIC), the beam increase has been a factor of 5 or greater, depending on ion species and charge state. Approximately 0.1 cc/min of the easily ionized support gas (argon, krypton, or xenon) is supplied to the ion source through a separate gas line and the primary gas flow is reduced by  $\sim 30\%$ . The proposed mechanism for increased intensity is as follows: The heavier support gas ionizes readily to a higher charge state, providing increased cathode heating. The increased heating permits a reduction in primary gas flow (lower pressure) and the subsequent beam increase.

### Introduction

Improvements in the performance characteristics of heavy ion sources have a direct impact upon the performance of heavy ion accelerators. Therefore, a large effort on positive ion source improvement has been carried out at ORNL in connection with the Oak Ridge Isochronous Cyclotron. In the past, mixing gases in the ion source had been viewed as resulting in poorer source performance, since the proportion of ions available for ionization would be diluted by the mixing ratio. In particular, this effect is obviously seen in enriched isotope gases (e.g., the intensity of  $^{180}$  versus enrichment factor).

Another observation is that the quantity of gas needed to support the arc varies with the element being ionized, namely, for protons the source requires a large gas flow, whereas for xenon the source requires a small gas flow. Assuming that the energy ( $E$ ) to heat the cold cathodes to the thermionic emission limit is the same for all gases, then the following relation can be written:

$$E = n_i \bar{q} V, \quad (1)$$

where  $n_i$  is the number of ions required for the cathodes to reach the thermionic emission limit and is related to the source gas flow,  $\bar{q}$  is the average charge in the plasma, and  $V$  is the arc voltage (the potential the ions fall through in bombarding the cathodes). For hydrogen,  $\bar{q}$  can be only  $\leq 1$ . As the ion source gas mass increases, the  $\bar{q}$  charge increases since the ionization energy decreases for ions of the same charge state.<sup>1</sup>

Effects in the source and near the cyclotron central region that are pressure dependent may then vary as different gases are used, since less gas flow is needed for the heavy mass gases.

\*Operated by Union Carbide Corp. for the U.S. ERDA.  
†Work supported by the National Science Foundation.

Another ion source characteristic that is known but not understood is that different cold cathode ion source geometries require different amounts of gas flow for source operation. For example, the present ion source of Oak Ridge<sup>2</sup> requires  $\sim 3-4$  cc/min gas flow for normal operation, whereas the ion source of Michigan State University and some other laboratories require a flow of 0.5 - 1 cc/min.<sup>3</sup> One would then expect central region pressure effects and ion source gas usage effects would be more readily detectable in the large gas flow source of Oak Ridge.

### Gas Mixing Experiments

Gas mixing experiments have been performed and large beam enhancements have been detected at ORIC. The experimental arrangement for gas mixing is schematically shown in Figure 1. The gases are fed to the ion source through separate gas lines and are mixed in the plasma chamber. Experiments of mixing the gases external to the ion source and feeding

ORNL-DWG 76-13811

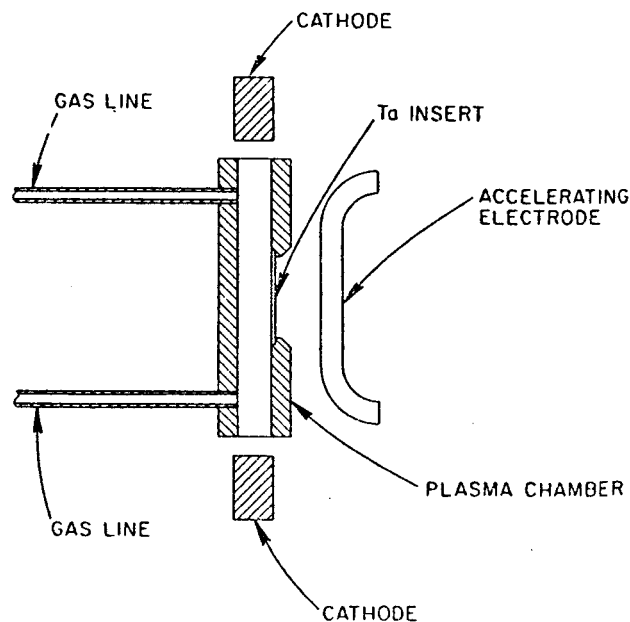


Fig. 1. A schematic view of the cold cathode ion source showing the gas inlet lines. In the gas mixing mode the primary arc gas is fed through one line and the support gas through the other. In mixing xenon with neon, visible observation of the arc through the extraction slit shows a two-colored arc, one side green (xenon) and the other side pink (neon).

## A QUICK CHANGE AXIAL COLD CATHODE ION SOURCE

M.L. Mallory, P.S. Miller, and W.S. Chien  
Michigan State University  
East Lansing, MI 48824

Summary

An axial cold cathode heavy ion source has been built and successfully operated on the Michigan State University Cyclotron. This ion source was designed to minimize the time to change cathodes and thereby increase the cyclotron efficiency. The ion source change time (i.e. the time to change the cathode and restrike the arc) can be less than 15 minutes. In particular, all source parts that need to be cleaned at the end of a source lifetime are easily removed and clean pieces substituted. No internal ion source vacuum and water seals are broken. The ion source operates at gas flows less than 1 cc/min. and typically at 1/2 cc/min. This reduced gas usage results in a good accelerating chamber pressure and small attenuation of the accelerated beam to the external beam stop. The external ion beam intensity for a given particle and charge state are comparable to the intensity obtained from Oak Ridge and Berkeley.

Introduction

Present cyclotron heavy ion sources are operated at power levels of  $\approx 2$  KW in order to produce high charge ions.<sup>1</sup> This high power operation mode results in rapid erosion of the ion source cathodes, hence necessitating frequent maintenance. This maintenance time represents an inefficiency in the acceleration operation, and attempts to decrease this ion source outage time has previously concentrated on use of various exotic cathode materials and on rotatable cathodes.<sup>2</sup> In this paper we report another approach at increasing the accelerator efficiency by minimizing the time to change the ion source cathodes. An axial cold cathode heavy ion source has been designed and is now operating in the Michigan State University (M.S.U.) cyclotron that has short ion source cathode maintenance time.

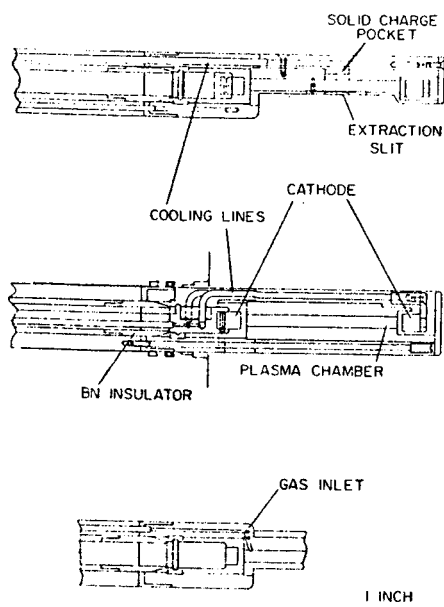


Figure 1.--The M.S.U. cold cathode axial heavy ion source is shown. The two cathodes are electrically connected by water cooled tubes. The ion source can be completely disassembled for maintenance without breaking any water and vacuum seals. A pocket for solid charge materials (e.g. for lithium beams) is provided directly behind the ion source extraction slit.

Ion Source Design

The axial cold cathode Penning ion source developed for the M.S.U. cyclotron is shown in figure 1. The ion source components that require maintenance (e.g. chimney and cathodes) can be easily disassembled without breaking water or vacuum seals. Duplicate and new ion source parts are substituted for the used pieces. The ion source is then re-assembled and put back into operation.

Ion Source Operating Experience

The ion source has now operated since September 1976. A list of particle beams and their intensity extracted from the cyclotron is shown in Table I. The measured intensities are comparable to the cyclotron extracted beam intensities of Oak Ridge and Berkeley. The ion source cathode lifetime is a strong function of accelerated ions. Lifetimes as long as 10 hours have been observed for a carbon beam where the ion source gas was CO. The ion source is maintained by the experimentalist and maintenance times of less than 15 minutes have been recorded.

The ion source gas usage is  $\approx 5$  cc/min. Gas mixing<sup>3</sup> of xenon with oxygen for an  $O^{6+}$  beam has resulted in increased stability and intensity. The ion source has also been used for the production of proton beams. The gas usage for hydrogen is greater than 5 cc/min. The heavy ion beam has required improvements in the cooling of the cyclotron accelerating slit (puller). The beam power dissipated from heavy ions is larger than for light ions. Large beam attenuation, due to charge exchange with residual vacuum in the accelerating chamber ( $\sim 5 \times 10^{-6}$  torr), has been observed only with the argon beam.

TABLE I.--The M.S.U. Cyclotron Laboratory Heavy Ion Beams (1/24/77).

Particle	Max Energy	Intensity (e $\mu$ A)
${}^6\text{Li}^{2+}$	38	3.0
${}^6\text{Li}^{3+}$	75	1.0
${}^7\text{Li}^{3+}$	74	1.0
${}^{11}\text{B}^{4+}$	85	.02
${}^{12}\text{C}^{4+}$	77	10.0
${}^{13}\text{C}^{4+}$	70	.003
${}^{14}\text{N}^{5+}$	103	1.0
${}^{16}\text{O}^{5+}$	90	1.0
${}^{16}\text{O}^{6+}$	130	.5
${}^{20}\text{Ne}^{4+}$	60	1.0
${}^{40}\text{Ar}^{8+}$	92	.03

References

1. E.D. Hudson, et al., IEEE Trans. Nucl. Sci. NS-18, No. 3(1971)113.
2. M.L. Mallory, et al., IEEE Trans. Nucl. Sci. NS-22, No. 3(1975)1669.
3. E.D. Hudson, et al., Proceeding this conference.

On Meson Exchange Currents\*

Dan Olof Riska  
Department of Physics  
Michigan State University  
East Lansing, Michigan 48824

and

Research Institute for Theoretical Physics  
Helsinki, Finland

Abstract

The construction of the simplest pion exchange current operators is reviewed. The effect of pion exchange current and charge operators on nuclear properties and reactions is discussed.

\* Research supported in part by the U.S. National Science Foundation

## Many-Body Dynamics of Heavy Ion Collisions

G.F. Bertsch

Cyclotron Laboratory and Physics Department  
Michigan State UniversityContents

1. Phenomena in Heavy Ion Collisions	1
1.1. Low Energy Collisions	
2.1. High Energy Collisions	
2. Quantum Equations of Motion	23
2.1. Density Matrix Formulation	
2.2. The Wigner Function	
2.3. Conservation Laws	
2.4. Quantum Mechanical Sum Rules	
2.5. Evolution of the Distribution Function	
3. Small Amplitude Oscillations in a Finite System	43
4. Bulk Properties of Nuclear Matter	53
4.1. Equation of State	
4.2. Tensile Strength of Nuclear Matter	
5. Dissipation of Collective Motion	53
5.1. Landau Damping	
5.2. Two-Body Dissipation	
5.3. Viscosity	
5.4. Collisions on Deformed Fermi Surfaces	
6. Theory at Low and Medium Energy	80
6.1. Shock Waves in One Dimension	
6.2. Friction	
6.3. Fragmentation and Escape of Particles	
6.4. Threshold Pion Production	
6.5. Three Dimensions	
6.6. Angular Momentum Transfer	
7. High Energy Theory	104
7.1. Phenomenology	
7.2. One-dimensional Slab Model	
7.3. Hydrodynamic Models in Three Dimensions	
7.4. Composite Particle Abundances	

Lecture Notes for the 1977 Les Houches Summer School  
Supported by the National Science Foundation